Molecular Cloning and Functional Characterization of Benzophenone Synthases from *Centaurium erythraea* and *Swertia chirata* (Gentianaceae)

Von der Fakultät für Lebenswissenschaften
der Technischen Universität Carolo-Wilhelmina zu Braunschweig
zur Erlangung des Grades einer
Doktorin der Naturwissenschaften
(Dr. rer. nat.)
genehmigte
D i s s e r t a t i o n

von Rabeia Ali
aus Benghazi / Libyen

1. Referent: Professor Dr. Ludger Beerhues
2. Referentin: Professorin Dr. Ute Wittstock
eingereicht am: 13. 03. 2019
mündliche Prüfung (Disputation) am: 20. 05. 2019

Druckjahr 2019

Vorveröffentlichungen der Dissertation

Teilergebnisse aus dieser Arbeit wurden mit Genehmigung der Fakultät für Lebenswissenschaften, vertreten durch den Mentor der Arbeit, in folgenden Beiträgen vorab veröffentlicht:

Posterbeiträge

Rabeia Ali, Pallavi Agarwal, Poonam Singh, Till Beuerle, Ludger Ernst, Adinpunya Mitra, Mariam Gaid, Benye Liu, Ludger Beerhues: Gentianaceae benzophenone synthases prefer 3-hydroxybenzoate CoA esters as starters. (Poster). Botanikertagung 2017, Kiel.

Acknowledgments

First of all, I would like to express my thanks to ***God***, who supported me in all the circumstances in my life.

I would like to express my sincere thanks and gratitude and my great respect to my supervisor Prof. Dr. ***Ludger Beerhues*** for giving me this opportunity to be a member of his research team. Thank you for your standing, assistance and valuable advice in this study. Especially, I would like to say to you: thank you for your support and encouragement to me during my PhD, despite the financial crises that have plagued me during my studies.

I am very grateful to Dr. ***Benye Liu*** for his constant support and for his continued efforts to elevate this work and to present it in the best possible way. Also, I do not want to forget the strong motivation he provided to get positive results during this work. I never experienced you would say no when asking for help. I really appreciate how your office door was always open to everyone to help and offer advice.

My great thanks to Dr. ***Rainer Lindigkeit*** for his help in software problems, to appreciate his great support and advice during this work. And thanks to Dr. ***Till Beuerle*** for his help in the chemical analysis, and friendly work conditions. I would like to thank Dr. ***Mariam Gaid*** for her helping during my study.

I want to say a big thank you to my close friend Dr. ***Ebtesam Khalil***, who introduced me to the group, for her great help, advice and tips. She helped me going through a lot of obstacles. I would like to thank Dr. ***Nargis Elgahmi*** for the special times we spent together in Germany and the shared cheering memories.

I would like to thank Dr. ***Mohamed Nagia*** for his care, support and the positive energy that made me forget all day work problems. I do not forget him to stand by my side in most of the problems and help me.

I would like to express my thanks to all, the old and new ***Colleagues*** for the wonderful time we have spent together. I thank them for the spirit of the one team to help me when I needed. I cannot forget to thank *Mrs.* ***Ines Rahaus*** and *Mrs.* ***Doris Glindemann*** for keeping the funny atmosphere during the hard working days and for their kind help during my work. Thanks a lot for keeping things bright and colorful. I sincerely appreciate the efforts of ***Bettina Böttner***, which made everyone's job much easier.

I am grateful to the *Libyan government*, *Technische Universität Braunschweig* and *International Office* for scholarships to support my stay in Germany and to finish my PhD study.

My big thanks to my husband, my soul *Fathi Issa* for standing by my side in all circumstances and helping to give me the patience and motivation to complete my study and to reach my goal, which was also his goal. I want to tell him: you were the basis of my success and if you were not by my side, I could not have been able to finish my way by this success. Thank you for all.

To my lovely children *Jana*, *Hamad*, and *Jaad*, you are the greatest thing in my life. You give me the strength and patience and carry the alienation. Listen to your voices laughing and hold you in my arms, all tiredness and stress of a hard working day just faded away, you will be always the most beautiful thing in my life.

All the words are not enough to introduce my big thanks to *my mother and my father*, who supported me with love and continuous prayer. My thanks to my *Brothe*r and *Sisters* for the continuous support and motivation to overcome all the difficulties, which I faced in my life.

Thanks to all who know who is *Rabeia Ali*

Contents

Contents

Contents

List of figures and tables

List of tables

List of figures

List of figures and tables

List of figures and tables

List of figures and tables

Abbreviations

List of abbreviations

[S]	Substrate concentration
C°	Degree Celsius
µl	Microliter
µM	Micromolar
M	Molar
2,4-D	2,4-Dichlorophenoxyacetic acid
NAA	Naphthaleneacetic acid
IBA	Indole-3-butyric acid
BAP	6-Benzylaminopurine
5` UTR	5` untranslated region
3` UTR	3` untranslated region
Bp	Base pair
BICS	Biphenylcarboxylate synthase
BIS	Biphenyl synthase
BLAST	Basic Local Alignment Search Tool
BPS	Benzophenone synthase
BSA	Bovine serum albumin
C. erythraea	*Centaurium erythraea*
Ce_St	*Centaurium erythraea* from Stuttgart
Ce_Kr	*Centaurium erythraea* from Karlsruhe
CeBPS	*Centaurium erythraea* benzophenone synthase
cDNA	Complementary deoxyribonucleic acid
CDS	Coding DNA sequence
CHS	Chalcone synthase
Contig	Set of overlapping DNA sequences
DNA	Deoxyribonucleic acid
dNTP	Deoxynucleoside triphosphate
DTT	Dithiothreitol
DOC	Deoxycholate
DW	Dry weigth
E. coli	*Escherichia coli*
G. lutea	*Gentiana lutea*
GlBICS	*Gentiana lutea* biphenylcarboxylase synthase
GSP	Gene specific primer
6X His	Hexa histidine tag
HPLC	High performance liquid chromatography
h	Hour
HaBPS	*Hypericum androsaemum* benzophenone synthase
IPTG	Isopropyl-1-thio-β-D-galactopyranoside
kDa	Kilo Dalton
K_{cat}	Catalytic constant
K_{cat}/K_m	Ratio catalytic constant / Michaelis constant

Abbreviations

K_m	Michaelis-Menten constant
L	Liter
LB	Luria Bertani
M. domestica	*Malus domestica*
mg	Milligram
ml	Milliliter
mM	Millimolar
MS	Murashig and Skooge
MeJ	Methyle jasmonate
RNA	Messenger ribonucleic acid
min	minute(s)
NCBI	National Center for Biotechnology Information
OD	Optical density
ORF	Open reading frame
PKSs	Polyketide synthases
PPS	Phenylpyrone synthase
Pfu-polymerase	*Pyrococcus furiosus* polymerase
rpm	Revolutions per minute
R.T	Room temperature
RT	Reverse transcription
RT-PCR	Reverse Transcription polymerase chain reaction
RNA	Ribonucleic acid
SDS-PAGE	Sodium dodecyl sulfate polyacrylamide gel electrophoresis
Sec	Second
S. chirata	*Swertia chirata*
SCBPS	*Swertia chirata* benzophenone synthase
TAE	Tris-acetate-EDTA
Taq	*Thermus aquaticus*
TEMED	N,N,N´,N´-tetramethylethylenediamine
TCA	Trichloroacetic acid
2,4,6 THB	2,4,6-Trihydroxybenzophenone
2,3´ ,4,6 THB	2,3` ,4,6-Tetrahydroxybenzophenone
T_m	melting temperature (primers)
U	Unit
V	Volt
V/V%	Volume per volume percentage
W/V%	Weight per volume percentage
YE	Yeast extract

Abbreviations

Amino acids:

Amino acid	Abbreviation		Amino acid	Abbreviation	
Alanine	A	Ala	Leucine	L	Leu
Arginine	R	Arg	Lysine	K	Lys
Asparine	N	Asn	Methionine	M	Met
Aspartic	D	Asp	Phenylalanine	F	Phe
Cysteine	C	Cys	Proline	P	Pro
Glutamic	E	Glu	Serine	S	Ser
Glutamine	Q	Gln	Threonine	T	Thr
Glycine	G	Gly	Tryptophan	W	Trp
Histidine	H	His	Tyrosine	Y	Tyr
Isoleucine	I	Ile	Valine	V	Val

Nucleotides

A Adenine C Cytosine T Thymine G Guanine

1 Introduction

1.1 Natural products

Plants produce a whopping variety of natural products, which have highly diverse and variable structures and play important roles in the biology of many different organisms. These products are commonly named "secondary metabolites", which play a significant role in the survival of the producing organism within its natural habitat. Conversely, the "primary metabolites" are essential for plant growth and development (Osbourn and Lanzotti 2009). Previously, the physiological roles of secondary metabolites in the plant were unexplained, but 30 years ago, it became evident, how these compounds have important roles in the interaction between plants and their environment. They include a vast array of compounds, which are classified according to their biosynthetic origin: alkaloids, polyketides, phenylpropanoids and terpenoids. To date, more than 200,000 structures of natural products from plants are defined (Hartmann 2007; Osbourn and Lanzotti 2009). These compounds serve, for example, as defence compounds against herbivores and pathogens, as flower pigments that attract pollinators, or as hormones or signal molecules. They have a strong effect on human health, besides their physiological role in plants. The plant-based system has advanced through the development of technology and it plays an essential role in the healthcare of many communities. Also, more than 50% of the most important prescribed drugs are related to natural products including plant metabolites or extracts (Bode and Müller 2003; Osbourn and Lanzotti 2009). One class of plant constituents are xanthones.

1.2 Xanthones

Xanthones or 9H-xanthen-9-on (dibenzo-γ-pyron) are secondary metabolites and constitute an important class of oxygenated heterocycles whose role is well-known in the medicinal field. They are most common in a few higher plant families, ferns, lichens, bacteria and fungi. The name "xanthone" comes from the Greek word "xanthos" and means yellow or blond, indicating their colour (Masters and Bräse 2012). Because of their important medicinal properties, xanthones have gradually risen to great significance. They are structured based on the planar dibenzo-γ-pyron skeleton (Scheme.1). This class of compounds have biological activities, which are associated with their tricyclic scaffold but vary depending on the nature and/or position of the different substituents. The acetate-derived ring is designated as ring A and is numbered 1–4, while the shikimate-derived ring is designated as ring B and is numbered 5–8 (Bennett and Lee 1989; Peres and Nagem 1997). Xanthones are typically polysubstituted and occur as either fully aromatized or dihydro-, tetrahydro-, and hexahydro derivatives.

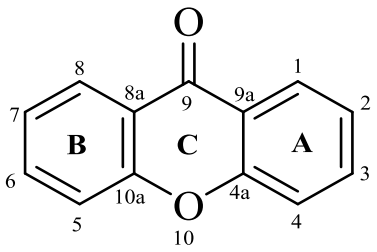

Scheme 1. Basic structure of xanthones

1.2.1 Classification of xanthones

Recently, more than 1500 xanthone-based compounds have been isolated from natural sources. They have been classified into six major groups: simple oxygenated xanthones, glycosylated xanthones, prenylated xanthones, xanthonolignoids, bis-xanthones and miscellaneous xanthones (Negi et al. 2013; Vieira and Kijjoa 2005). Furthermore, simple oxygenated xanthones classified into six groups, depending on the degree of oxygenation. They are found in these plant families: Gentianaceae, Guttiferae, Moraceae, Annonaceae, Betulaceae, Euphorbiaceae, Polygalaceae, Hypericaceae, and Calophyllaceae (Peres and Nagem 1997).

1.2.2 Bioactivity of xanthones

Xanthones are very interesting due to their broad array of biological activities, depending on their diverse structures which are derived from a different type of substitution on the free positions on the ring system. Their pharmacological activities include antioxidant, antithrombic, and anticancer properties (El-Seedi et al. 2010; Jia et al. 2015; Obolskiy et al. 2009), which have led the xanthones being designated as 'privileged structures' (Masters and Bräse 2012). The following Table shows pharmaceutical activities of xanthones.

Table 1. List of some (natural and synthetic) xanthones with their bioactivities.

Source	Xanthone	Biological activity	Reference
Garcinia paucinervis "leaves"	• Paucinervin H • Paucinervin I • Paucinervin J • α-mangostin • β- mangostin • γ- mangostin	Antiproliferative activity against human cells	**(Li et al. 2016)**
Garcinia mangostana	• mangostinone • garcinone E • 2-isoprenyl-1,7-dihydroxy-3-methoxyxanthone	Promyelocytic leukemia	**(Matsumoto et al. 2003)**

Comastoma pedunculatum	• Comastomaxanthone A • Comastomaxanthone B • Comastomaxanthone C	Anti-tobacco mosaic virus activity (Anti-TMV)	**(Zhou et al. 2015a)**
Garcinia paucinervis	• Paucinervin E • Paucinervin F • Paucinervin G • 8-*O*-*β*-D-glucopyranosyl-1-hydroxy-2,3,5-trimethoxyxanthone	Anti-TMV	**(Wu et al. 2013)**
Swertia mussotii	• 8-*O*-[*β*-D-xylopyranosyl-(1 → 6)-*β*-D-glucopyranosyl]-1-hydroxy-2,3,5-trimethoxyxanthone	Anti-hepatitis B virus	**(Cao et al. 2013)**
Swertia bimaculata	• 1-O-[β-D-xylopyranosyl-(1 → 6)-β-D-glucopyranosyl]-8-hydroxy-2,3,4,5-tetramethoxyxanthone.	α-glucosidase inhibitory activity	**(Yue et al. 2014)**
Hypericum perforatum root	• 1,6-dihydroxy-5-methoxy-4′,5′-dihydro-4′,4′,5′-trimethylfurano-(2′,3′,3,4)-xanthone • 4,6-dihydroxy-2,3-dimethoxyxanthone • *cis*-kielcorin	Anti-inflammatory against species of *Phomopsis*	**(Crockett et al. 2011)**
Garcinia hanburyi	• Garcinolic acid and other derivatives	Cytotoxic activity	**(Jia et al. 2015)**
Cudrania cochinchinensis	• Isoprenoid-substituted xanthones	Anti-microbial against vancomycin-resistant enterococci	**(Fukai et al. 2005)**
Garcinia mangostana		Antimicrobial against methicillin-	**(Iinuma et al. 1996)**

	• α-mangostin and other related xanthones	resistant *Staphylococcus aureus*	
Garcinia mangostana *Hoppea fastigiata*	• α-mangostin • 8-deoxygartanin • Gartanin • Garciniafuran • Garcinone C • Garcinone D • γ-mangostin • Mangosteen • 1,5,7-trihydroxy-3-methoxyxanthone • 1,5-dihydroxy-3,7-dimethoxyxanthone • 1,3,5-trihydroxy-8-methoxyxanthone	Treatment of Alzheimer's disease	**(Chin and Kinghorn 2008; Wang et al. 2016)** **(Moon et al. 2015)**

Trihydroxy- and tetrahydroxybenzophenones are the building blocks of xanthones and prenylated benzophenone derivatives, which are considered as an important group of phenolic natural products. They possess fascinating pharmacological activities on cardiovascular, renal, hepatic, and immune systems. They also exhibit anti-tumour activity; e.g. **psorospermin**, antiviral, anti-HIV and antioxidant activities; e.g. **guttiferone F**, antibacterial properties against methicillin-resistant *Staphylococcus aureus*, platelet aggregation-inhibitory activity; e.g. **rubraxanthone** (Jantan et al. 2009), antifungal, antimalarial, antitubercular, antiplatelet, antithrombotic and antimutagenic properties; e.g. **garcinol** (Klundt et al. 2009; Liu et al. 2003) and **gambogic acid** (Li et al. 2013), anti-tumor activity.

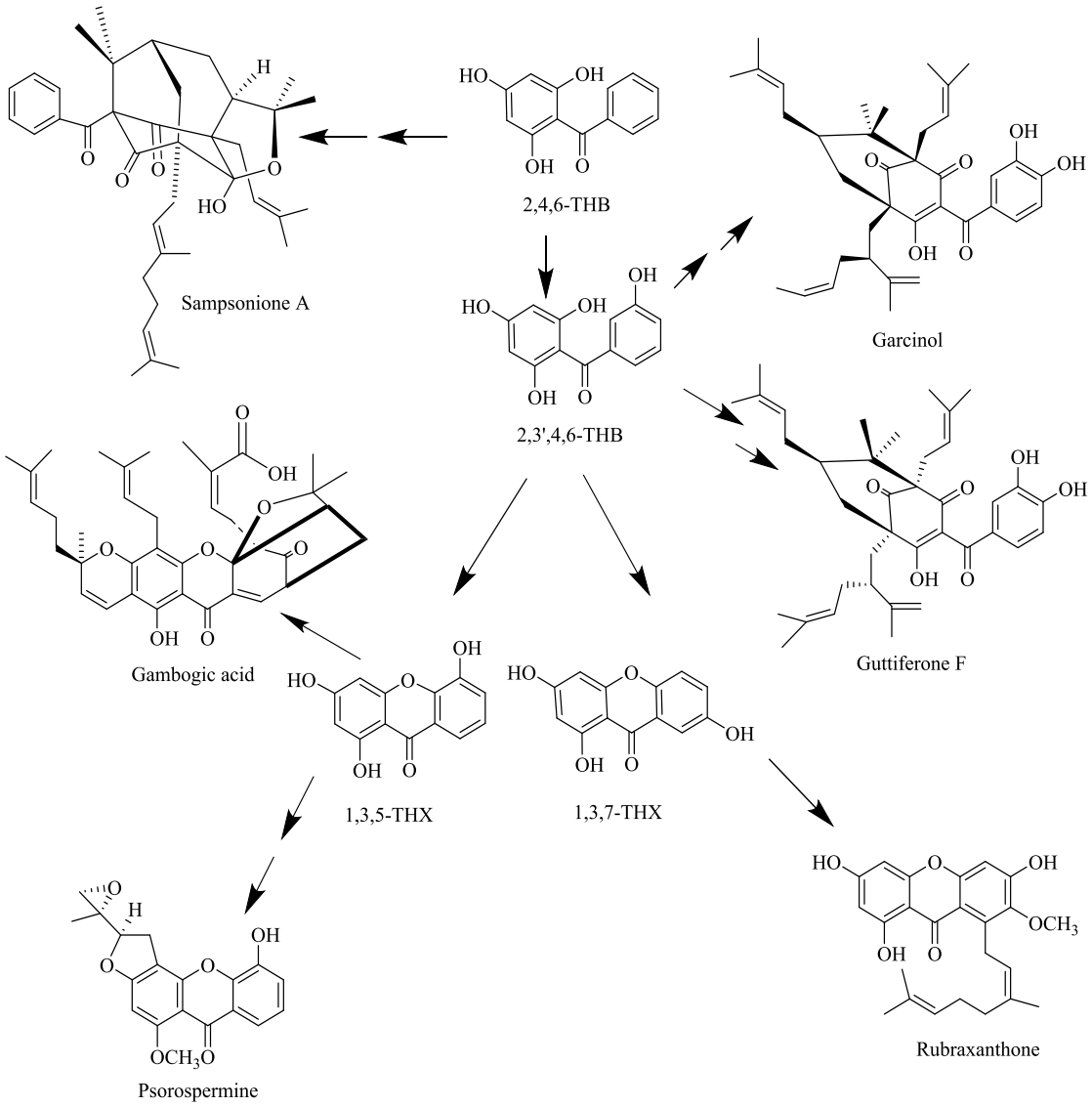

Figure 1. Examples of pharmacologically active benzophenone derivatives and their biogenic relationships (Klundt et al. 2009; Liu et al. 2003).

1.3 Amarogentin (chirantin)

Another interesting constituent of Gentianaceae is amarogentin, which is a secoiridoid glycoside restricted in occurrence to this family, naturally distributed in *Gentiana lutea* and *Swertia chirata* (Aberham et al. 2007; Arino et al. 1997; Keil et al. 2000; VanHaelen and Vanhaelen-Fastre 1983). This compound is bitter even at a dilution of 1:58,000,000. It is composed of a secoiridiod glycoside attached to 3,3` ,5-trihydroxybiphenyl-2-carboxylic acid (Scheme 2). A retrobiosynthetic ^{13}C NMR study indicated that the sweroside moiety is formed from DMAPP and IPP, which are derived from the deoxyxylulose phosphate pathway. The chemical synthesis of the biphenyl carboxylate moiety was reported (Kumar et al. 2015; Wang et al. 2000).

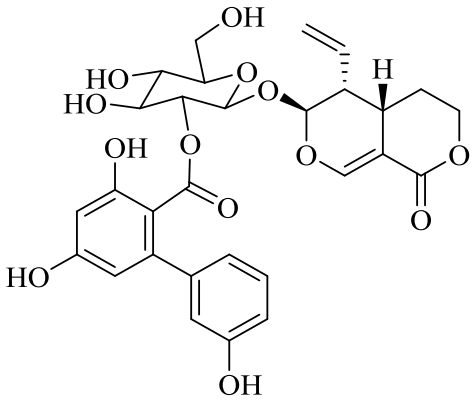

Scheme 2. Amarogentin structure

1.3.1 Bioactivity of amarogentin

In recent years, interesting novel bioactivities of amarogentin have been observed, especially, its activity against human leishmaniasis. This disease is caused by parasites of the *Leishmania* type, humans can be infected by more than 20 species of *Leishmania*. Approximately, 4-12 million people are currently infected in some 98 different countries around the world, and the number of deaths was 50,000 per year. So, amarogentin is an interesting compound, which was isolated mostly from *Swertia chirata* plants and showed activity in both liposomal and niosomal forms (Medda et al. 1999). It was recognized as a potent inhibitor of topoisomerase I of *L. donovani*. It interacts with topoisomerase I and prevents the binary complex formation, which is essential for cell replication and protein synthesis (de Carvalho and Ferreira 2001; Ray et al. 1996) . In addition, amarogentin has a range of pharmacological activities not limited to leishmanicidal properties, such as antioxidant, antiglycosidase, and anti-acetylcholinesterase activities (Gargi et al. 2015). Also, it has anti-tumor activity (Kumar and Van Staden 2015) and hypoglycemic properties (Phoboo et al. 2013). The major amarogentin source, *S. chirata*, belongs, like a number of xanthone-containing species, to the family Gentianaceae.

1.4 Gentianaceae

The plant family Gentianaceae described by Jussieu 1789 comprises 87 genera and about 1600 species (Meszaros et al. 1996). This family contains diverse species with interesting pharmacological activities, which have been widely used in traditional medicines. The most promising groups of compounds are secoiridoid glycosides and xanthones. Gentianaceae are a rich source of oxygenated and glycosylated xanthones (Bennett and Lee 1989). Some interesting species are as follows.

1.4.1 *Centaurium erythraea* (centaury)

Centaurium erythraea Rafn is a species of flowering plants known by common names “centaury”, “feverfoullie”, or “gentian” (Kumarasamy et al. 2003). The name *C. erythraea* is derived from the Greek erythros (red), reflecting on the colour of the flowers. Earlier, it was known as *Chironia*, derived from the name Centaur Chiron, a prominent personality in Greek mythology who was famous for his skills in herbal medicine. The genus *Centaurium* consists

of approximately 40 species (annuals or biennual herbs). The aerial parts of the plant are used in folk medicine drugs (Centaurii herba). The plant is described in pharmacopoeias of many countries in Europe and America (Piątczak and Wysokińska 2013). This species is native all over Europe, South to North Africa and through Eastern Europe to the Middle East and Pakistan. It has spread in other areas, including Australia, New Zealand, Canada, the United States and dispersed localities in Central and South America (Mroueh et al. 2004b). A plant of *C. erythraea* is shown in Fig. 2

Figure 2. *Centaurium erythraea* (https://upload.wikimedia.org/wikipedia/commons/4/45/Flickr_-_don_macauley_-_Common_*Centaury*.jpg)

C. erythraea is used as a support for the digestion process, especially within the stomach for stimulating the stomach secretion, and enhances the appetite and stimulates the bile production (Valentão et al. 2003). Other therapeutic strengths of *Centaurium* are against fever, anorexia, dyspepsia, asthma, eczema, rheumatism, wounds and sores. The constituents of *C. erythraea* were shown to have a significant hepatoprotective effect (Mroueh et al. 2004a) as well as a strong antimutagenic activity (Schimmer and Mauthner 1996). The major components distributed in *C. erythraea* are secoiridoid glucosides, which are characteristic bitter-tasting compounds of the plant such as swertiamarin, gentiopicroside, and sweroside. Swertiamarin is the major component in all parts of the plant. In addition there are secoiridoid alkaloids (gentianine and gentianidine), xanthone derivatives, alkaloids, phenolic acids, triterpenes, oleanic acid and resins (Aberham et al. 2011; Kaouadji et al. 1986; Kumarasamy et al. 2003; Piatczak et al. 2005; Valentão et al. 2001).

1.4.2 *Swertia chirata*

Swertia chirayita (Roxb. ex Fleming) H. Karst, in the literature also mentioned as *Swertia chirata* Buch.-Ham., *Ophelia chirata* Grisebach, *Agathotes chirayita* Don., *Gentiana chirayita* Roxburgh and *Gentiana floribunda* Don., is a popular and important medicinal herb indigenous to the temperate Himalayas. It belongs to Gentianaceae, which include a large group of annual and perennial herbs (almost 135 species). In India, 40 species were recorded as herbal medicines (Clarke 1885; Saxena et al. 1984). The common name of *S. chirata* is "Chiretta'', which is a valuable herbal medicine growing at high altitudes in the Himalayas, i.e. at heights of 1200 to 2100 m from Kashmir to Bhutan (Bentley and Trimen 1880; Clarke 1885). Chiretta is a widespread herb and known by different names such as Anaryatika, Bhunimba, Chiratitka, Kairata in Sunskrit, Qasabuzzarirah in Arab and Farsi, Chiaravata in Urdu, Sekhagi in Burma, and Chirrato or Chirata in Nepal (Joshi and Dhawan 2005). A plant of *S. chirata* is shown in Fig. 3.

Figure 3. *Swertia chirata* (https://paulhaider.files.wordpress.com/2014/05/swertia-chirata.jpg)

This traditional herb is known by its characteristic bitter taste, mainly due to the presence of amarogentin (the most bitter molecule isolated till now) as a main active constituent, besides swerchirin and swertiamarin. The whole plant is used traditionally in the treatment of digestive disorders and as anti-inflammatory and anti-hepatitis agents (Bhatt et al. 2006). However, the root is the most important part of the plant as mentioned in the literature. *Swertia chirata* was used in treatment of a lot of chronic diseases such as hypertension, epilepsy, diabetes, mental disorders, bronchial asthma, chronic fever, anemia, and malaria (Banerjee et al. 2000; Chen et al. 2011; Karan et al. 1999; Phoboo et al. 2014; Rai et al. 2000; Zhou et al. 2015b). For this

reason researchers are encouraged to analyze the active principles present in the plant, which are responsible for its medicinal properties. Active constituents of *S. chirata* are secoiridoid glycosides (amarogentin, amaroswerin), xanthones (swerchirine), flavonoids, terpenoids, iridoids, and alkaloids (gentianine) (Bajpai et al. 1991; Ghosal et al. 1973b; Niiho et al. 2006; Pant et al. 2000; Ray et al. 1996; Ya et al. 1999).

1.4.3 *Gentiana lutea* (gentian)

Gentiana lutea is a perennial herb, which also belongs to the same family of the two above plants (Gentianaceae). It has different names such as bitterroot, bitterwort, Enzian, pale gentian, and yellow gentian. Most of the plants grow at a height between 600 and 2,500 m in mountain regions of Alpine and sub-Alpine areas of Europe (central and south). The name of the plant comes from the person who is thought to have found it as a valuable medicinal herb, king Gentius, king of lllyria (west Jogoslavia) in the period of 180-167 B.C. The Gentians (approximately 180 species) are distributed around the world. *G. lutea* was used in traditional medicine. Gentianae radix is the officinal drug reported in European and Japanese Pharmacopoeias (Aberham et al. 2007; Bruneton 1995; Lange 1998; Menković et al. 2000; Ueno et al. 2003). A plant of *G. lutea* is shown in Fig. 4.

Figure 4. *Gentiana lutea* (https://commons.wikimedia.org/wiki/File:*Gentiana_lutea*_DSCF1579.JPG).

The bitter nature of the plant is mainly related to the main active ingredients, amarogentin and amaroswerin (Skrzypczak et al. 1993). The bitter compounds were supposed to be responsible for stimulating the secretion of digestive juice in the stomach and thereby the appetite (Weiss 1988). It is used as an alternative bittering agent for quinine in soft drinks (Capasso et al. 2003;

Keil et al. 2000). *G. lutea* is beneficial in states of exhaustion from chronic disease and signs of weakness of the digestive system or lack of appetite. *Gentiana* root also has anthelmintic, anti-inflammatory, antiseptic, cholagogue, emmenagogue, stomachic, antifungal, antiviral, antibacterial, and liver-protecting properties and is helpful in improving the overall function of the kidneys (Kusšar et al. 2006; Menković et al. 2000; Öztürk et al. 1998; Suzuki et al. 1978). The main active constituents in *G. lutea* are iridoids, secoiridoid glucosides (amarogentin, swertiamarin, gentiopicroside, sweroside), xanthones, and glycosidic xanthones (Haraguchi et al. 2004; Mustafa et al. 2015; Waltenberger et al. 2015). Many of the above-mentioned compound classes involve polyketide synthases in their biosynthetic pathways.

1.5 Polyketide synthases (PKSs)

Polyketide synthases are a family of multi-domain enzymes or a group of complex enzymes that form polyketides, a large class of secondary metabolites in plants, bacteria and fungi. Polyketides are complex organic compounds, which often have pharmaceutical activities, for example, antimicrobial, immunosuppressant, antiparasitic and anticancer properties (David 1998). PKSs are a group of enzymes structurally and functionally similar to fatty acid synthases (FASs). Both have a *β*-ketoacyl synthase (KS) activity that stimulates the successive head-to-tail addition of two-carbon acetate units into a developing polyketide chain (Austin and Noel 2003). Recently, PKSs and the polyketide compounds have reached the highest proportion in the biopharmaceutical researches due to their biological activities. The total market for polyketide natural products exceeds $10 billion annually and the provocation to find new drug candidates becomes a must, notably after the resistance of pathogens to many kinds of known molecules (Staunton and Weissman 2001). Based on their own domain structures, PKSs are classified into three types: type I, type II and type III. Type I PKS resembles the yeast and animal FASs, which are typically a protein complex with large subunits such as ketoacylsynthase (KS), acyl carrier protein (ACP), and acyltransferase (AT) as essential domains (Shimizu et al. 2017). Biosynthesis of erythromycin in the bacterium *Saccharopolyspora erythraea* is an example of a modular type I PKS (Austin and Noel 2003). Type II PKSs are typically multienzyme complexes composed of KS and chain-length-factor subunits and ACP (Shimizu et al. 2017). Actinorhodin biosynthesis in *Streptomyces coelicolor* is catalyzed by a typical type II PKS (Frandsen 2010). By contrast, type III or CHS-like PKS enzymes have relatively simple architecture, that is, a homodimer of KS monomeric domains, which make them much more flexible to *in vitro* investigations and structural analyses (Austin and Noel 2003; Hertweck 2009). Plant type III PKSs are discussed in the following section.

1.5.1 Plant type III PKSs

Plant type III PKSs maintain a simple architecture (a homodimer of identical KS monomeric domains). Since the first type III PKS (CHS) was discovered, various studies were achieved (Austin and Noel 2003). This group of enzymes synthesize an important type of secondary metabolites, which have a surprising usage in the medicinal field, such as flavonoids, phloroglucinols, resorcinols, benzophenones, biphenyls, chromones, isocoumarins, 4-hydroxycoumarins, acridones, pyrones, curcuminoids, stilbenes, etc (Abe 2008; Liu et al.

2009). They form an array of secondary metabolites by varying the starter substrate (aromatic or aliphatic) (Fig. 5), the number of acetyl additions (mostly malonyl-CoA) from 1 to 7 molecules and the mechanism of ring formation used to cyclize linear polyketide intermediates (Claisen condensation, aldol condensation, or heterocyclic lactone formation) (Austin and Noel 2003; Dibyenda 2015; Lukačin et al. 2005; Reimold et al. 1983). Furthermore, a large number of type III PKSs have been studied, successfully cloned and characterized such as stilbene synthase STS (Morita et al. 2001), benzophenone synthase BPS (Liu et al. 2003), biphenyl synthase BIS (Liu et al. 2004), acridone synthase ACS (Lukačin et al. 2001; Lukačin et al. 1999; Morita et al. 2007; Wanibuchi et al. 2007), benzalacetone synthase BAS (Abe et al. 2001; Abe et al. 2007), aloesone synthase ALS (Abe et al. 2004), 2-pyrone synthase 2-PS (Eckermann et al. 1998; Jez et al. 2000), and quinolone synthase QNS (Resmi et al. 2013).

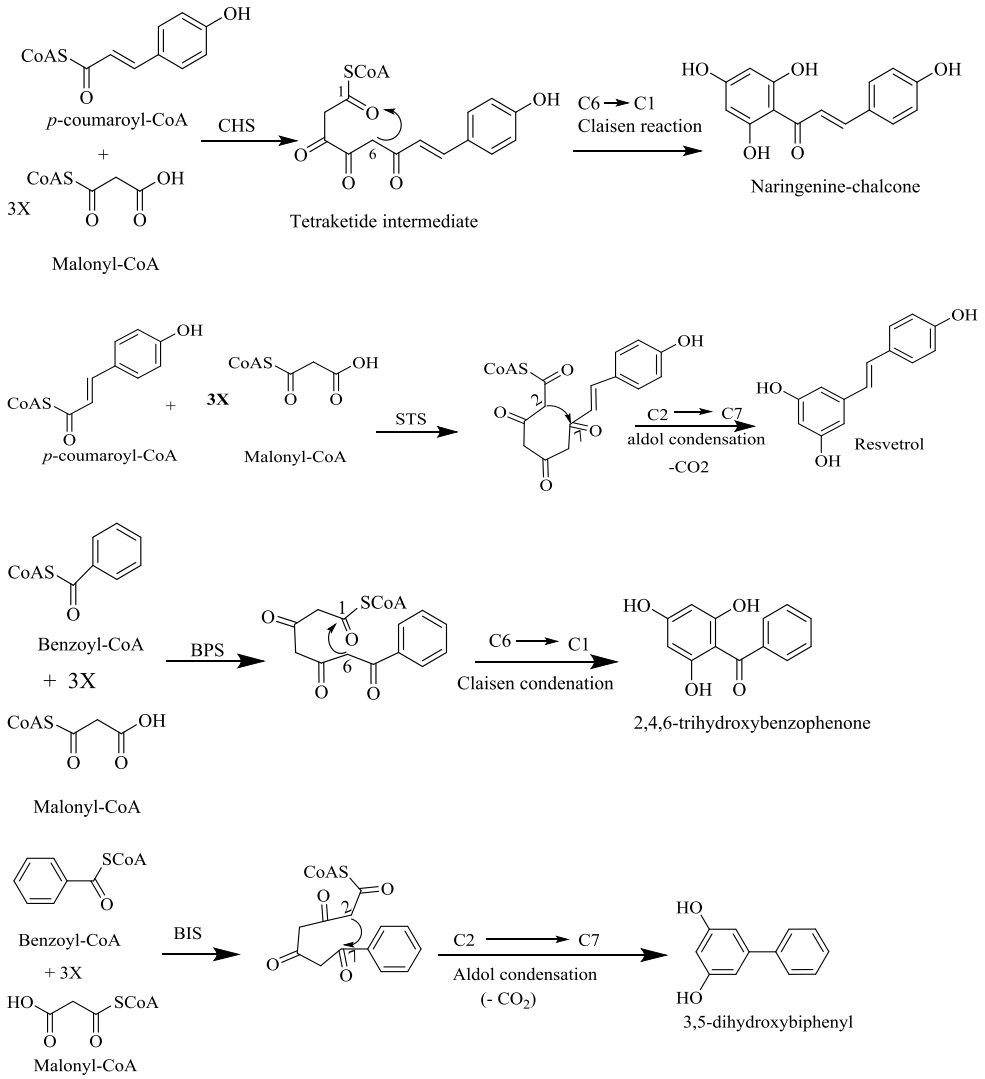

Figure 5. Biosynthesis of some plant polyketides by type III polyketide synthases (CHS super family). Chalcone synthase CHS; stilbene synthase STS; benzophenone synthase BPS; biphenyl synthase BIS.

1.5.2 Proposed type III PKS reaction mechanism

All polyketide synthases possess a conserved catalytic triad in the active site cavity composed of Cys_{164}, His_{303}, Asn_{336} as the amino acid residues. The imidazole-N of His plays a base by removing a proton from the Cys sulfhydryl group generating a reactive anion ($\mathbf{S^-}$), which attacks the carbonyl carbon of starter-CoA and replaces the CoA moiety. Malonyl-CoA as extender molecule binds near the Asn residue and forms a H-bond by NH_2 of Asn and carbonyl oxygen of malonyl-CoA, that simplifies the CO_2 to release, resulting in acetyl carbanion attack on the carbonyl carbon of ester (starter-Cys-complex) and producing a diketide intermediate. Then, the triketide is formed by attaching the second equivalent molecule of malonyl-CoA to the Asn residue, this triketide intermediate undergoes another elongation step by binding to the active site Cys and acetate addition to form a tetraketide intermediate. The final product is formed by a series of cyclization and aromatization steps in the active site of the enzyme (Fig. 6). The mechanism of polyketide formation can be summarized in the main four steps (Abe 2008; Austin and Noel 2003; Staunton and Weissman 2001):

- Loading the starter substrate.
- Decarboxylation of extender substrate (malonyl-CoA).
- Elongation of polyketide chain.
- Final product formation.

Accordingly, the remarkable functional diversity of the PKS enzymes derives from the differences in the selection of the starter molecules, the number of the malonyl-CoA condensations, and the mechanisms of cyclization reactions. PKSs that are related to the present work are presented in more detail.

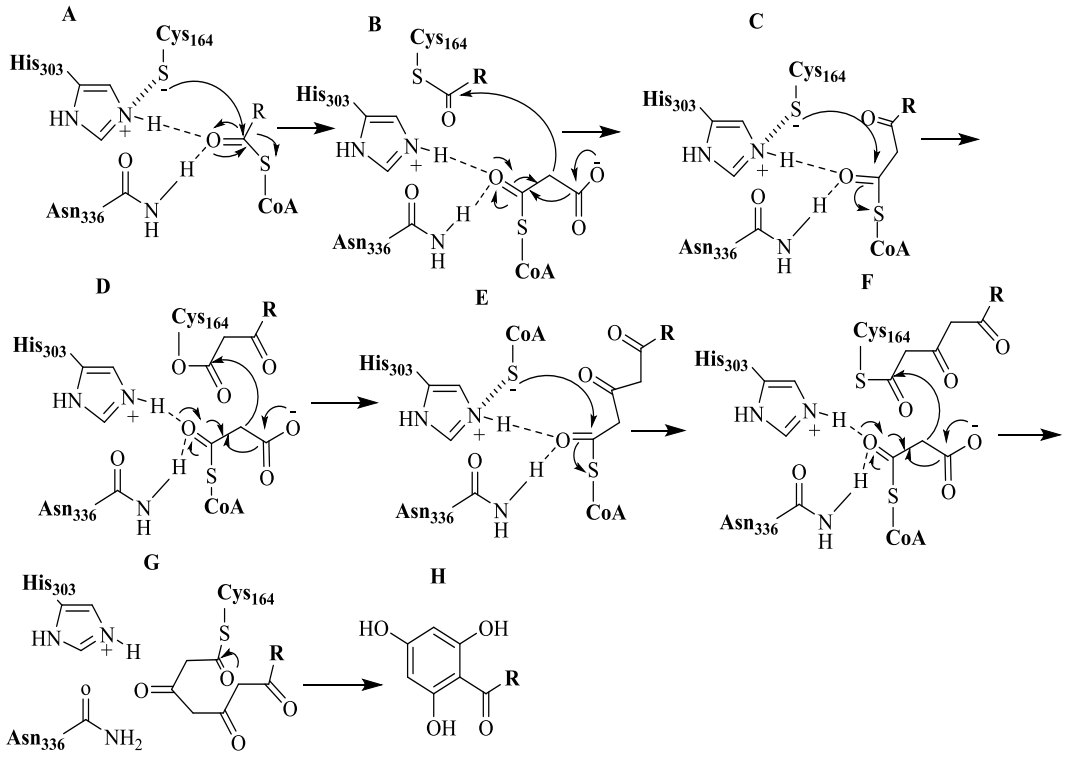

Figure 6. Proposed mechanism of the reaction catalyzed by type III PKSs (Abe 2008).

1.5.3 Chalcone synthase (CHS)

CHS is the first type III polyketide synthase investigated and isolated in 1983 from parsley (*Petroselinum hortense*) (Reimold et al. 1983). CHS is the best known representative for type III PKSs. It provides the starting material for a group of metabolites (flavonoids), which play important biological functions in flowering plants by providing floral pigments, UV-protectants and insect repellents (Austin and Noel 2003). Flavonoids have significant impact on human health such as anticancer (Jang et al. 1997), antimitotic and anti-proliferative activities (Boumendjel et al. 2008). Furthermore, antimalarial (Li et al. 1995), antileishmanial (Nielsen et al. 1998), antibacterial, antifungal and antiviral (Cushnie and Lamb 2005) properties were reported. CHS catalyzes the reaction to produce naringenin_chalcone by iterative condensation of *p*-coumaroyl-CoA with three molecules of the extender substrate malonyl-CoA in the active site cavity, followed by intramolecular cyclization (Claisen) and aromatization (Fig. 5) (Austin and Noel 2003). The crystal structure of *Medicago sativa* chalcone synthase 2 alone and complexed with substrates and products was determined and used to explain the catalytic mechanism for most of PKS type III (Ferrer et al. 1999).

1.5.4 Benzophenone synthase (BPS)

This enzyme is the focus of the present study, so it will be explained in more detail. BPS catalyzes the formation of a C_{13} skeleton, *i.e*. benzophenone, which is a central step in xanthone biosynthesis. The activity of BPS was detected for the first time in cell-free extracts from cell cultures of *Centaurium erythraea* (Beerhues 1996). Benzophenone synthase catalyzes the stepwise or iterative condensation of three molecules of malonyl-CoA with one molecule of 3-hydroxybenzoyl-CoA as starter substrate and forms 2,3` ,4,6-tetrahydroxybenzophenone as a final product (Fig. 7). Benzophenone synthase from cultured cells of *Hypericum androsaemum* (HaBPS) was the first one to be cloned and characterized. HaBPS preferred benzoyl-CoA as starter substrate, and it formed 2,4,6-trihydroxybenzophenone (2,4,6-THB) by sequential condensation with three molecules of malonyl-CoA (Fig. 7) (Liu et al. 2003).

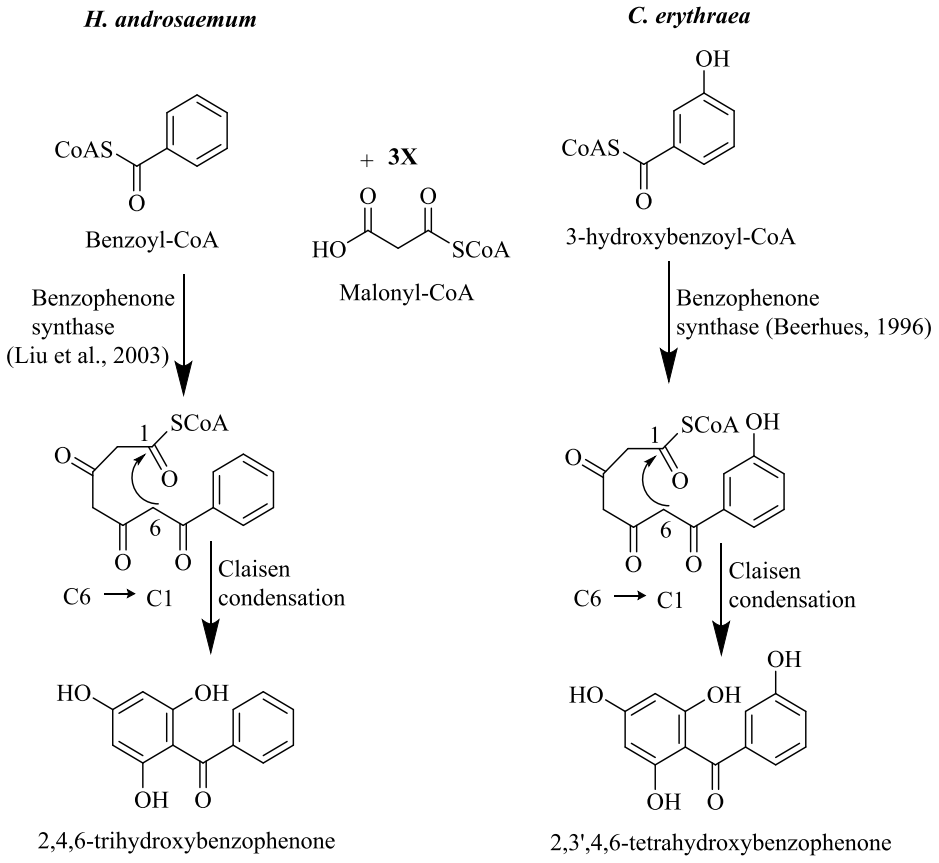

Figure 7. Reactions catalyzed by benzophenone synthases from *Centaurium erythraea* (Beerhues 1996) and *Hypericum androsaemum* (Liu et al. 2003).

Two recent BPSs were cloned from *Garcinia mangostana* and *Hypericum sampsonii* (Clusiaceae) (Huang et al. 2012; Nualkaew et al. 2012). Both enzymes prefer benzoyl-CoA as does HaBPS to produce 2,4,6-trihydroxybenzophenone. By contrast, biphenyl synthase (BIS) forms 3,5-dihydroxybiphenyl. It is the second enzyme of type III PKSs to accept and prefer benzoyl-CoA. The activity of the enzyme was detected in yeast-extract treated cell cultures of *Sorbus aucuparia* (Liu et al. 2004). The cDNA for the enzyme was cloned and characterized

by Liu et al. (2007). It catalyzes the iterative condensation of benzoyl-CoA with three malonyl-CoAs to form a tetraketide intermediate, which undergoes intramolecular C2 → C7 aldol condensation with loss of C1 as CO_2 and thus forms 3,5-dihydroxybiphenyl (Fig. 5).

A series of mutations were performed at the active site residues of HaBPS and MsCHS2 based on the crystal structure of *Medicago sativa* (Fabaceae) CHS2 (Ferrer et al. 1999). A number of the resulting enzyme mutants were either inactive or inhibited the growth of their host (*E. coli*) cells or functionally resembled the wild-type enzyme. However, a dramatic change was observed in the functional behavior of HaBPS with the substitution of a single amino acid (threonine) at position 135 with leucine. The mutant T135L formed phenylpyrone as a major product and only traces of 2,4,6-trihydroxybenzophenone when incubated with benzoyl-CoA and malonyl-CoA (Klundt et al. 2009). This means, the functional behavior of BPS was changed by a single amino acid substitution in the active site cavity to phenylpyrone synthase PPS. Phenylpyrone synthase catalyzes only two condensations of malonyl-CoA to form a triketide intermediate, followed by C5-oxy ⟶C1 lactonization to form 6-phenyl-4-hydroxy-2-pyrone (Fig. 8).

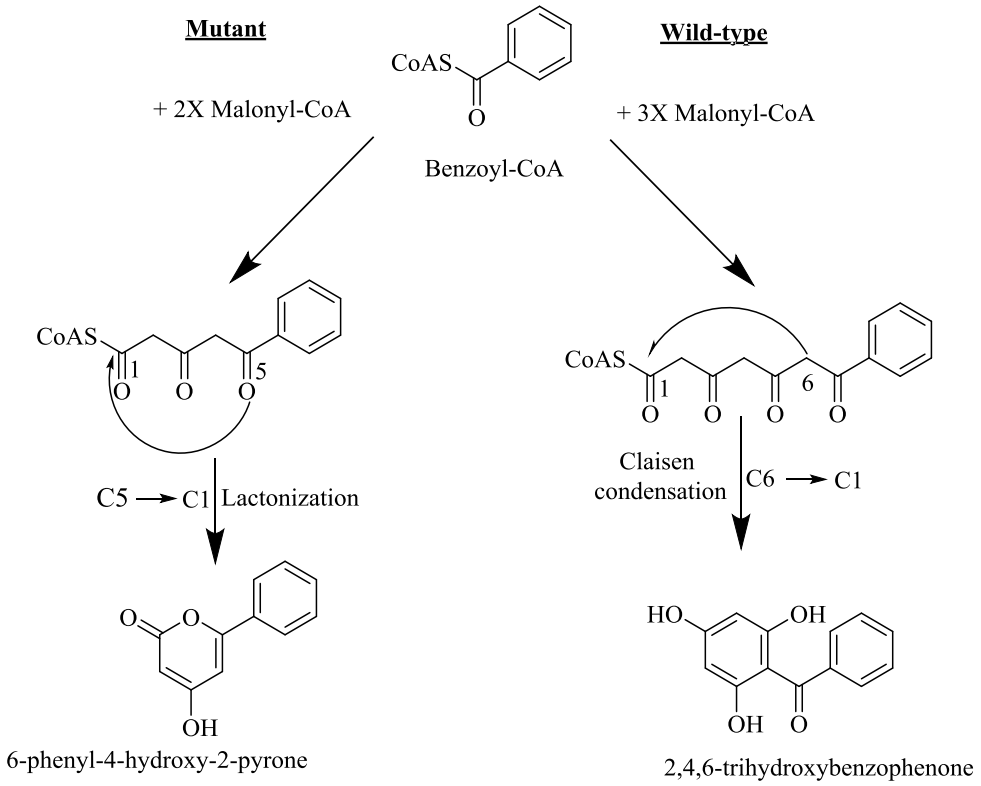

Figure 8. Reactions catalyzed by wild-type BPS and the T135L mutant (Klundt et al. 2009).

Benzoic acids are involved in the biosynthesis of benzophenones and xanthones. Benzophenone is formed by BPS and has a central step in xanthone biosynthesis. Xanthone biosynthesis has been extensively studied in cultured cells of *C. erythraea*, *C. littorale*

(Gentianaceae) and *H. androsaemum* (Hypericaceae) (Beerhues and Berger 1995; Peters et al. 1997; Schmidt and Beerhues 1997). In xanthone biosynthesis, either benzoyl-CoA or 3-hydroxybenzoyl-CoA is subjected to iterative condensations with three acetate units from malonyl-CoA to yield an intermediate benzophenone (Beerhues 1996). In different systems, the benzoic acid moiety has been proposed to come either from cinnamic acid via phenylalanine (Abd El-Mawla et al. 2001) or from the shikimate pathway as revealed by retro NMR studies (Wang et al. 2003). In *C. erythraea* cell cultures, the results showed that 3-hydroxybenzoic acid was the only radioactive precursor to be incorporated into xanthones, and benzoic acid is a poor substrate of 3-hydroxybenzoate:CoA ligase (Barillas and Beerhues 1997). In addition, benzoyl-CoA was the second best substrate of CeBPS (Beerhues 1996). The lack of incorporation of cinnamic acid indicated that the formation of 3-hydroxybenzoic acid in this species proceeds through a PAL-independent pathway (Abd El-Mawla and Beerhues 2002; Abd El-Mawla et al. 2001). Other benzoic acids also appear to be produced from the shikimate pathway, for example, gallic acid in leaves of *Rhus typhina*, and 2,3-dihydroxybenzoic acid in cell cultures of *Catharanthus roseus* (Moreno et al. 1994). Formation of benzoic acid in *H. androsaemum* originates from side chain degradation of cinnamic acid and the mechanism underlying side chain shortening is CoA-dependent and non-β-oxidative. The enzymes involved are cinnamate:CoA ligase, cinnamoyl-CoA hydratase/lyase and benzaldehyde dehydrogenase (Fig. 9) (Abd El-Mawla and Beerhues 2002).

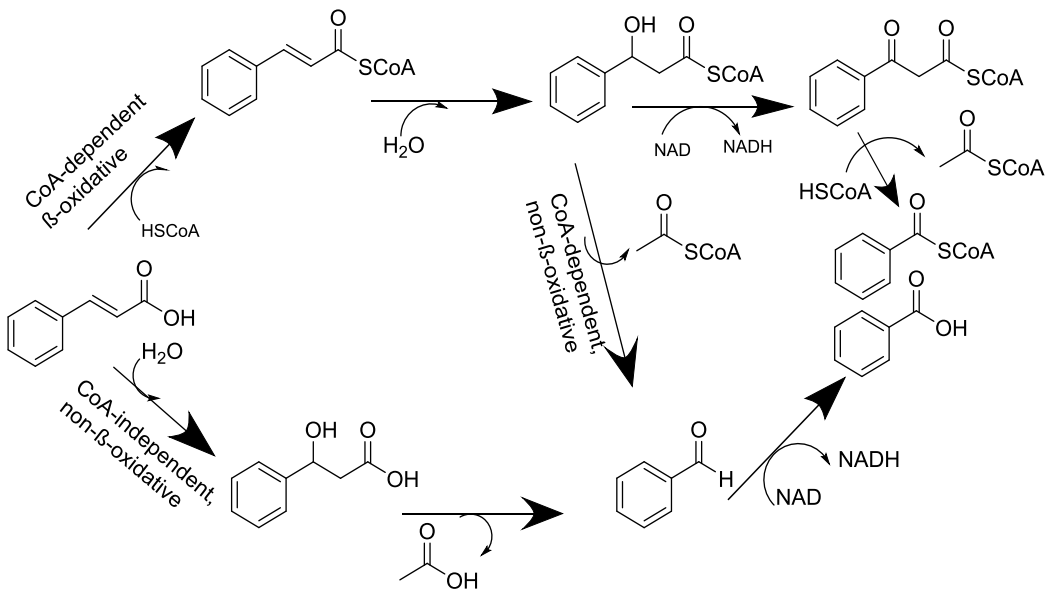

Figure 9. Proposed pathways for benzoic acid biosynthesis via cinnamic acid (Abd El-Mawla and Beerhues 2002).

Biosynthesis of xanthones is catalyzed by BPS to form 2,4,6-THB and 2,3` ,4,6-THB in Hypericaceae and Gentianaceae, respectively. In Hypericaceae, 2,4,6-THB was converted to 2,3′,4,6-THB by benzophenone 3′-hydroxylase (B3′H) activity (Beerhues 1996; Schmidt and

Beerhues 1997). The key intermediate 2,3′,4,6-THB undergoes regioselective intramolecular oxidative C–O phenol coupling reactions to give 1,3,7- trihydroxyxanthones in cell cultures of *Hypericum androsaemum* and 1,3,5-trihydroxyxanthones in cell cultures of *Centaurium erythraea*, the reactions being catalyzed by two distinct P450s known as 1,3,7- and 1,3,5 trihydroxyxanthone synthases TXSs (El-Awaad et al. 2016; Peters et al. 1997). Those are known as precursors for all types of xanthones (Bennett and Lee 1989). In addition, there is the possibility of adding a hydroxyl group to different positions, as shown in Fig. 10. At position 6, the hydroxyl group is added by xanthone 6-hydroxylase (X6H) to form 1,3,5,6-THX and 1,3,6,7-THX, respectively (Schmidt et al. 2000b). In bacteria, 2-hydroxybenzoyl-CoA, 2,3-dihydroxybenzoic acid and 4-hydroxybenzoic acid originate directly from intermediates of shikimate pathway (Marshall and Ratledge 1972; Sakaitani et al. 1990; Siebert et al. 1994). Alternatively, xanthones are synthesized in other organisms like fungi and lichens from acetate moieties.

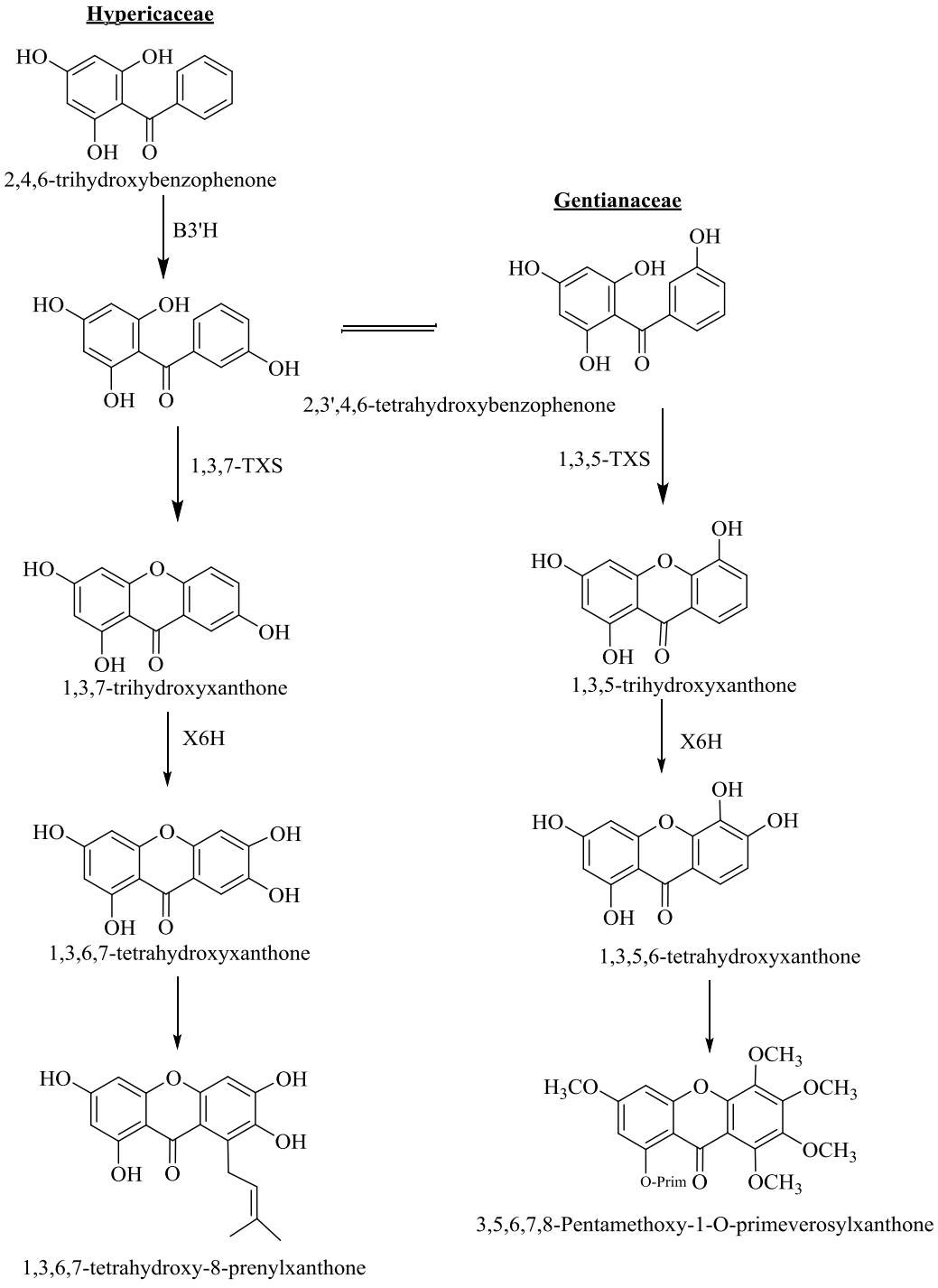

Figure 10. Biosynthesis of xanthones in Hypericaceae and Gentianaceae

1.5.5 Biphenylcarboxylate synthase (BICS)

The biphenylcarboxylate moiety of amarogentin seems to be synthesized via a polyketide pathway, using three molecules of malonyl-CoA and one molecule of 3-hydroxybenzoyl-CoA. The enzyme biphenylcarboxylate synthase was supposed to be the enzyme that catalyzes this reaction (Fig. 11). A chemical synthesis of the biphenyl carboxylate moiety was reported (Wang et al. 2000), however, the biosynthesis was neither studied at the enzyme nor the gene levels.

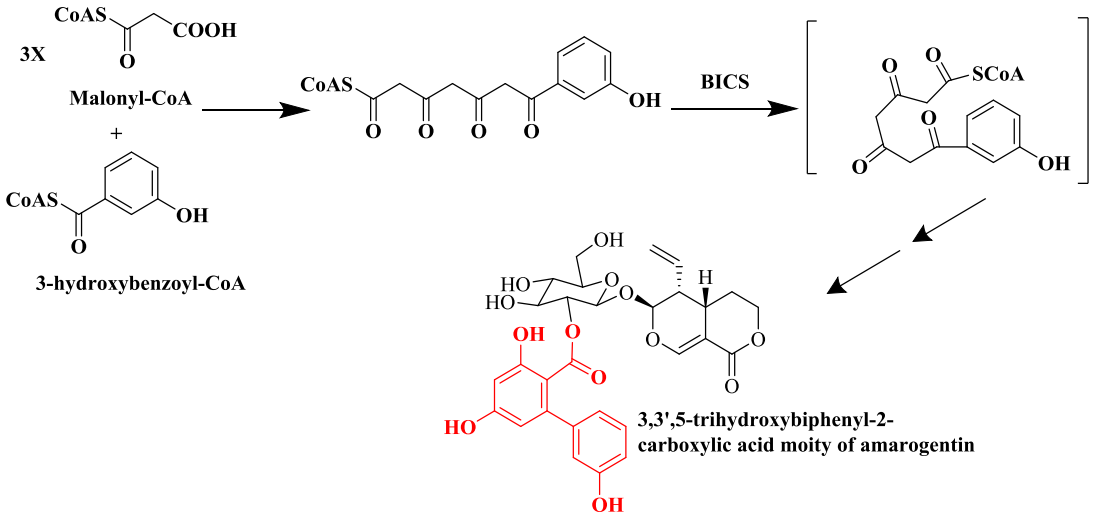

Figure 11. Proposed biosynthetic pathway of amarogentin.

1.6 Aim of the work

Benzophenone synthase and biphenylcarboxylate synthase are type III PKSs and play important roles in the biosynthesis of xanthones and amarogentin, respectively. To date, no benzophenone synthase or biphenylcarboxylate synthase from the *Gentianaceae* family were cloned and functionally characterized, although many trials were carried out to isolate the genes that encode the enzymes.

- The goals were achieved by handling plants belonging to the Gentianaceae family in order to accomplish the following aims :
  - Induction of xanthone production in cell suspension cultures of ***Centaurium erythraea*** treated with methyl jasmonate and yeast extract as elicitors.
  - cDNA cloning and functional characterization of benzophenone synthase from cell cultures of ***Centaurium erythraea***.
  - Functional characterization of a putative benzophenone synthase that has been cloned recently in our lab from root cultures of ***Swertia chirata*** (Agarwal 2013).
  - Cloning of a full length cDNA encoding BICS from ***Gentiana lutea***, based on a 3' end fragment cloned in our lab before (Swiddan 2010).
  - Studying expression kinetics of the *BPS* gene in cell suspension cultures of ***Centaurium erythraea*** after elicitor treatment.

2 Materials and Methods

2.1 Materials

2.1.1 Biological (plant materials)

2.1.1.1 *Centaurium erythraea*

The cultures of *C. erythraea* were established by Dr. M. Gaid from different geographical sources of Germany (Stuttgart, Jena, Kalsruhe) (Fig. 12.1). The calli were maintained on solid LS medium (2.2.3.1) supplemented with hormones 2,4-D 1mg/ml and NAA 1mg/ml. This callus was transferred to 250 ml Erlenmeyer flasks containing 50 ml of LS liquid medium and allowed to grow under dark and continuous shaking conditions at 120 rpm. Once a fine cell suspension culture was established (Fig. 12.2), the cells (3g) were subcultured to fresh medium every 10-14 days.

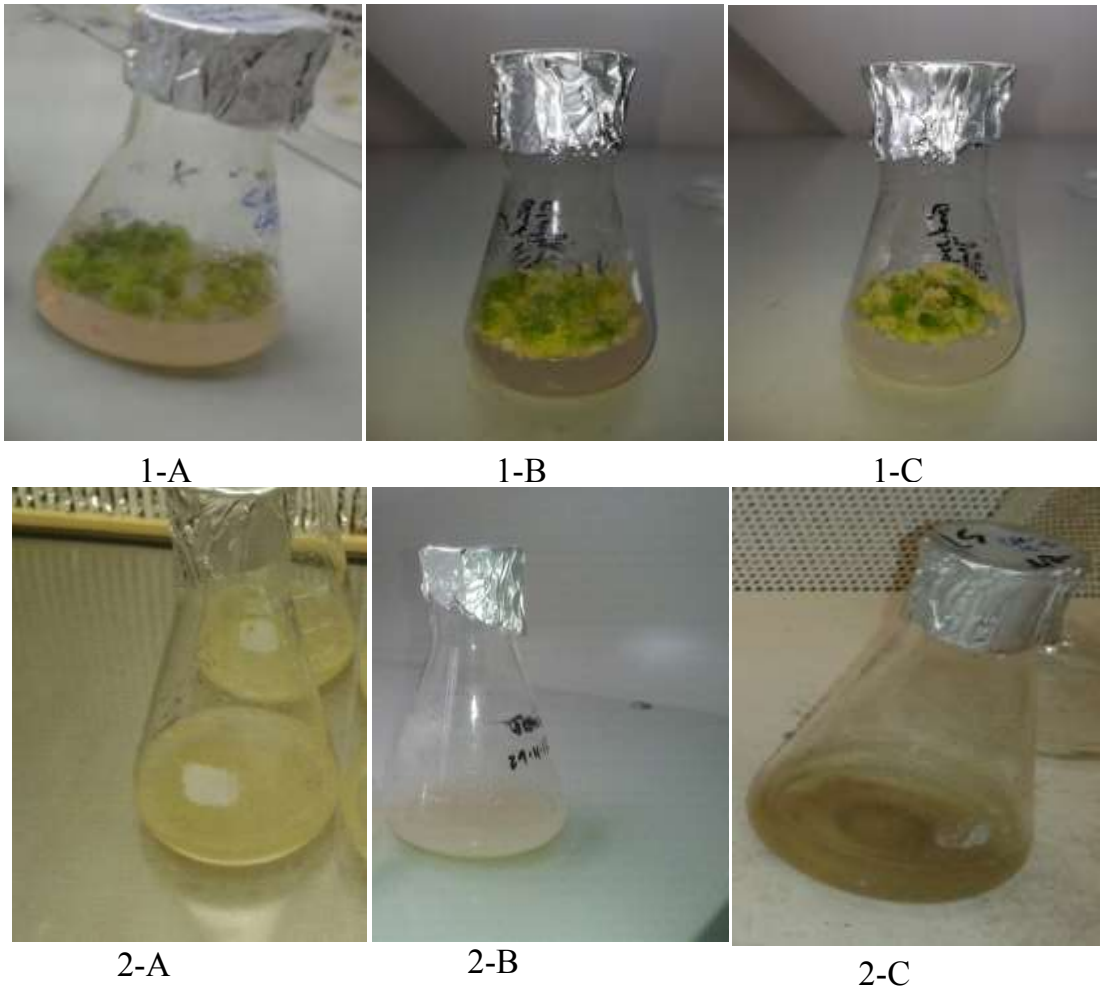

Figure 12. Tissue cultures of *Centaurium erythraea*. 1) Callus cultures from A) Stuttgart, B) Jena, C) Kalsruhe. 2) Cell suspension cultures A) Stuttgart, B) Jena, C) Karlsruhe.

2.1.1.2 *Swertia chirata*

In vitro cultures of *S. chirata* roots and plantlets were previously established in our group as described before (Agarwal 2013). The roots were grown in ½ MS medium (2.1.3.2) supplemented with 1 mg/l IBA, while the plantlets were grown in ½ MS medium supplemented with 1 mg/l BAP and 0.2 mg/l NAA (Fig. 13).

A B

Figure 13. *In vitro* cultures of *Swertia chirata*: A) Shoot cultures, B) Root cultures.

2.1.2 Chemicals and reagents for plant cultures

Most chemicals and solvents were purchased from the following companies: Roth, Sigma-Aldrich, Applichem, Fischer Scientific and Fluka. Deionized water was supplied from Milli-Q water purification system (Sartorius, Germany), and used in preparing all aqueous solutions. The solutions and culture media were autoclaved at 120°C for 20 min. Thermolabile compounds, for example ampicillin 100 mg/ml, IPTG 0.5 M, yeast extract 150 mg/ml were prepared under sterile conditions (sterile filtration) and added to autoclaved solutions.

2.1.3 Nutrient media for plant tissue cultures

2.1.3.1 LS medium for cell suspension cultures of *C. erythraea*

LS medium (Linsmaire and Skooge ,1965)	Stock solution components		Supplier	For 1 liter volume
Macroelement 10 (X)	NH_4NO_3	16.5 g	Sigma-Aldrich, Roth	100 ml
	KNO_3	19.0 g		
	$MgSO_4X7H_2O$	3.7 g		
	KH_2PO_4	1.7 g		
	$CaCl_2$	4.4 g		
	Na_2EDTA	0.413 g		
	$FeSO_4$	0.278 g		
	H_2O add up to	1 L		

Microelement 1000 (X)	H_3BO_3 620 mg $MnSO_4xH_2O$ 1690 mg KJ 83 mg $ZnSO_4x7H_2O$ 1060 mg $NaMoO_4x2H_2O$ 25 mg $CuSO_4x5H_2O$ 2.5 mg $CoCl_2x6H_2O$ 2.5 mg H_2O add up to 100 ml	Sigma-Aldrich, Roth	1 ml
Vitamins 100 (X)	Thiamine hydrochloride 4 mg Myo-Inositol 1000 mg Dissolved in dH_2O 100 ml	Serva Sigma-Aldrich	10 ml
Hormones	2,4-Dichlorophenoxyacetic acid (2,4 D) 1 mg/ml 1-Naphthylacetic acid (NAA) 1 mg/ml Dissolved in absolute ethanol	Fluka Fluka	220 µl 186 µl
Sucrose	Sucrose	Fluka	30 g
pH	pH-adjusted to 5.8 with 0.5 N NaOH		6-6.3
Agar	Agar added prior to autoclaving	Applich-em	0.6 %

2.1.3.2 MS medium for *in vitro* cultures of *Swertia chirata*

MS medium(Murashig and Skooge,1962)	Stock solution components	Supplier	For 1 liter volume
Makroelements (20X)	NH_4NO_3 33 g KNO_3 38 g $MgSO_4X7H_2O$ 7.4 g KH_2PO_4 3.4 g $CaCl_2X2H_2O$ 8.8 g Dissolved in 1L dH_2O	Sigma - Aldrich, Roth	50 ml
Microelements 1000(X)	H_3BO_3 0.62 g $MnSO_4XH_2O$ 2.23 g $ZnSO_4X7H_2O$ 0.87 g KJ 0.083 g $NaMoO_4X2H_2O$ 0.025 g $CuSO_4X5H_2O$ 0.0025 g $CoCl_2X6H_2O$ 0.0025 g Glycin 0.2 g Dissolved in dH_2O 100 ml	Sigma-Aldrich, Roth	1 ml

Vitamins100(X)	Nicotic acid 0.005 g Thiamine hydrochlorid 0.001 g Pyridoxalhydrochloride 0.005 g Myo-Inositol 1g Dissolved in dH_2O 100 ml	Serva, Sigma-Aldrich	10 ml
Iron salt 200(X)	NaFeEDTA 0.73 g Dissolved in dH_2O 100 ml		5 ml
Hormones	IBA 1 mg/ml for roots subcultures BAP 1 mg/ml for shoot Regeneration NAA 0.2 mg/ml for shoot regeneration		1 ml 1 ml 200 µl
Sucrose	Sucrose	Fluka	30 g
pH	pH-adjusted to 5.8 with 0.5 N NaOH		5.7-5.8
Agar for solid medium	Agar added prior to autoclaving	Applichem	0.6%

2.1.3.3 Special chemicals

Chemical used for enzyme assays

Compound	Source
3-(3-hydroxybenzoyloxy) benzoyl-CoA	Synthesized by Dr. B.Liu (2016) in our lab (unpublished) The analysis results for all substrates in Appendix
3-hydroxybenzoyl-coA	
3-((3-hydroxybenzoyloxy)3-hydroxylbenzoyloxy)-benzoyl-CoA	
Benzoyl-CoA	Sigma-Aldrich
Cinnamoy-CoA	Synthesized in our lab
Malonyl-CoA	Sigma-Aldrich
2-hydroxybenzoyl-CoA	Synthesized in our lab
4-hydroxybenzoyl-CoA	Synthesized in our lab
4-Comaroyl-CoA	Synthesized in our lab
2-Coumaroyl-CoA	Synthesized in our lab

3-Coumaroyl-CoA	Synthesized in our lab
dihydrocinnamoyl-CoA	Synthesized in our lab
dihydro-4-cumaroyl-CoA	Synthesized in our lab
Acetyl-CoA	Sigma-Aldrich
Caffeoyl-CoA	Synthesized in our lab
2,4,6-THB	ICN Biomedicals
2,3`,4,6-THB	Synthesized in our lab
Feruloyl-CoA	Synthesized in our lab
N-methylanthraniloyl-CoA	As gift from Prof: Matern, U. Uni_Marburg
Desmethoxyjangonin	AvaChem Scientific
Naringenin	Sigma-Aldrich

2.1.4 Elicitors

The elicitors were used for treatment of cell suspension cultures of *C. erythraea*.

Elicitor	**Supplier**	**Preparation and storage**
Yeast extract (YE)	Applichem	Stock solution of 3g/l was prepared in water, then sterilized by 0.20 µM filter and kept at 4°C.
Methyl jasmonate (MeJ)	Serva	11 µl MeJ was dissolved in 989 µl ethanol. The solution should be freshly prepared before each experiment.

2.1.5 Nutrient media for bacterial cultures

Medium	**Components**		**Supplier**	**Notices and storage**
LB medium(Luria – Bertani)	Bacto-pepton	10 g/l	Roth	pH 7
	Yeast extract	5 g/l	Applichem	Stored at refrigirator
	NaCl	10 g/l	Appichem	
For solid medium	Agar	1 % (w/v)	Roth	
SOC-Medium	Bacto Peptone	20 g/l	Roth	pH 7
	Yeast extract	5 g/l	Applichem	Stored at -20°C
	1 M NaCl	10 ml/l		
	1 M KCl	2.5 ml/l		
	Autoclave and addition of the			

	following sterile filtered solutions: 2M Glucose 10 ml/l 2M Mg^{+2} 10 ml/l		
IPTG 0.5 M	Dissolve freshly 60 mg IPTG in 500 µl dH_2O sterile-filtrate, the final concentration for the induction is 0.1mM		Stored at -20°C
Ampicillin	100 mg in 1ml distilled water, sterile filtrate		Stored at -20°C
Chloramphenicol	30 mg/ml in absolute ethanol.		Stored at -20°C

2.1.6 Solutions and buffers for biochemical analysis

2.1.6.1 Buffer for extraction and enzyme incubation

Buffer	**Composition**	**Preparation and storage**
0.1 M potassium dihydrogen phosphate containing 0.5 M DTT	potassium dihydrogen phosphate 1.36 g DTT 15.4 mg Water add 100 ml	pH adjusted by KOH, stored at 4°C DTT is added freshly

2.1.6.2 Buffers used for gel electrophoresis

2.1.6.2.1 Buffer for DNA- agarose electrophoresis preparation

Purpose	**Buffer**	**Composition**
DNA- agarose electrophoresis	50X TAE buffer	Tris-HCl 2 M EDTA 0.05 M Adjust pH to 8 by glacial acetic acid. To examine DNA products less than 300 bp, 2% agarose gel was prepared; for larger sizes, 1% agarose gel was prepared.

2.1.6.2.2 Buffers for SDS-PAGE electrophoresis

SDS-PAGE electrophoresis	**Composition**
Staking gel (for 2 small gels)	Water 2.72 ml 1 M Tris-HCl (pH 6.8) 504 µl 30% Acrylamide/Bis 664 µl 10% (w/v) SDS 40 µl 10% (w/v) APS 40 µl TEMED 4 µl
Resolving gel (for 2 small gels)	Water 2.3 ml

	1.5 M Tris-HCl (pH 8.8)	1.75 ml
	30% acrylamide/Bis	2.8 ml
	10% (w/v) SDS	70 µl
	10% (w/v) APS	70 µl
	TEMED	2.8 µl
Protein loading buffer (2X)	Water	2.7 ml
	0.5 M Tris-HCl (pH 6.8)	1.0 ml
	Glycerol	2.0 ml
	10% (w/v) SDS	3.3 ml
	β-mercaptoethanol	0.5 ml
	0.5% (w/v) bromophenol blue	0.5 ml
SDS-electrode buffer (10X)	Tris base	15 g
	Glycine	72 g
	SDS	5 g
	Water add	500 ml
Staining solution	Coomassie blue R-250	1 g
	Mathanol	500 ml
	Acetic acid	75 ml
	Water add	1000 ml
Destaining solution	Methanol	200 ml
	Acetic acid	76 ml
	Water add	1000 ml

2.1.6.3 Buffers for extraction and purification of His_6-tagged fusion protein

Buffers for extraction and purification of His_6-tagged fusion protein

Buffer	**Composition**	**Storage**
Lysis buffer	50 mM NaH_2PO_4 300 mM NaCl 20 mM Immidazole	at -20°C
Wash buffer	50 mM NaH_2PO_4 1.5 M NaCl 50 mM Immidazole	at -20°C
Elution buffer	50 mM NaH_2PO_4 300 mM NaCl 250 mM Immidazole	at -20°C

***** pH of all buffers adjusted to 8 with HCl.

2.1.6.4 Buffers for plasmid isolation (miniprep)

Buffer	**Composition**	
Buffer I (pH 8)	50 mM Tris-HCl	1.5 g/250 ml

	10 mM EDTA 10 µl/ml RNase A RNase A was added freshly before use	0.93 g/250 ml
Buffer II	0.2 M NaOH 1% (w/v) SDS	2g/250 ml 2.5 g/250 ml
Buffer III (pH 5.5)	2.55 M K-acetate Glacial acetic acid to adjust pH	62.57 g/250 ml

2.1.6.5 Solution to determine the protein amount

Bradford-dye solution	Coomassie-Brilliant blue G-250 Ethanol 96% Phosphoric acid 85% dH_2O ad Dissolve well Coomassie®-Brilliant G250 in ethanol, add orthophosphoric acid and make volume up to 1 L with water. Filter the solution through filter paper (Whatman No. 1) until no blue color can be seen. Keep it at 4°C in amber glass bottle (dark bottle).	100 mg 50 ml 100 ml 1000 ml

2.1.6.6 Solutions for PD10 washing and Ni-NTA agarose regeneration

2.1.6.6.1 Solutions for PD10 washing

Solution	**Composition**
NaOH (0.16 M)	Wash PD10 column with 5 column volumes of NaOH cleaning solution then wash with water till getting a neutral eluent by testing the eluent with litmus paper.

2.1.6.6.2 Re-Charge of the Ni-NTA agarose beads

Ni-NTA Agarose tends, after two or three usages, to change the color light blue to brownish-gray. The following steps for recharging are recommended:

- Wash the column with **2** volumes of regeneration buffer (6M GuHCl, 0.2 M acetic acid).
- Wash the column with **5** volumes of H_2O.
- Followed by washing the column with **3** volumes of 2% SDS.
- Then wash the column with **1** volume of 25% EtOH, 50% EtOH, 75% EtOH.
- Wash the column with **5** volumes of 100% EtOH.
- Followed by washing the column with **1** volume of 75% EtOH, 50% EtOH, 25% EtOH.
- Wash the column with 1 volume of H_2O.
- Followed by washing the column with 5 volumes of 100 mM EDTA, pH 8.

- Then wash the column with H_2O.
- Recharge the column with 2 volumes of 100 mM $NiSO_4$.
- Wash the column with 2 volumes of H_2O.
- Wash the column with 2 volumes of Regeneration Buffer.
- Equilibrate with 2 volumes of lysis buffer.
- Then collect the Ni-NTA with a spatula and keep it with an equal volume of 30% EtOH. and store at 4°C.

2.1.6.6.3 Regeneration of the Ni-NTA agarose beads

Wash 10 volumes of Ni agarose as follows:

- 0.2 M acetic acid
- 30% glycerol
- H_2O

Then collect the Ni-NTA with a spatula and keep it with an equal volume of 30% EtOH and store at 4°C.

2.1.7 Materials used for molecular biology

2.1.7.1 Kits for molecular biology

Purpose	Kit	Supplier
RNA isolation	Rneasy® Plant mini Kit	Qiagen
DNA isolation	Dneasy™ plant maxi Kit	Qiagen
First strand cDNA synthesis	Maxima first strand cDNA synthesis Kit	Thermo Scientific
purification of PCR product or DNA from gel	DNA Purification Kit from gel	Analytic Jena

2.1.7.2 Host cells

Strain	Purpose	Genotype
E. coli DH5α	It was used for the initial cloning of target DNA into cloning vector.	F' φ80δlacZ9M15 end A1 hsdR17(rk-mk+)supE44thi-1 λ-gyrA96 relA1 9(lacZYA-argFV169) deoR
E. coli BL21(DE3)pLysS	Used for protein expression of target gene cloned in pRSETB vector.	F⁻ *ompT hsdS*B (rB⁻mB⁻) *gal dcm* (DE3) pLysS (CamR)

2.1.7.3 Cloning vector and expression vector

Vector	Character/Purpose	Supplier
pJET1.2/blunt Cloning vector	2.974 kb for cloning DNA fragments with 5` - or 3` - overhangs generated by restriction enzyme digestion.	Thermo scientific
pRSET B expression vector	2.9 kb vector with N-terminal His_6-tag and ampicillin resistance gene	Invitrogen

2.1.7.4 The enzymes used in cloning part

Enzyme	Purpose	Supplier
RevertAid H Minus Reverse transcriptase	Reverse transcription	Thermo Scientific
FastAP Thermosensitive Alkaline Phosphatase	Catalyzes the release of 5'- and 3'-phosphate groups from linearized vector DNA and preventing its recircularization	Thermo Scientific
Taq DNA polymerase	Amplification of DNA	Thermo Scientific
Kpn I and *Nhe* I	Production of sticky ends	Thermo Scientific
DNA Blunting enzyme	Blunting reaction	Thermo Scientific
T4 DNA Ligase	Ligation	Thermo Scientific
RNase A	Digestion of RNA by plasmid isolation	Thermo Scientific
Phusion Hot Start II High fidelity DNA polymerase	High fidelity amplification of DNA	Thermo Scientific

2.1.7.5 Primers

All primers were synthesized in HPSF (high purity salt free) quality at MWG-Biotech AG (Ebersberg) Germany or Microsynth AG, Switzerland.

Purpose	Name	Sequence

Reverse transcription	3'CDS primer A	5´-AAG CAG TGG TAA CAA CGC AGAGTA C(T)30 N-1N-3´
	5'CDS primer A	5´-(T)25 N-1N-3'
	SMART II	5` -AAG CAG TGG TAA CAA CGC AGA GTA CGC GGG-3´
RACE	RACE-long	5` -CTA ATA CGA CTC ACT ATA GGG CAA GCA GTG GTA ACA ACG CAG AGT-3’
	RACE-short	5` -CTA ATA CGA CTC ACT ATA GGG C-3'
Degenerate Primers	PKSdegF1	5'TA(CT)(CA)A(ATGC)CA(AG)GG(ATGC)TG(C T)TT(CT) GC- 3'
	PKSdegR1	5'TC(ATGC)AC(ATGC)GTIA(AG)(ATGC)CCIGG (ATGC) CC -3'
Ce cDNA control	CeBPS6 F	5´ATC**GCTAGC**ATGGTGATGGCCAAGGAGCT CAAAAG-3`
	CeBPS6 R	5` ATG**GGTACC**TTAGATTGCTACACTACGTA GG-3`
18s gene Gentianaceae Specific	Forward	5'-ACCTGCGGAAGGATCATTGTC-3'
	Reverse	5'-AACTTGCGTTCAAAGACTCGATGG-3'
Vector specific primer (for sequencing DNA insert)	PJET 1.2 F	5'-CGA CTC ACT ATA GGG AGA GCG GC-3'
	PJET1.2 R	5'-AAG AAC ATC GAT TTT CCA TGG CAG-3'
	pRSETB F	5`-GAG ACC ACA ACG GTT TCC CTC-3`
	pRSETB R	5`-CTA GTT ATT GCT CAG CGG TGG-3`
Ce gene Specific Primers	P1_4 R1	5'-CAA ACA AAG CTT GTC CGA CAA GAC-3'
	P1_4 R2	5'-ATT GGG GCC TCG GAA AAA GAT G-3'
Overexpression Primers for BPS of	P16_F_*Nhe* I	5'-ATT **GCT AGC** ATG GTG GCG GCC GTC GAG-3'
	P16_R_*Kpn* I	5'-ACT **GGT ACC** CTA AAT GGA GAC GCT ACG CAG AAC CA-3'

Centaurium erythraea	P13_F_*Nhe* I	5'-**CTG CTA GC**A TGA GAA GTT TTT TGG GTG TAG TGA GAT TGG-3'
Primers used for RT-PCR	CeBPS_RT_Rev CeBPS_RT_For Ce18srRNA_F Ce18srRNA_R	5` -AAG CCC TGT CTC GCG GA-3` 5` -GTC CCA AAG CTT GCG AAA CTT G-3` 5` -ATT AAC AGG GAC AGT CGG GG-3` 5` -TGC ACC ACC ACC CAT AGA ATC-3`
BICS primers	GL2_3 *Kpn* I GL2_5 *Nhe* I GL2_F GL2_cutintron_F GL2_cutintron_R	5` -AGT GGT ACC TTA AAT TGC TAC ACT GCG TAA AAC AAC AG-3` 5` -AGT GCT AGC ATG ATG ACT GAG AAG GAG CTC AGA AG-3` 5` -CCA ATT TCG TCG AAG AGA TCT CAT AC-3` 5` -TAA GCG CAT TTG TGA AAA GTC AAT GAT AAG GAA GCG CCA-3` 5` -TGA CTT TTC ACA AAT GCG CTT AAA CTT TTC CTT AAG CTC-3`

2.1.8 Equipment

Equipment	**Model**	**Company**
Balance Balance Balance	2254 Kern 572 LA230S	Sartorius Kern & Sohn GmbH Sartorius
pH Meter	Digital pH meter 325	WTW
Autoclave	VX-120	Systec
Clean bench	LaminarAir HLB 2472 Laminar Air HBB 2460	Heraeus Heraeus
Dry block heater	Dri-Block DB-3D	Techne
Spectrophotometer Spectrophotometer Spectrophotometer	Ultrospect 1000 SimpliNano™ Ultrospec 3100 pro	Pharmacia Biotech GE Lifesciences GE Healthcare
Water purification system	Arium 611 VF	Sartorius, Germany

-80°C Freezer	Hera Freeze	Heraeus
Incubator shaker Incubator shaker	HT Multitrone	Infors HT
Centrifuges	Universal 32R Biofuge 13 Avanti®- J-E Centrifuge Sigma 1-15K	Hettich Heraeus Sepatech Beckman Coulter Sigma Centrifuges
Electrophoresis	Mini-Sub Cell Sub Cell GT Protein Chamber	BioRad BioRad Biometra
Heating circulator water bath	MW-4	Julabo
Ultrasonic Cell-Disruptor	Sonifier 250	Branson (G. Heinemann
Magnetic rotator	VF2	IKA-Labortechnik (Janke & Kunkel)
PCR cycler	T-Proffessional basic Gradient	Biometra
Gel documentation MultiImage T^M	Light Cabient	Alpha In. Corp
Speed vacuum	RVC 2-18	Christ
Lyophilizer	Gamma -20	Christ Lyophilizing apparatuses GmbH

2.2 Methods

2.2.1 Biochemical methods

2.2.1.1 Treatment of *in vitro* cultures with elicitors

Cells (3g) of *C. erythraea* (Ce_St and Ce_Kr) were inoculated to 50 ml medium (LS- medium. 5 days after subculture, MeJ at final concentration 100 µM and YE at final concentration 3g/l were added to the culture. For control, the cultures were treated by an identical amount of water instead of YE, and ethanol instead of MeJ.

2.2.1.2 Extraction of metabolites from cell suspension cultures of *C. erythraea*

Three gram of cells (Ce_St/ Ce_Kr) were homogenized with seasand and methanol in a mortar. The total volume of methanol was 20 ml. The cells were crushed for 5 to 10 min, then placed on a sonicator for 15 min. The homogenized cells were filtered and then the filtrate was dried using rotary evaporator. The residue was re-dissolved in 3 ml methanol, then the mixture was centrifuged at maximum velocity for 5 min. From the mixture, 100 µl was diluted with 900 µl methanol and 40 µl were injected to HPLC for analysis.

2.2.1.2.1 Extraction of media

Culture media were combined and extracted twice with 50 ml ethyl acetate. The organic phase was combined and evaporated to dryness. The residue was taken up in 1 ml methanol and 40 µl were injected to HPLC for analysis.

2.2.1.2.2 Acid hydrolysis of extract

For hydrolysis with 2 N HCl, 61 µl of 2 N HCl were added to 1 ml of the extracts from cells and medium, and the mixtures were heated at 60°C for 1h. The solvent was evaporated and the residue was re-dissolved in 5 ml water and extracted with 10 ml ethyl acetate. The organic layer was evaporated to dryness and the residues were redissolved in HPLC methanol and analyzed by HPLC.

2.2.1.2.3 Extraction and analysis of xanthone accumulation in cell cultures of *C. erythraea* (Ce_Kr)

The cells were lyophilized and the dried cells were weighted at culture growth and post-induction by YE (3g/l) at time intervals (0, 2, 4, 6, 8, 10, 24, 48, 72, 96 h). The same weight of the cells was taken and incubated overnight with methanol HPLC. The following day, the cells were vortexed for 30 min and centrifuged at maximum speed (13000 rpm) for 20 min. The supernatant was collected. The supernatant (50 µl) was diluted 1:10 and 20 µl 1 N HCl was added to 200 µl sample and the mixture was left overnight. The following day, 20 µl was injected to analyze by HPLC.

2.2.1.3 Crude protein extraction

2.2.1.3.1 Preparation of cell-free extracts

Cell cultures of *C. erythraea* (Ce_St) were harvested 6 h, and 9 h post-induction by MeJ and YE. Cells (6 g) were mixed with seasand (50% w/w), polyclar AT (10% w/w). The mixture

was homogenized in a mortar for 15 min in 6 ml of 0.1 M KH_2PO_4 buffer pH 7 containing 0.5 M DTT. Homogenized cells were centrifuged at 9000 rpm for 20 min. The supernatant was applied to PD10 column, which was already equilibrated with 25 ml extraction buffer. The fraction (high-molecular weight) was eluted with 3.5 ml of 0.1 M KH_2PO_4 buffer (pH 7). These crude protein extracts were used in the test activity of *C. erythraea* benzophenone synthase.

2.2.1.3.2 Protein determination

Protein concentration measured by the method of Bradford protein assay (Bradford 1976). By binding of proteins to Coomassie® brilliant Blue G 250, the concentration of protein was determined. The binding ability causes a shift in the absorbance from 465 nm to 595 nm in the photometric assay. The assay was carried out by the addition of 900 µl Bradford-dye solution to 5 µl sample and 95 µl water in a cuvette of one cm width. The absorbance was measured at 595 nm in a UV/VIS spectrophotometer. Protein concentration was calculated from a calibration curve, which was prepared for each determination using 1 mg/ml bovine serum albumin (BSA) as standard.

2.2.1.4 Benzophenone synthase (BPS) assay (crude protein)

According to Beerhues (1996), benzophenone synthase activity was determined. The reaction mixture contained 37.4 µM malonyl-CoA as extender substrate, 13.7 µM benzoyl-CoA as starter CoA, 0.1 M KH_2PO_4 buffer pH 7, and approximately 100 µg protein in a total volume of 250 µl. The mixture was incubated for 30 min at 37°C, and the reaction was terminated by adding 27 µl 50% acetic acid. Ethyl acetate (300 µl) was added to extract the product. Followed by vigorous mixing and centrifugation at 13000 rpm for 5 min, the organic phase was collected and evaporated to dryness. 50 µl of methanol was added to dissolve the residue and 40 µl were injected and analyzed by HPLC (VWR-HPLC). The control reaction mixture contained denatured crude protein extract.
*Benzoyl-CoA was the starter substrate used, because of its availability in the lab, whereas synthesis of 3-hydroxybenzoyl-CoA was under process.

2.2.1.5 Time course changes in benzophenone synthase activities

C. erythraea BPS activity was measured at 3 time points (9, 12, 15 h) after elicitor treatment (MeJ and YE at maximum concentrations of 100 µM and 3g/l, respectively). The experiment was carried out as mentioned above (2.2.1.4).

2.2.1.6 Enzyme assays for recombinant enzymes (CeBPS and ScBPS)

The standard assay was performed according to Liu et al. (2003). The following initial starter substrates were used to determine CeBPS activity and ScBPS activity: 3-((3-hydroxybenzoyl)-oxy)benzoyl-CoA, 3-((3-hydroxybenzoyloxy)3-hydroxylbenzoyloxy)-benzoyl-CoA, 3-hydroxybenzoyl-CoA, and benzoyl-CoA, at concentrations of 11.9, 10.3, 27.16, and 13.7 µM, respectively. Malonyl-CoA (37.4 µM) was used as an extender with all starter substrates

and the reaction was incubated at 37°C for 10-15 min and stopped by 27 µl 50% acetic acid. The product formed was extracted twice by 300 µl ethyl acetate, vortexed and centrifuged at 13000 rpm for 5 min. The organic phase was collected, dried and the residue was dissolved in 50 µl HPLC methanol, 40 µl was injected in HPLC (VWR-HPLC) for analysis.

2.2.1.7 Biochemical characterization of *Centaurium erythraea* and *Swertia chirata* benzophenone synthases

2.2.1.7.1 Stability test for CeBPS and ScBPS

To determine the activity of CeBPS and ScBPS at different temperatures (0°C, 4°C, -20°C and -80°C), aliquots of the pure protein fractions (2.2.3.6.9) were stored immediately after elution with elution buffer (2.1.6.3) on ice at 0°C and in a refrigerator at 4°C. The other fractions were eluted with 50 mM Tris-HCl buffer using PD10 column (Amersham Biosciences). The column was firstly equilibrated with 25 ml 50 mM Tris-HCl buffer pH 7.5. Then 2.5 ml from the other protein fractions were loaded to the PD10 column. The elution was performed with 3.5 ml of 50 mM Tris-HCl buffer. The collected samples were stored after concentration measurement at -20°C and -80°C. The stored fractions of protein under different conditions (0°C, 4°C,-20°C and -80°C) and at different time intervals (days and weeks) were incubated with different substrates (benzoyl-CoA, 3-hydroxybenzoyl-CoA, and 3-((3-hydroxybenzoyl)-oxy)benzoyl-CoA) and the activity was compared with the activity of fresh protein.

2.2.1.7.2 Determination of pH and temperature optima

To determinate the pH optimum, 0.1 M KH_2PO_4 buffer ranging from 5.5 – 9 values were used for optimum buffer capacity. The enzymes (CeBPS, ScBPS) were incubated in standard assay at this different pH values with purified protein at 37°C for 10 min. The enzymatic product was analyzed by HPLC and the optimum pH value for both enzymes was determined. At the optimum pH, other incubations were carried out at different temperatures from 20 - 50°C.

2.2.1.7.3 Linearity with protein amount and incubation time

The incubations were carried out at the pH and temperature optima. The amount of enzymatically formed product was determined as a function of the protein amount in the standard assay (0.5-16 µg) and incubation time (5, 10, 15, 20, 25, 30 min) for CeBPS and (5, 10, 15, 20, 25, 30, 35 min) for ScBPS.

2.2.1.7.4 Effect of DTT on enzyme activity

In series of incubations at the standard conditions for CeBPS and ScBPS, the activity of both newly cloned benzophenone synthases was detected at different concentrations of DTT (0, 10, 25, 50, 100, 200, 250, 500, and 1000 µM).

2.2.1.7.5 Study of substrate specificity

At optimum pH, temperature, protein amount and time, enzyme assays were performed using malonyl-CoA as extender and a series of substrates: benzoyl-CoA, 2-hydroxybenzoyl-CoA, 3-hydroxybenzoyl-CoA, 3-(3-hydroxybenzoyloxy)benzoyl-CoA, 3-((3-hydroxybenzoyloxy)3-

hydroxylbenzoyloxy)benzoyl-CoA, 4-hydroxybenzoyl-CoA, cinnamoyl-CoA, 2-coumaroyl-CoA, 3-coumaroyl-CoA, 4-comaroyl-CoA, dihydrocinnamoyl-CoA, dihydro-4-cumaroyl-CoA, acetyl-CoA, caffeoyl-CoA, feruloyl-CoA and *N*-methylanthraniloyl-CoA. The samples were incubated for 10 min in case of CeBPS and 15 min in case of ScBPS. The product was collected as mentioned above (2.2.1.6). The residue was redissolved in 50 µl HPLC-methanol and 40 µl was injected in HPLC for analysis. Three independent experiments were performed and the mean values were calculated.

2.2.1.8 Determination of kinetic parameters

The kinetic parameters of the enzymes were determined at optimum conditions (fresh protein, pH 7.5, temperature 37°C) for both enzymes. The time was adjusted to 10 min for CeBPS and 15 min for ScBPS. The amounts were adjusted to 5 µg protein for CeBPS and 7.5 µg for ScBPS. Different concentrations of potential starter substrates and the extender malonyl-CoA were used. The kinetic parameters of BPSs (CeBPS, ScBPS) were determined from Lineweaver-Burk plots. The products were extracted and analyzed by VWR-HPLC. Two independent experiments were performed and mean values were calculated. The apparent K_m and V_{max} values were calculated from Lineweaver-Burk plot, which is a linear regression of the Michaelis-Menten equation, by using hyper 32 http://hyper32.software.informer.com/.

2.2.2 Analytical methods

2.2.2.1 HPLC analysis

The analysis of all enzymatic products was performed by HPLC (VWR-Hitachi) EZChrome vers.3.3.2 SP1 supplied with a diode array detector L-2455 and Hyper Clone ODS column (C18, 250 X 4.6 mm, 3 µm) or Symmetry® glass lined column (C8, 150 x 4.6 mm, 3.5 µm). The liquid phase consisted of the distilled acidified water (A) pH 2.5 and methanol (B). For this purpose (the analysis of enzymatic products), different gradients composed of water and methanol were used. **Gr. 1** was as follows:

Gr.1	
Time (min)	**%B**
0	**30**
2	**30**
22	**90**
27	**95**
29	**95**
31	**30**
40	**30**

The same HPLC (VWR-Hitachi) EZChrome vers.3.3.2 SP1 was used to analysis the metabolites from cell suspension cultures of *C. erythraea* (Ce_Kr). The same column was used as mentioned above. The gradient of the liquid phase **Gr. 2** was used as follows:

Gr.2	
Time (min)	**%B**
0	**10**
2	**10**
22	**90**
27	**95**
29	**95**
31	**10**
40	**10**

The analysis of metabolites from cell cultures of *C. erythraea* (Ce_St) was performed by using HPLC (Agilent 1260 Infinity Quaternary LC System; Agilent Technologies, Santa Clara, CA, USA) supplied with a diode array detector (DAD; G1315D DAD VL) and a column Symmetry® glass lined column (C8, 150 x 4.6 mm, 3.5 µm). The liquid phase was used for different gradients, acidified water (1% formic acid pH 3) (A) and acetonitrile (C) **Gr. 3**. Then, we used two optimized gradients **Gr. 4** and **Gr. 5** to enhance the separation of two induced compound peaks.

Gr. 3	
Time (min)	**% C**
0	**5**
2	**5**
45	**90**
46	**95**
48	**95**
50	**5**
60	**5**

Gr. 4	
Time (min)	**% C**
0	**25**
2	**25**
22	**85**
23	**0**
25	**0**
27	**25**
35	**25**

Gr. 5	
Time (min)	**% B**
0	**30**
2	**30**
22	**85**
23	**100**
25	**100**
27	**30**
35	**30**

2.2.2.2 LC-MS analysis (Liquid chromatography-mass spectrometry)

All compounds and enzymatic products were analyzed by mass-spectrometry. They were firstly purified by HPLC and the corresponding peaks were collected as individual peaks. Secondly, the concerned compounds were directly infused into the mass spectrometer with a flow rate of 5-10 µl/min. Mass spectrum analysis was carried out through "Positive Full-Scan Mode". MS/MS experiment was done with EPI^+ (enhanced product ion scan, positive mode). Mass calibration and instrument tuning were based on molecular ion peak $[M+M]^+$ through the whole fragmentation pattern.

2.2.3 Molecular biology methods

2.2.3.1 Isolation of nucleic acids

2.2.3.1.1 Isolation of total RNA

Total RNA was isolated from *C. erythraea* cells treated with MeJ and YE by RNeasy® Mini Kit (Qiagen). The frozen (-80°C) cells ~150 mg at were homogenized with liquid nitrogen in precooled mortar and pestle and used as a material for extraction. The cells disrupted immediately in a lysis buffer containing a strong denaturating agent. Following cell lysis, centrifugation through QIAshredder^{TM} was conducted to remove undesirable material and to reduce the viscosity of the lysate. The lysate was transferred to RNeasy Mini Spin columns in the presence of ethanol (100%), which promotes a selective binding of RNA to the silica-gel-based membrane of the RNeasy Mini Spin column. By centrifugation the contaminants including small RNAs were efficiently washed away, high-quality RNAs were eluted in RNase-free water and used either directly for reverse transcription or stored at -80°C.

2.2.3.1.2 Isolation of genomic DNA

Genomic DNA from root cultures of *S. chirata* was isolated by using DNeasy® Plant Mini Kit (Qiagen). The plant material (root) ~100 mg was pulverized in liquid nitrogen and lysed in a buffer containing RNase. To exclude any clumps, which affect the yield of DNA, the mixture was centrifuged through a QIAshredder Mini spin column. Binding buffer and ethanol were added to precipitate most of the proteins, detergent, and polysaccharides and allow to DNA adsorption on the membrane, which occurred in presence of high concentration of Chaotropic salts, which removed water from hydrated molecules in solution. The pure DNA was eluted in 50 µl elution buffer and stored at - 20°C until use.

2.2.3.1.3 DNA extraction from agarose gel slices

After gel electrophoresis (2.2.3.5) a DNA fragment of the right size was excised from agarose gel by sharp scalpel then transferred to a suitable tube. Purification of DNA fragment was performed by using the Innu PREP DOUBLE Pure Kit (Analytic Jena bioslution). The gel matrix was solubilized in a solubilizer buffer by 50°C, then the solution was mixed by the binding optimizer and transferred into Nucleospin filter. The DNA fragment was bound well with the silica membrane, but the undesirable compounds were washed with washing buffer. Finally, DNA fragment was eluted by 20 µl elution buffer. In case of extraction of DNA fragments after digestion, wash buffer was added instead of gel solubilizer buffer, then the process was continued as mentioned before.

2.2.3.2 Determination of RNA and DNA concentrations

The concentration of nucleic acid solutions was determined spectrophotometrically by measuring the UV absorbance at 260 nm.
The following equation was used (Sambrook and Russell 2001):
Concentration of RNA = absorbance at 260 nm x dilution factor x 40 µg/ml
Concentration of DNA = absorbance at 260 nm x dilution factor x 50 µg/ml

By calculating the ratio of absorbance at 260 nm to absorbance at 280 nm, the purity was determined. Pure samples having an A260/A280 ratio of (1.7-1.9) ensure the appropriate quality.

2.2.3.3 Reverse transcription (RT)

Reverse transcription is a technique used to synthesize a first strand cDNA from an RNA template. Reverse transcriptase is the enzyme catalyzed this reaction and known as RNA-dependent DNA polymerase. For the synthesis of the first strand cDNA, total RNA was used as a template and an oligo-dT as a primer, which annealed to the poly-A tail of the mRNA. The RNA template is degraded by incubation with RNase H. RNaseH is an endoribonuclease that specifically hydrolyzes the 5` -phosphodiester bonds of RNA, which is hybridized to DNA. The reverse transcription reaction product can be directly used or stored at -20°C.

2.2.3.3.1 Rapid Amplification of cDNA Ends (RACE)

Two complementary steps were involved in RACE technique: firstly, reverse transcriptase was used to introduce 3´ or 5´ anchor by primer extension, as a result to single strand cDNA synthesis. Secondly, PCR amplification by using the gene-specific primer (GSP), which designed from the known internal sequence together with a primer similar to the anchor sequence. The amplification product is subsequently cloned into a suitable vector and sequenced to detect any missing part.

2.2.3.3.2 3´CDS-cDNA synthesis (3´ RACE)

In the 3′-RACE, an oligo-dT primer with a unique anchor sequence at its 5′-end primes, the single strand cDNA was synthesized, starting from the poly (A) tail by the action of reverse transcriptase. Following, a PCR amplifies by using a forward GSP and a reverse primer similar to the sequence of the introduced anchor. The PCR product will be from the poly (A) tail to the middle of the gene as presented in the following scheme.

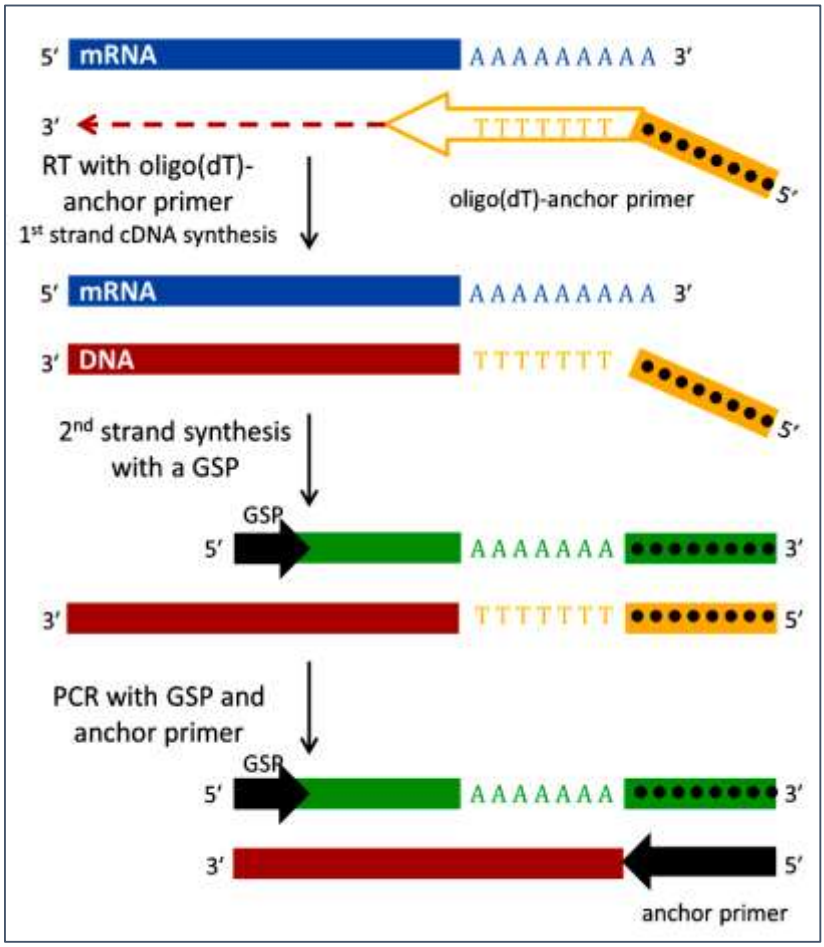

Scheme 3. Representation of 3` -RACE synthesis (El-Awaad 2016).

The first strand cDNA for 3´ -RACE was synthesized over the following steps:

1. Mix 2 µg RNA + 10 pmol 3´CDS primer + water to a final volume of 11 µl.
2. Centrifuge briefly, incubate at 70°C for 5 min, then chill on ice.
3. Add 4 µl (5x) reaction buffer + 20 units Riboblock™ RNase inhibitor + 2µl dNTP (1 mM final concentration from each + RNase free water to a total volume 20 µl.
4. Incubate at 37°C for 5 minutes.
5. Add 200 units of RevertAid H Minus M-MuLV Reverse Transcriptase and incubate the reaction at 42°C for 90 min.
6. Stop the reaction by heating at 70 °C for 10 min, then chill on ice.

The product was used directly or stored at -20°C.

2.2.3.3.3 5´_ cDNA-synthesis using SMART-RACE protocol

SMARTscribe™ reverse transcriptase based on reverse transcriptase from M-MuLV (Moloney Murine Leukemia Virus) was used for 5` RACE. The enzyme exhibit a terminal transferase activity, it adds to the 3´_ end of the first strand cDNA from 3 to 5 cytosine (C) residues.

SMART II primer contains a terminal stretch of guanine (G) residues that anneal to the dC-rich cDNA tail and serves as an extended template for reverse transcriptase as presented in the following scheme.

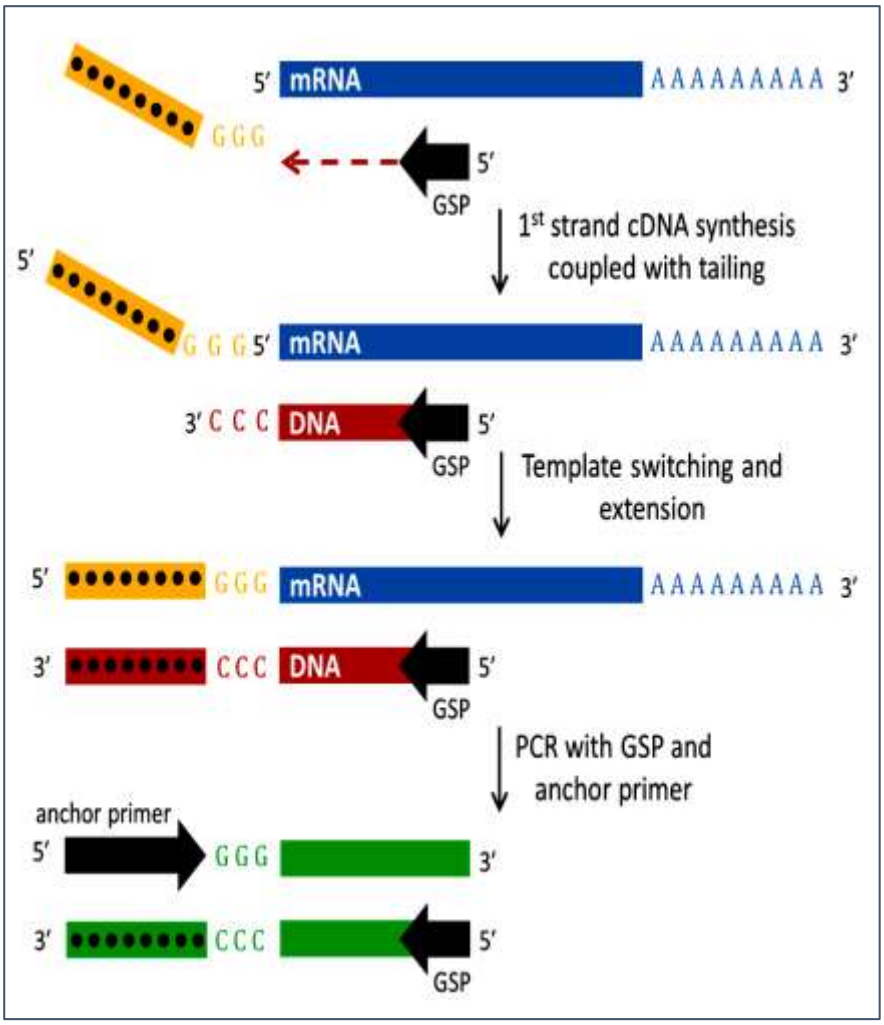

Scheme 4. Representation of 5´ -RACE PCR using SMART system (El-Awaad 2016).

The following components were added for cDNA synthesis:

Component	**Volume**
Total RNA	3 µl
5` CDS primer	1 µl
Smart II A oligo	1 µl
Nuclease-free water	3 µl
The tubes were incubated 2 min at 70°C. Then the following components were added:	
5x first strand buffer	4 µl

DTT	1 µl
dNTPs	2 µl
Reverse Transcriptase (SMART scribe™)	2 µl
After mix all of these components, the tubes incubated at 42°C for 90 min.	

Synthesized 3` CDS cDNA was used in the following PCR reactions, whereas 5` CDS cDNA was used together with reverse gene-specific primers for expression studies and as template for terminal transferase protocol.

❖ **Gene specific primer design**

The primers are a short strand of nucleic acids synthesized from DNA or RNA sequence. It is important to design high-quality primers to get successful PCR results. The primers should contain a target part or area which binds specifically and accurately at the cDNA template. As mentioned elsewhere, certain recommendations should be taken into consideration for primer design. It is not necessary to include all the mentioned recommendations.

- The length of primers should be between 15-30 base pairs, their length should be enough to increase the level of specificity and to anneal with a DNA template.
- The 3` prime end and 5` prime end should design in the right direction.
- Melting temperature T_m is the important factor for the annealing phase of PCR reaction. The melting temperature should be in the range of 50°C and 60°C and the difference between forward and reverse primer temperatures not more than 2°C.
- The content of G-C should be relatively higher than A-T content in a whole sequence of primer and the ratio about 50-60 %. To enhance the efficiency of the annealing the 3` end of the primer should finish with G or C.
- Should not contain many complementary areas in the base sequence of reverse and forward primers, to avoid binding to each other or binding to themselves and form primer dimer.

In the case of primers with sticky-ends, exemplified in case of overexpression using the pRSETB vector, the restriction sites are introduced at the beginning of the primers. Between the start codon of the forward primer and the introduced restriction sites, one, two, or no nucleotide should be introduced to keep the coding sequence in frame.

2.2.3.4 Polymerase chain reaction (PCR)

The polymerase chain reaction is a technique used to amplify a single copy of DNA, through successive cycles of amplification generating thousands to millions of copies of a particular DNA sequence. The reaction of PCR depending on thermal cyclic which consisting of repeating heating and cooling of the reaction, three cycles are applied:

a) **Denaturation**: The DNA is heated to 95°C to denature DNA, the temperature breaks the weak hydrogen bonds that hold DNA double strands to single strands.
b) **Annealing:** The binding of primers to single DNA strands. This binding is the first starting point for DNA polymerase enzyme. The temperature of annealing depends on

the melting temperature of primers (Tm). It should be neither so high (no binding occurs), nor so low (miss-priming occurs). It is usually about 5°C less than the Tm.

c) **Extension or elongation:** The reaction is heated to 72°C, which is the optimum temperature for DNA polymerase activity. DNA polymerase extends the primers till getting double stranded DNA again. Adding nucleotides onto the primer in a sequential manner, using the target DNA as a template. The duration of this step depends on the length of the fragment to be amplified and the speed by which the enzyme adds nucleotides to the newly_synthesized strand.

2.2.3.4.1 Standard PCR

This method was used to check for proper ligation of the insert in the constructed plasmids and occasionally in RACE-PCR. The components of standard PCR are as follows.

Component	Volume to
10x reaction buffer	2.5 µl
dNTPs (10 mM each)	1 µl
Forward primer (10 pmol)	1 µl
Reverse primer (10 pmol)	1 µl
Template DNA from RT-reaction	0.5 µl
Taq DNA polymerase (5U/µL)	0.1 µl
Water	25 µl

The cycling was achieved as fallows.

Step	Temp °C	Time	Cycles
Initial denaturation	95	3 min	1
Denaturation	95	30 sec	
Annealing	50	30 sec	35
Extention	72	3 min	
Final extention	72	10 min	1
Stop (storage)	15	pause	

2.2.3.4.2 Touch down PCR

To increase the specificity of the amplification and decrease the possibility of non-specific amplifications (mispairing), this method was used by adjusting in the melting temperatures of pairs of the primers. The annealing temperature of touch down PCR during the initial cycles is 5-10 °C higher than melting temperature (T_m) of the primers. Then in the subsequent cycles, the annealing temperature was decreased by 0.5°C/cycle. The reaction components were the same as in standard PCR, but the cycling was performed as follows:

Step	Temp °C	Time	Cycles
Initial denaturation	95	3 min	
Stop	70	Pause	
Denaturation	95	30 sec	
Annealing	Tm (ΔT = -0.5 °C/cycle)	40 sec	X 9
Extension	72	1 min	
Denaturation	95	30 sec	
Annealing	Tm - 5 °C	40 sec	X 29
Extension	72	1 min	
Final extension	72	10 min	
Stop(storage)	15	Pause	

2.2.3.4.3 Nested PCR

This method of PCR was used in the present work to increase the amplification specificity of the product. The PCR product of the first amplification is used directly in the next PCR reaction as a template. The primer pairs used in the second amplification to 3` -direction of those the same were used in the first amplification. The reaction components were the same as in standard PCR, while in the cyclic program was used standard PCR program or touch down PCR program.

2.2.3.4.4 PCR using proof reading DNA polymerase

In the present work, it is important to be sure that the whole DNA sequence for protein expression is completely correct, that why to use the Phusion DNA polymerase ''proofreading'' for faithful replication of the desired template. Specifically, this involves multiple steps, including its ability to read the template strand, select the appropriate nucleotide triphosphate and insert the correct nucleotide at a 3` prime end (3` to 5` exonuclease activity), thus increase the fidelity. The components of PCR were as follows:

Component	Volume to
5x Phusion HF buffer	5 µl
dNTPs (10 mM each)	1 µl
Forward primer (10 pmol)	1 µl
Reverse primer (10 pmol)	1 µl
Template DNA from RT-reaction	1 µl
Phusion DNA polymerase (5U/µL)	0.1 µl
Water	to 25 µl

The cycling was performed as follows:

Step	Temp °C	Time	Cycles
Initial denaturation	98	3 min	
Stop	80	Pause	
Denaturation	98	30 sec	
Annealing	(T_m- 5 °C)	30 sec	X30
Extension	72	1 min	
Final extension	72	10 min	
Stop (storage)	15	Pause	

2.2.3.4.5 Gene transcript analysis (CeBPS) by RT-PCR

PCR reaction is one method in our field to determine the expression of mRNA from a target gene, which achieved by the following steps:

- Specific primers are designed to amplify a 500 bp length from the target gene CeBPS_RT_F and CeBPS_RT_R. At the same time two primers are designed to use as control in PCR reaction, Ce18srRNA_F and Ce18srRNA_R.
- Total RNA was extracted from control and yeast-extract treated *C. erythraea* cell suspension cultures at 3, 6, 9, 15, 20, 24, 30 hours post-elicitation. The genomic DNA was eliminated by treatment with DNase I (Qiagen). The RNA concentrations at 260/280 ratios were determined using spectrophotometer.
- cDNA synthesis at all time points from an equal amount of RNA.
- Sample cDNAs were 10 times diluted with DNase-free water.
- RT-PCR amplification was carried out by using the synthesized cDNA in all-time points as a template with gene specific-primers.
- The number of cycles was optimized to 25 after comparing the band intensities obtained from the amplification and 23 cycles in case of amplification with *C. erythraea* 18S primers (Ce18srRNA_F and Ce18srRNA_R). 18S ribosomal RNA served to normalize RT-PCR results.
- The components of reaction and temperatures cycles were performed as in a standard PCR.

2.2.3.5 Agarose gel electrophoresis

According to the number of samples, the corresponding volume of TAE buffer and agarose weight mixed. The mixture was boiled in a microwave oven to dissolve the agarose. The medori green was added after cooling down the mixture, which helps in visualization the bands. The mixture was poured in a suitable gel try and allow it to solidify at room temperature. Samples were loaded on the gel after mixing with loading dye along with Generuler mix (ladder). Thereafter, samples were run in a gel chamber filled with TAE buffer and under electric current (120 V, 400 mA. 25-30 min). The gel is visualized under UV-equipped transilluminator. The concentration of agarose was determined depending on the expected band size, in order that the small DNA molecules enable to separate well on high agarose concentration, it cause reducing in the migration speed and the separation.

2.2.3.6 Cloning of PCR product

2.2.3.6.1 Cloning into pJET1.2/blunt cloning vector

The first and second fragments of CeBPS were ligated into a pJET1.2/blunt cloning vector for the purpose of sequencing. According to the instruction in the kit, the blunting and ligation were performed as follows:

Firstly, the following components were mixed.

Component	Volume to
2x Reaction buffer	5 µl
PCR product	1 µl
Water, nuclease-free	2.5 µl
DNA blunting enzyme	0.5 µl

Vortex briefly and centrifuge for 5 sec.

Secondly, incubate all at 70°C for 5 min, then chill on ice.

Finally, ligation reaction was done on ice by adding this mixture:

pJET1.2/blunt cloning vector (50 ng/ µl)	0.5 µl
T4 DNA Ligase	0.5 µl
Total	10 µl

Blunting program was as follows:

Step	Temp °C	Time
1	70	Pause
2	70	5 min
3	15	Pause

Ligation program was as follows:

Step	Temp °C	Time
1	22	Pause
2	22	10 min
3	12	Pause

Note: The ligation mixture was used directly for transformation to the host bacteria.

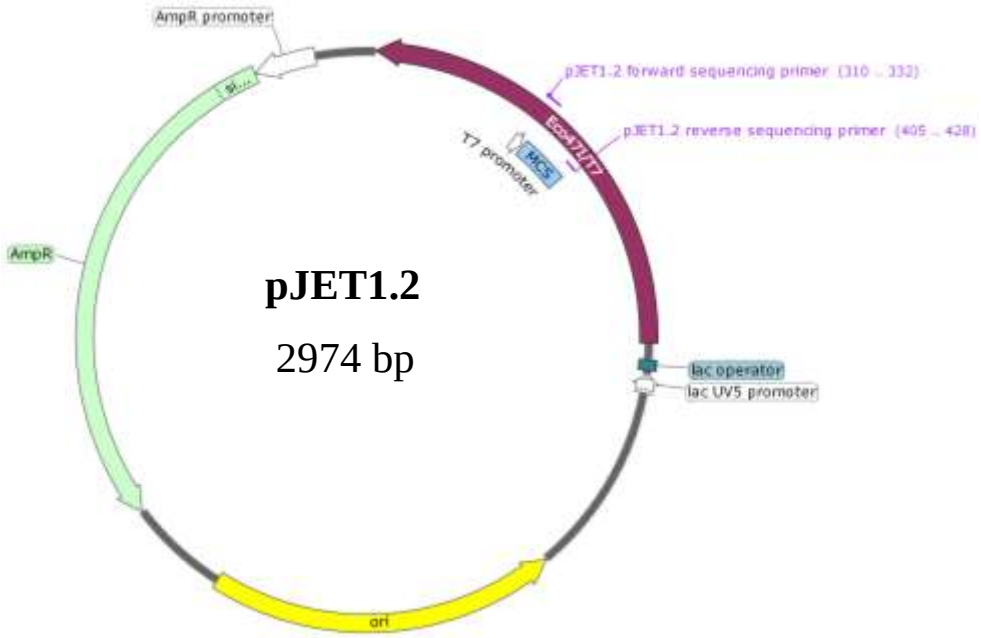

Figure 14. pJET1.2/blunt cloning vector.

2.2.3.6.2 Transformation into *E. coli* DH5α

Competent cells were prepared in our lab according to the modified method "calcium chloride method" (Cohen et al. 1972; Dagert and Ehrlich 1979; Mandel and Higa 1970). The competent cells were stored at -80°C as 50 µl aliquots. This treatment enhances the attachment of plasmid DNA to the bacterial membrane. Competent cells (50 µl) were mixed with the ligated product after stirring with a pipet tip. The mixture was incubated at 4°C for 20 min, then transferred to a water bath at 42°C for 45 s followed by immediate incubation on ice for 5 min. SOC medium (250 µl) was added to the mix and shaken up at 37°C for one hour, to increase the efficiency of transformation. Then 200 µl was spread on LB-agar plates containing ampicillin (100 mg/ml), high yield of plasmid was produced during overnight incubation at 37°C.

2.2.3.6.3 Isolation of plasmid DNA by alkaline hydrolysis (miniprep)

This method was developed by Birnboim and Doly (1979).

A single colony of the transformed *E. coli*-DH5α was inoculated into 5 ml liquid LB medium containing an appropriate concentration of ampicillin (100 mg/ml) and grown overnight at 37°C. The next day, 4 ml from the cultures were centrifuged at 5000 rpm for 5 min. The accumulated pellets were resuspended in buffer I (300 µl) (2.1.6.3) containing 3 µl RNase A. Buffer II (300 µl) (2.1.6.3) was added and the bacterial suspension was mixed by inverting cautiously 6 times and incubated at room temperature for 5 min. Denaturation of large chromosomal DNA and lysis of cell wall took place. Ice-cooled buffer III (300 µl) (2.1.6.3) was added to precipitate the proteins and to denature large chromosomal DNA, gentle mixing by inversion upside-down 6 times and incubation on ice for 15 min. To exclude the denaturated proteins, centrifugation at maximum speed for 15 min was done. The clean supernatant ~ 800

µl containing the DNA solution was transferred to a new Eppendorf tube. 800 µl chloroform were added to extract the residual contaminants and hydrolyzed protein, vortexed and then centrifugated at 13000 rpm for 15 min. The aqueous layer was transferred to a new Eppendorf tube. Isopropanol (0.7 volume of the aqueous layer volume) was added, mixed carefully 6 times and followed by centrifugation at 13000 rpm for 30 min to precipitate plasmid DNA. For washing the pellet, 500 µl 70 % ethanol was added and centrifuged at 13000 rpm for 10 min, then the sample was dried in an oven for 15 min or by speed vacuum. The sample was dissolved in 50 µl PCR water and can be directly used after measuring the concentration or stored at -20 °C.

Restriction analysis

Plasmid DNA obtained from mini preparations was digested with an appropriate restriction enzyme at the optimal condition suggested by the manufacturer. The choice of that enzyme depends on the knowledge of restriction sites within the DNA sequence of interest and the vector used for cloning.

2.2.3.6.4 Cloning of CeBPS into expression vector (pRSETB)

For heterologous expression of the target gene, the amplified PCR product (ORF) should be inserted into an expression vector (plasmid), which can later be transferred to the host bacterium *E. coli* BL21 lys s. To achieve this, both vector and PCR product were digested with endonuclease(s) to produce either sticky or blunt ends. These complementary ends are then ligated. The target gene sequence should not include recognition sites, therefore used endonucleases to digest the site including in the vector. In our case, the overexpression vector was pRSETB (Invitrogen). The ORF of CeBPS was amplified with Phusion Hot start II and overexpression primers (2.1.7.5). The PCR product were digested with *Nhe* I and *Kpn* I and then ligated with the digested dephosphorylated vector. Double digestion has a recommendation and the ratio between two endonucleases can be determined from the website http://www.thermoscientificbio.com/webtools/doubledigest/.

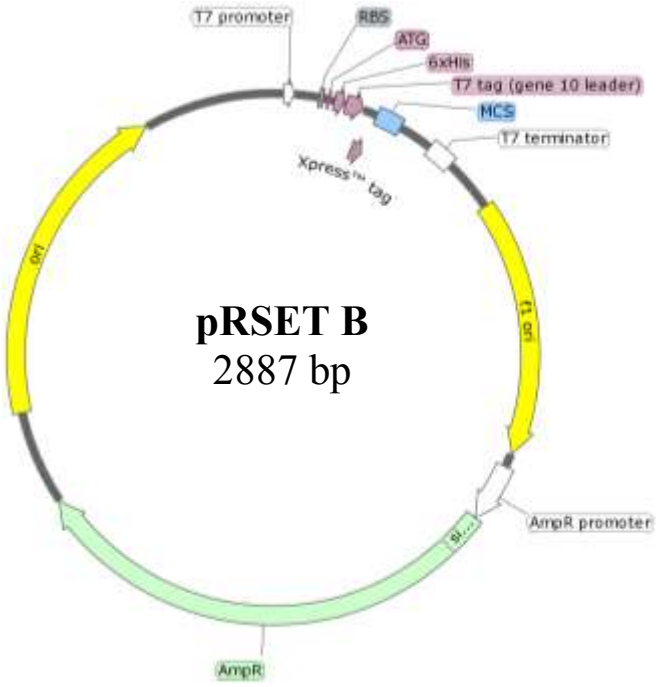

Figure 15. pRSETB cloning vector

2.2.3.6.5 Standard restriction reaction

The restriction reaction was as follows.

Component	**Insert**	**Vector**
Template (DNA)	20 µl (direct after gel extraction)	1 µl
Nhe I (endonuclease)	2 µl	2 µl
Kpn I (endonuclease)	1 µl	1 µl
10x buffer *Kpn* I	4 µl	2 µl
Water to	40 µl	20 µl

The mixture (vector and insert) were incubated at 37°C for 3h, while plasmid digestion was incubated for 1 h at 37°C. Digestion products were subjected to purification using a kit (2.2.3.1.3) to exclude all the undesirable materials that may affect in the next steps.

2.2.3.6.6 Dephosphorylation of the digested vectors

The digested vector was dephosphorylated with Thermosensitive Alkaline Phosphatase (Fast AP), to prevent self-ligation of the vector during the ligation step. That recommended to remove 5` phosphate group before ligation. The composition of the dephosphorylation reaction was as follows.

Component	**Volume**
Digested vector	17 µl
10x reaction buffer	2 µl
Fast AP enzyme	1 µl

The mixture reaction was incubated for 15 min at 37 °C, then the enzyme was inactivated by 75°C for 5 min. The product was subjected to purification by a kit (2.2.3.1.3) to get a pure vector.

2.2.3.6.7 Ligation of DNA fragments

To construct a recombinant plasmid is connecting the insert (digested insert) with compatible vector backbone (dephosphorylated digested vector). T4 ligase enzyme which more specificity to form a phosphodiester bond between 3` -hydroxy of one DNA molecule with 5` -phosphate of the other, which permanently join the nucleotides together. The constituents of the mixture were as follows:

Component	Volume
Digested dephosphorylated vector	1 µl
Digested insert	7.5 µl
T_4 ligase	0.5 µl
10x buffer	1 µl

A negative control reaction was prepared parallel, which contains all the components except the insert. The components were incubated at 16°C for 3h, then incubated at 4°C overnight.

2.2.3.6.8 Heterologous expression of recombinant protein

An *E. coli* BL21 Lys s colony containing the desired heterologous gene was used for expression of protein. This strain suitable for expression and production of protein at a high level. The transformation was done as mentioned in the transformation of plasmid into *E. coli* DH5α (2.2.3.6.2) except, the heat shock time was 20 sec, and addition of chloramphenicol (30 mg/ml) to the selection medium. After grown the transformed bacteria on agar plate overnight, on the following day, one colony inoculated into 50 ml LB medium containing ampicillin and chloramphenicol (2.1.5) at 200 rpm by 37°C in the shaker overnight. On the following day, 25 ml from the grown culture transferred to 400 ml LB medium at the same condition of growth. The cultures were grown by 37°C until OD600 of 0.6-0.8 was reached. Then 0.1 mM IPTG was added to bacterial suspension. The flasks were incubated at 23°C in the shaker for 4 hours. Then the cells (pellet) were harvested in a suitable tube by centrifugation at 5000 rpm at 4°C for 15 min and stored at -20°C for subsequent uses.

2.2.3.6.9 Conservation of bacteria containing a target gene

Bacterial culture was taken and mixed with the stock solution (40% LB medium and 60% glycerol) vortexed and stored at - 80°C for long-term using. The bacterial culture was collected when it reached to OD 600, and before adding IPTG as mentioned above. Carefully, the culture was used at -80°C. Sterile pipet was used to take a very little on top of the pippet and spread directly on an LB agar plate containing the appropriate antibiotics as mentioned above.

2.2.3.6.10 Extraction of the expressed protein

Heterologously expressed protein was extracted from *E. coli* cells to determine its biochemical activity. The frozen cells (pellet) from 400 ml cultures were resuspended in lysis buffer, pH 8 at 4°C. Mechanical disruption of the cell membrane (sonication) is a common method to

degrading the cell wall and segregating the soluble protein. The cell wall was disrupted by sonifier for 5 min at duty cycle 40% and output control of 1.5. Cell debris was separated by centrifugation at 13000 rpm for 10 min. The supernatant was mixed with Ni-NTA agarose beads (200 µl) and rotated for 1 h at 4°C to allow the whole protein to bind with Ni ions. The mixture was loaded into a column then started for washing undesirable protein by adding 4-5 times 1 ml washing buffer (2.1.6.3). The His_6-tagged-fusion protein (target protein) was eluted using 3.5 ml elution buffer (2.1.6.3) containing a high concentration of imidazole.

2.2.3.6.11 SDS-PAGE (sodium dodycyl sulfate polyacrylamide gel electrophoresis)

SDS-PAGE is the most common analytical method used to separate and characterize proteins according to their molecular masses. The samples were denatured in presence of SDS buffer at 95°C for 5 min. The protein mixed with SDS (anionic detergent) that denature the structure of the protein and becomes uniformly coated with negative charges from SDS in the buffer. To ensure the samples were sunk down in the pocket of the SDS-PAGE, glycerol was added to the mixture, whereas bromophenol blue was added to help in tracing the development of the gel. When samples are loaded on the SDS-PAGE gel, proteins migrate through the two zones; namely, stacking zone gel and resolving zone gel and start for separation depending on the difference of molecular mass (Laemmli 1970). The lower molecular mass will be faster than the larger molecular mass proteins. Bisacrylamide interconnects the polymer chains of acrylamide. The concentration of acrylamide and bisacrylamide in the separating gel was 12%, which enhance the highest resolution of proteins between 10 and 200 kDa. Some factors are affected in the properties of gel. Firstly, lower stability, elasticity and faster gelation were the results of high concentrations of APS (ammonium peroxydisulfate) and TEMED, (N,N,N′,N′-tetramethylethylenediamine). Secondly, the temperature will effect on the gel stability, whereas at low temperature the gel becomes more turbid, porous and inelastic. The optimum temperature is 23-25°C. Lastly, the pH of the buffer should be neutral and time of the gel preparing should be limited in 20-30 min. Samples are loaded on the gel and run at 200 v, parallel with the samples 10-170 KDa protein marker was loaded to detect the actual mass of our target protein. The run time ends when the dye bromophenol blue reaches the front of the gel. The gel transferred to stain by Coomassie blue solution under gentle shaking for 30 min and then distained by immersing in distaining solution overnight.

2.2.3.6.12 DNA sequencing

The samples for sequencing were sent to Source Bio Science, Germany, as per their instructions.

2.2.3.6.13 Computer-assisted sequence analysis

DNA sequences were analyzed using programs such as:

Program	**Purpose**
Lasergene-DNA star 7.0 Include: MegAlign, EditSeq, SeqMan, SeqBuilder	The software was used for different purposes, such as analyzing DNA, protein sequences, generating pairwise, multiple sequence alignments of DNA. It was used in alignment of different sequences of proteins, which was helpful when calculating the percent of identity between each other. The program helps select the suitable region for primer design. It also supports editing protein and nucleotide sequences as well as assembling contigs from individual overlapping sequences.
➢ Basic Local Alignment Search Tool (BLAST) **http://blast.ncbi.nlm.nih.gov/**	blastn: Search a nucleotide database using a nucleotide query. blastp: Search protein database using a protein query. blastx: Search protein database using a translated nucleotide query in all possible frames. tblastn: Search translated nucleotide database using a protein query.
➢ ExPASy translate tool **https://web.expasy.org/translate/**	Translation of DNA sequences in all 6 forward and reverse frames.
➢ Primer 3.0 **http://primer3.ut.ee/**	Verifying the properties of the designed RT-PCR primers.

3 Results

3.1 Cloning of benzophenone synthase from *Centaurium erythraea* and *Swertia chirata*

3.1.1 Benzophenone synthase activity in crude protein extract of *Centaurium erythraea*

Cell suspension cultures of *C. erythraea* were treated on the 5th day after transfer into new medium with methyl jasmonate (MeJ, 100 µM) and yeast extract (YE, 3g/l). At different time points (9, 12, 15 h), the harvested cells were used to extract crude protein (2.2.1.3.1). The Bradford method was used to measure the protein concentration, followed by measuring the benzophenone synthase (BPS) activity of the crude protein. Benzoyl-CoA (13.7 µM) was used as a starter substrate together with the extender molecule malonyl-CoA (37.5 µM) for incubation at 37 °C for 30 min. The enzymatic product was analyzed by HPLC using gradient 1 (2.2.2.1). The enzymatic product was 2,4,6-trihydroxybenzophenone (2,4,6-THB), as confirmed by comparing its UV spectrum and retention time with those of an authentic reference compound (Fig. 16). When heat-denatured protein was used, no product was detected.

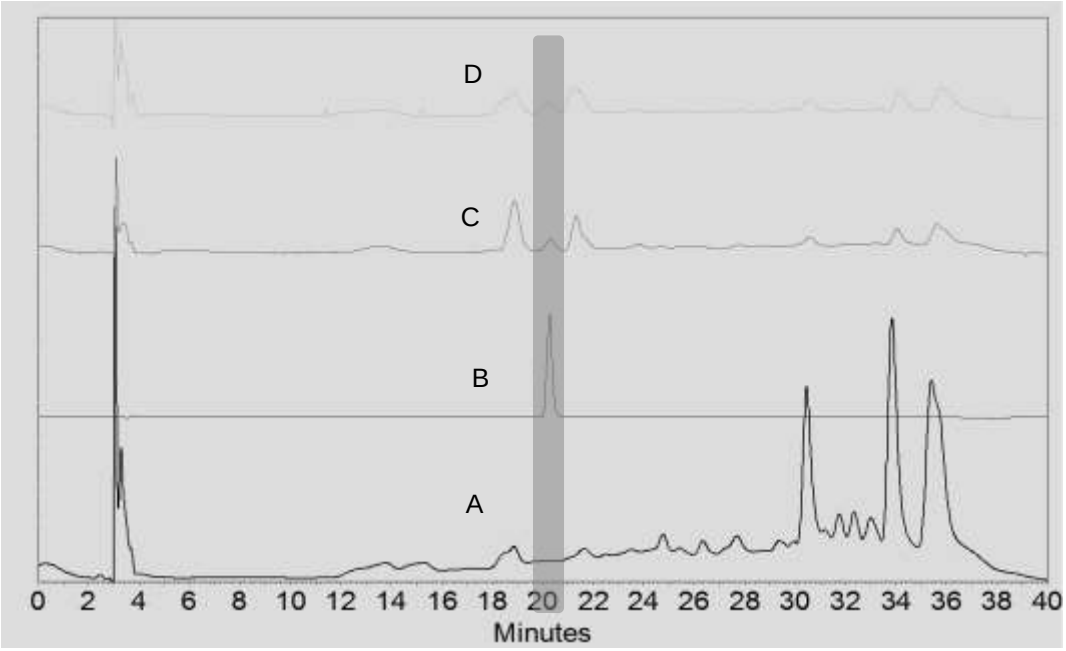

Figure 16. HPLC analysis of assays containing crude protein extract from cell cultures of *C. erythraea*. A) Control assay containing boiled protein, B) reference compound 2,4,6-THB, C) post-MeJ induction, D) post-YE induction.

Before collecting samples for molecular investigations, it is important to determine BPS activity after elicitation. Based on these analytical results, samples for further steps can be accurately collected. Elicitation was carried out as mentioned above and cells were harvested, followed by extraction of crude protein and determination of the BPS activity. The activity of

BPS can be detected starting from 9 h after elicitation with both yeast extract and methyl jasmonate (Fig. 17).

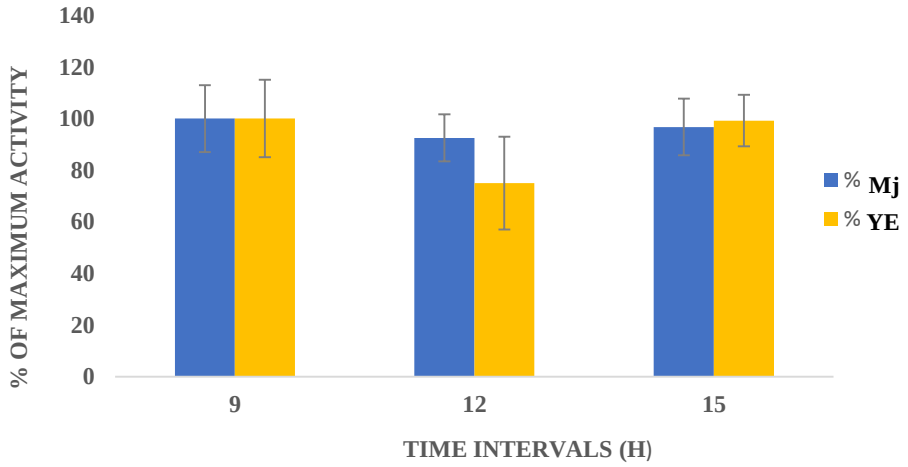

Figure 17. Benzophenone synthase activity in crude protein extract post-induction with methyl jasmonate and yeast extract. Data are means of two replicates.

3.1.2 Cloning of full-length benzophenone synthase cDNA (CeBPS) from cell suspension cultures of *Centaurium erythraea*

3.1.2.1 Isolation of total RNA

Five-day old cultured cells were treated with yeast extract (YE) and methyl jasmonate (MeJ). Total RNA was isolated from freshly harvested cells or frozen cells (150 mg) after 6h and 9h as described (2.2.3.1.1). Two µg of mRNA was used to synthesize cDNA, which was employed as a template to amplify the CeBPS sequence. 3´ -RACE cDNA was synthesized and used in the subsequent PCR reactions.

3.1.2.2 Amplification of 3´ cDNA

3.1.2.2.1 cDNA quality control

To check the quality of the synthesized 3` cDNA, gene-specific primers for the *C. erythraea 18S rRNA* gene were used to perform a standard PCR. A 300 bp band was amplified from both the cDNAs post-induction with MeJ and YE (Fig. 18 A). At the same time, phenylpyrone synthase CePPS (cloned in our lab) was also used as a control and amplified (1200 bp) from both newly synthesized cDNA pools by using two primers available in the lab (2.1.7.5) (Fig. 18 B). The results indicated that the syntheses of cDNA were successful.

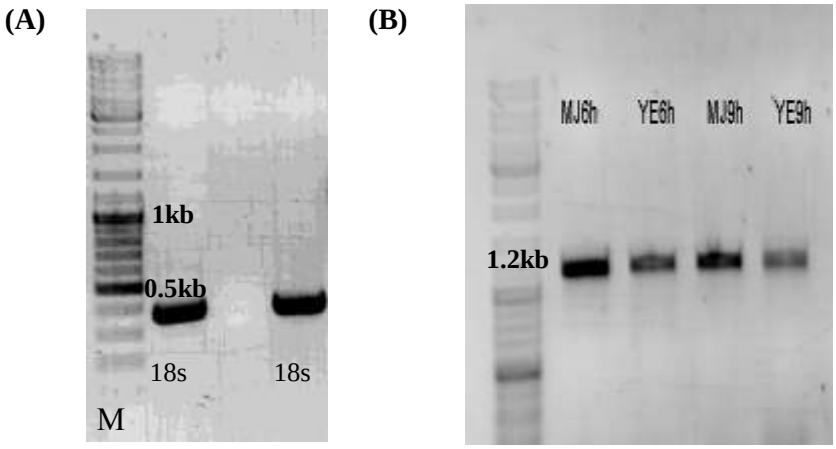

Figure 18. A) Quality control of cDNA template B) PCR amplification of full-length *C. erythraea* phenylpyrone synthase CePPS after MeJ and YE treatment.

3.1.2.2.2 Designing degenerate primers

Degenerate primers were designed to single out a core fragment of type III PKS, according to the conserved regions of amino acid sequences available in NCBI comprising BPSs and CHSs from different plants. Moreover, the sequences were aligned using the MegAlign software of DNA Star. The forward primer (PKSdpF1) and the reverse primer (PKSdpR1) were designed according to the guidance of research scholars at IIT Kharagpur, Chiranjit Mukherjee and Utkarsh Moon (Agarwal 2013).

3.1.2.2.3 First fragment of CeBPS amplification

For PCR amplification of the core fragment of CeBPS, we used a degenerate forward primer with RACE long in the first and second PCR amplifications to direct fishing of the 3′ end. After extraction, bands resulted in lanes 2, 3, and 4 (Fig. 19). The fragments were cloned into the pJET1.2 vector (2.2.3.6.1) and sent for sequencing. After analysis, band number 4 showed the most interesting sequence, because it exhibited the highest percent identity with *Swertia chirata* BPS (ScBPS), which has been cloned recently in the host laboratory.

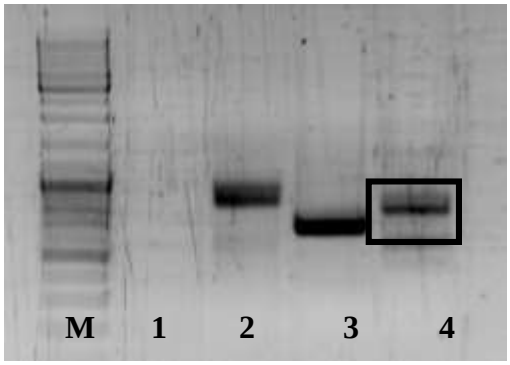

Figure 19. PCR amplification of a PKS gene from 3´ CDS cDNA of cell suspension cultures of *C. erthraea*: Lanes **1** and **2,** first amplification product; Lane **3** and **4,** second amplification product. In **1** and **3**, PKS degenerate forward primer and PKS degenerate reverse primer were used, giving a ~ 663 bp size. In **2** and **4**, the PKS degenerate forward and RACE long primers were used.

The DNA sequence was analyzed, using the Lasergene software (Fig. 20). A stop codon TAG (red highlight), poly A tail (blue highlight), and 3´ UTR (yellow highlight) were marked. For further procedures, two reverse primers (**pink GSPR1** and **dark brown-GSPR2**) were designed, as documented in the following figure.

TACCAGCAGGGTTGTTTCGCCGGTGGAACGGTCATCCGTGTAGCCAAGGACAT
CGCCGAGAACAACAAAGGTGCTCGTGTCCTTATCGCGTGCTCGGAAATCACTG
C**CATCTTTTTCCGAGGCCCCAAT**GAGGACTACATTGATG**GTCTTGTCGGACAA**
GCTTTGTTTGGGGATGGGTCCGCAGCAATGATCATTGGTGCGGATCCCATTCC
CCAAGTGGAAAAGCCACTATTTGAGCTGGTTTCTGCAGCTCAAACAGTTGTCC
CCGATAGTCATGGGGCTATCAAGGGACTTGTCCGCGAGACAGGGCTTGTCCTG
CATCTACACAAGGACATTCCCGGCCTTATCGCCAAGAACATAGACTCATGCTT
GGAGGAGGCTTTCGAACCACTTGGAATCTCTGATTGGAACTCGATTTTCTGGG
CCGTACACCCTGGTGGCACCGCGATTCTGGACCAACTGGAAAAGAAATTTTCT
CTAGACACCGCGAGGCTACGTGCTACAAGACACGTCCTAAGCGAGTATGGAAA
CATGTCAAGTGTATGTGTGTTTTTCATACTGGATGAGATACGAAAGTCGTCGG
TAAAGAAGCAACACAAGACCACCGGAGAAGGGCTGGAATGGGGAGTGCTGTTT
GGGCTTGGACCAGGGATCACTGTTGAGACTGTGGTTCTGCGTAGCGTCTCCAT
T**TAG**GAAGATGCTTATATGATTGTTCTACAGTTTTATT**AAAAAA**

Figure 20. Analysis of the newly cloned *C. erythraea* BPS 3'end.

The first comparison was with PKSs cloned in our lab from Gentianaceae (*Centaurium erythraea* PPS, *Swertia chirata* BPS, *Gentiana lutea* CHS). The analysis showed a maximum of 82.7% identity with ScBPS.

Percent Identity

	1	2	3	4	5	6	7	8	9	10		
1		71.0	79.2	78.4	77.6	77.6	70.4	83.3	71.0	70.0	1	ScPKS1.pro
2	36.7		67.6	66.8	66.1	65.8	66.6	69.4	69.2	82.7	2	ScPKS2.pro
3	24.4	42.3		99.0	93.6	93.8	69.2	76.6	67.9	66.1	3	CeBPSVI old.pro
4	25.5	43.6	1.0		92.8	93.3	68.9	75.1	67.1	65.2	4	CePPS.pro
5	26.6	45.0	6.7	7.6		93.3	68.6	75.6	67.6	66.1	5	Cs1.pro
6	26.6	45.5	6.4	7.0	7.0		68.6	76.6	67.6	66.1	6	Cs2.pro
7	37.6	44.1	39.6	40.1	40.6	40.6		68.9	78.0	71.7	7	Asya fr.1.pro
8	19.0	39.3	28.2	30.3	29.6	28.2	40.1		68.9	67.9	8	Asya Fr.2.pro
9	36.7	39.7	41.9	43.2	42.3	42.3	26.1	40.1		70.4	9	GlCHS.pro
10	38.3	19.7	45.0	46.5	45.0	45.0	35.5	41.7	37.6		10	3' frag.pro
	1	2	3	4	5	6	7	8	9	10		

Figure 21. Identity of the CeBPS 3'end with lab-internal Gentianaceae sequences.

Analysis by NCBI BLAST of the 3′ fragment with amino acid sequences available in the data bank showed a maximum of 74%, which was with a *CHS* gene.

RecName: Full=Naringenin-chalcone synthase

Sequence ID: Q8RVK9.1 Length: 389 Number of Matches: 1

▶See 1 more title(s)

Range 1: 160 to 389 GenPept Graphics ▼ Next Match ▲ Previous Match

Score	Expect	Method	Identities	Positives	Gaps	Frame
368 bits(945)	4e-125	Compositional matrix adjust.	170/230(74%)	199/230(86%)	0/230(0%)	+1

```
Query  1    YQQGCFAGGTVIRVAKDIAENNKGARVLIACSEITAIFFRGPNEDYIDGLVGQALFGDGS  180
            YQQGCFAGGTV+R+AKD+AENNKGARVL+ CSEITA+ FRGPN+ ++D LVGQALFGDGS
Sbjct  160  YQQGCFAGGTVLRLAKDLAENNKGARVLVVCSEITAVTFRGPNDTHLDSLVGQALFGDGS  219

Query  181  AAMIIGADPIPQVEKPLFELVSAAQTVVPDSHGAIKGLVRETGLVLHLHKDIPGLIAKNI  360
            AA+I+G+DPIP+VEKP+FELVSAAQT++PDS GAI G +RE GL  HL KD+PGLI+KNI
Sbjct  220  AALIVGSDPIPEVEKPIFELVSAAQTILPDSDGAIDGHLREVGLTFHLLKDVPGLISKNI  279

Query  361  DSCLEEAFEPLGISDWNSIFWAVHPGGTAILDQLEKKFSLDTARLRATRHVLSEYGNMSS  540
            + L EAF+PLGISDWNS+FW  HPGG AILDQ+E K +L T +LRATRHVLSEYGNMSS
Sbjct  280  EKSLNEAFKPLGISDWNSLFWIAHPGGPAILDQVESKLALKTEKLRATRHVLSEYGNMSS  339

Query  541  VCVFFILDEIRKSSVKKQHKTTGEGLEWGVLFGLGPGITVETVVLRSVSI  690
             CV FILDE+R+  V+     TTGEGLEWGVLFG GPG+TVETVVL SV+I
Sbjct  340  ACVLFILDEMRRKCVEDGLNTTGEGLEWGVLFGFGPGLTVETVVLHSVAI  389
```

Figure 22. Comparison of the CeBPS 3'end with databank entries, yielding a CHS hit.

3.1.2.2.4 PCR amplification using gene-specific primers for fishing out the 5′ end

For fishing out the 5′ end of the desired *C. erythraea* sequence, two gene-specific reverse primers were designed, based on the first fragment (marked pink and dark brown in the first fragment, Fig. 20), and named P1_4 R1 (reverse primer R1) and P1_4 R2 (reverse primer R2) (2.1.7.5).

- **Extension of the PCR core fragment in 5′ direction**

To clone the 5′ end, 5′ CDS cDNA was initially synthesized as described (2.2.3.3). For PCR amplification, we used the reverse primer R1 and RACE long in the first amplification, followed by a second amplification with reverse primer R2 and RACE short. The amplification was implemented from 5′ CDS cDNA using a terminal transferase protocol (2.2.3.3.3). The

gel obtained (Fig. 23) showed the expected band at ~700 bp. The band was extracted from the gel, cloned into a pJET1.2/blunt cloning vector (2.2.3.6.1) and sent for sequencing.

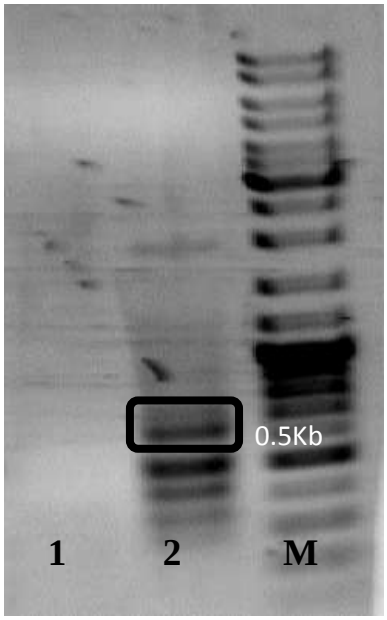

Figure 23. PCR amplification of 5´ CDS cDNA using P1_4 R1 with RACE long and P1_4 R2 with RACE short for 1st and 2nd amplification in Lane 1 and Lane 2, respectively..

- **Nucleotide sequence of the 5` end (CeBPS fragment 2)**

Blasting the sequence revealed a maximum of 75% identity with *CHS* genes. The Lasergene software was used to clean the sequence (EditSeq, SeqMan). The start codon and the nucleotide sequence of the 5´ UTR were identified. In Fig. 24, the start codon **ATG** and the **5` UTR** are highlighted.

5′ATTGGGGCCTCGGAAAAGATGAGAAGTTTTTTGGGTGTAGTGAGATTGG
AAGGTGAGGAGCTGATCGGGAGACCCCAAAGAGCCGAGGGACTGGCGGCGG
TGTTGTCCATCGGAACCGCCACGCCACCCAACTGTATCGACCAAAGCACCT
ACCCTGATGCCTACTTCAGAATCACTAATAGCGAACATATGGTTGAGCTCA
AAGAAAAATTCAAGCGCATCTGTGATAAGTCATCCATTAAGAGGCGTTACA
TGCACTTGACTGACGAGATCTTGAAAGCAAATCCGAGTATTACTGAACCTA
TGGGAGCTTCATTTGATGCTAGACAAGAAATCCTAGTAAATGAGGTCCTAA
AGCTTGCGAAACTTGCTGCTGATAAGGCAATTGATGAATGGGGTCAGCCCA
AATCTAGCATCACTCACTTGGTGTTCTGTACCTCTAGTGGTGTGGACATGC
CGGGGGCCGATTACCAGCTCGCTAGACTTCTTGGTCTTAGCCCATCTGTGA
AGCGTCTGATGTTTTACCAACAAGGTTGTTTCGCCGGTGGAACGGTCATCC
GTGTAGCCAAGGACATCGCCGAGAACAACAAAGGTGCTCGTGTCCTTATCG
CGTGCTCGGAAATCACTGCCATCTTTTTCCGAGGCCCCAAT-**3`**

Figure 24. 5` Stretch of CeBPS.

Since the 3` end and the 5` end nucleotide sequences were available (fragment 1 and 2), we used the SeqMan software to find the overlapping region, yielding contig 1. Moreover, the information obtained from the two sequences allowed to design two gene-specific primers (overexpression primers) to clone the whole sequence (ORF) of CeBPS from the start codon ATG to the stop codon TAG, as represented in the following scheme.

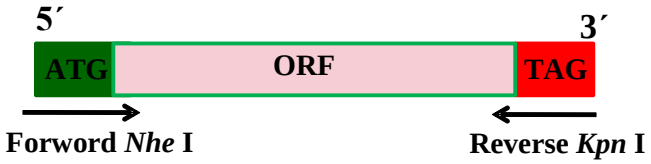

Scheme 5. Schematic representation to obtain the full-length CeBPS ORF from start codon (green highlighted) to stop codon (red highlighted) by using the two primers (overexpression primers) forward *Nhe* I and reverse *Kpn* I.

Phusion-polymerase was used to re-amplify the CeBPS ORF from reverse-transcribed mRNA of *C. erythraea* as a template in a standard PCR amplification at an annealing temperature of 56°C with two primers designed as follows. The forward primer P16_F_*Nhe* I contained a *Nhe* I restriction site directly before the start codon ATG. The reverse primer P16_R_*Kpn* I contained a *Kpn* I restriction site directly behind the stop codon TGA. The restriction sites were introduced to allow the cloning of the CeBPS ORF into the expression vector pRSETB (2.1.7.5).

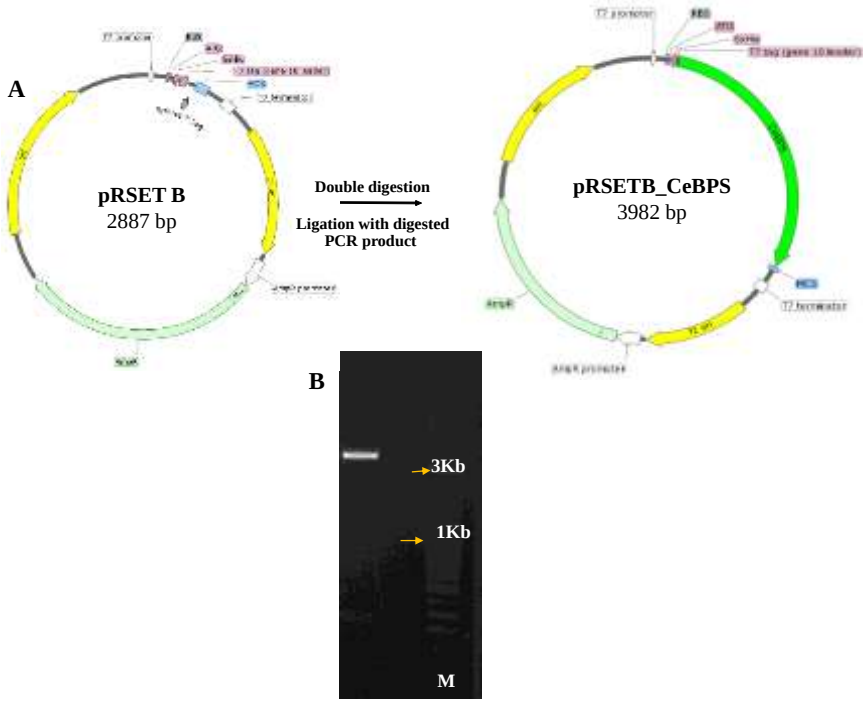

Figure 25. Construction of the expression vector for the CeBPS cDNA. A) vector maps, B) Confirmation of successful ligation and presence of the insert.

3.1.2.3 Analysis of the CeBPS amino acid sequence

The constructed plasmid was sequenced to confirm that the reading frame was continuous and lacked frame shifts and that the right insert was present. In addition, the sequence was identical to that obtained by *Taq* DNA polymerase amplification. The sequence contained the start codon ATG and the stop codon TAG and in between 1170 bp open reading frame (Appendix 7.1.1). The protein consisted of 389 amino acids and had a molecular mass of 42.3 kDa.

CeBPS was aligned with the other PKSs cloned recently in our laboratory from *C. erythraea* and *S. chirata*. The following alignment was obtained using the MegAlign software (Fig. 26). The light brown highlights are the catalytic triad in the active site pocket, which is conserved in all type III PKSs. The green highlights are amino acids of the elongation pocket and the blue highlights are those of the initiation pocket.

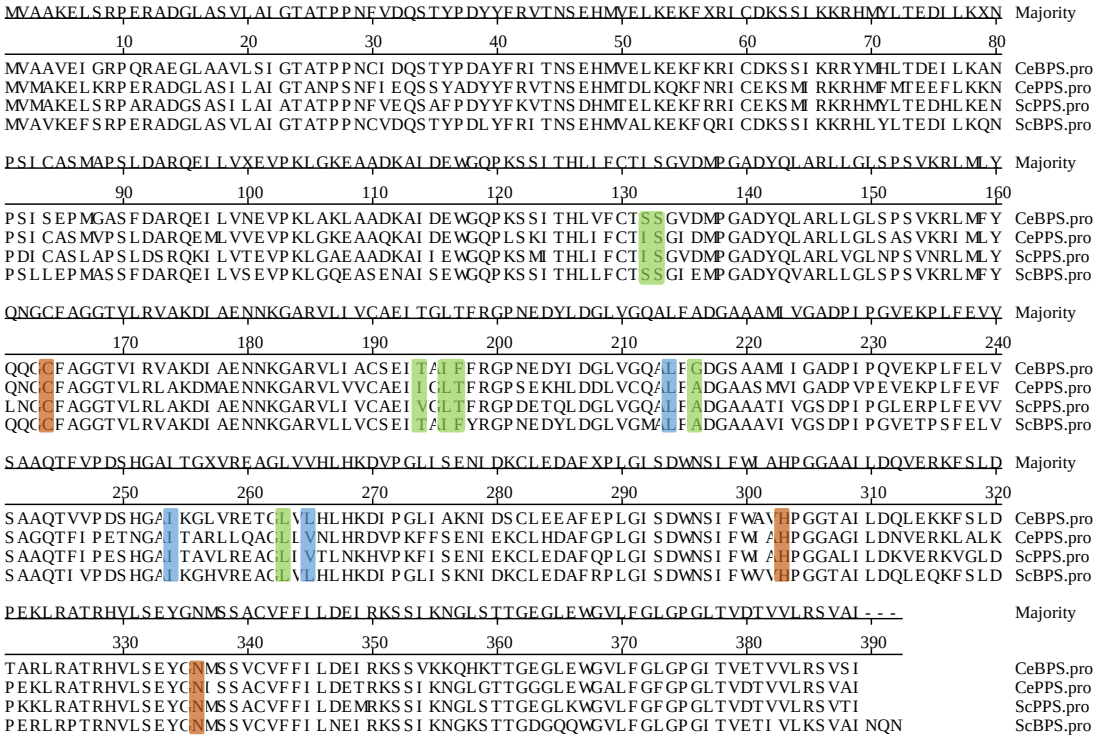

Figure 26. Amino acid sequence alignment of CeBPS with enzymes of *C. erythraea* (CePPS) and *S. chirata* (ScPPS and ScBPS). The sequences CePPS, ScBPS, and ScPPS were present in our laboratory. The brown highlights are the catalytic triad, green highlights are the elongation pocket and the blue highlights are the initiation pocket.

3.1.2.4 Expression of CeBPS in *E. coli*

IPTG was added to induce the expression of the recombinant protein. The cloned target gene was successfully expressed in the *E. coli* BL21 strain. The efficiency of the expression was detected by SDS-PAGE (Fig. 27). The expected band (pure protein sample) matched the subunit size of ~ 42.0 kDa.

.

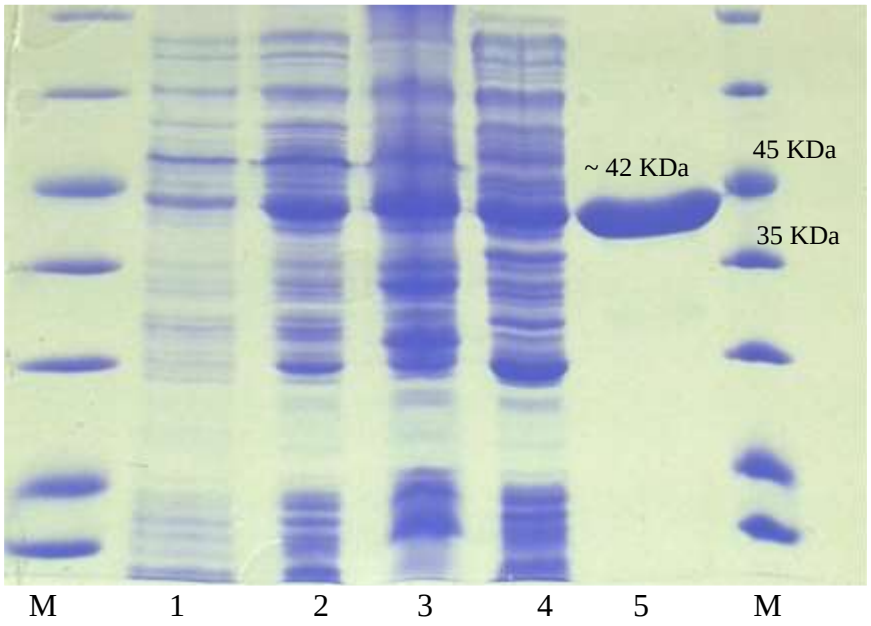

Figure 27. SDS-PAGE (12%) of fractions containing CeBPS protein after the following purification steps, 1: pre-induction. 2: post-induction. 3: pellet. 4: crude protein (supernatant). 5: pure CeBPS protein.

3.1.3 Test for enzymatic activity

3.1.3.1 *Centaurium erythraea* benzophenone synthase assay

Affinity-purified recombinant CeBPS (2 µg/assay) was incubated with the following CoA esters as starter substrates to detect activity. Malonyl-CoA (37.5 µM) was added as extender substrate.

1. Benzoyl-CoA (13.7 µM) was incubated for 10 min at 37°C. The assay was carried out as described in 2.2.1.6. The product was confirmed by HPLC analysis (2.2.2.1) using gradient 1 at 305 nm wavelength. Previously, benzophenone synthases have been cloned from *Hypericum* species and showed activity with benzoyl-CoA, the final product being 2,4,6-trihydroxybenzophenone (2,4,6-THB) after three stepwise condensations with malonyl-CoA. Similarly, CeBPS formed 2,4,6-THB as the main component, which had the same R_t as the authentic reference compound, as shown in the stacked HPLC-DAD chromatograms (Fig. 28 A). Its UV spectrum showed the characteristic absorption maxima at 305 and 259 nm, which matched those of the authentic substance (Fig. 28 B).

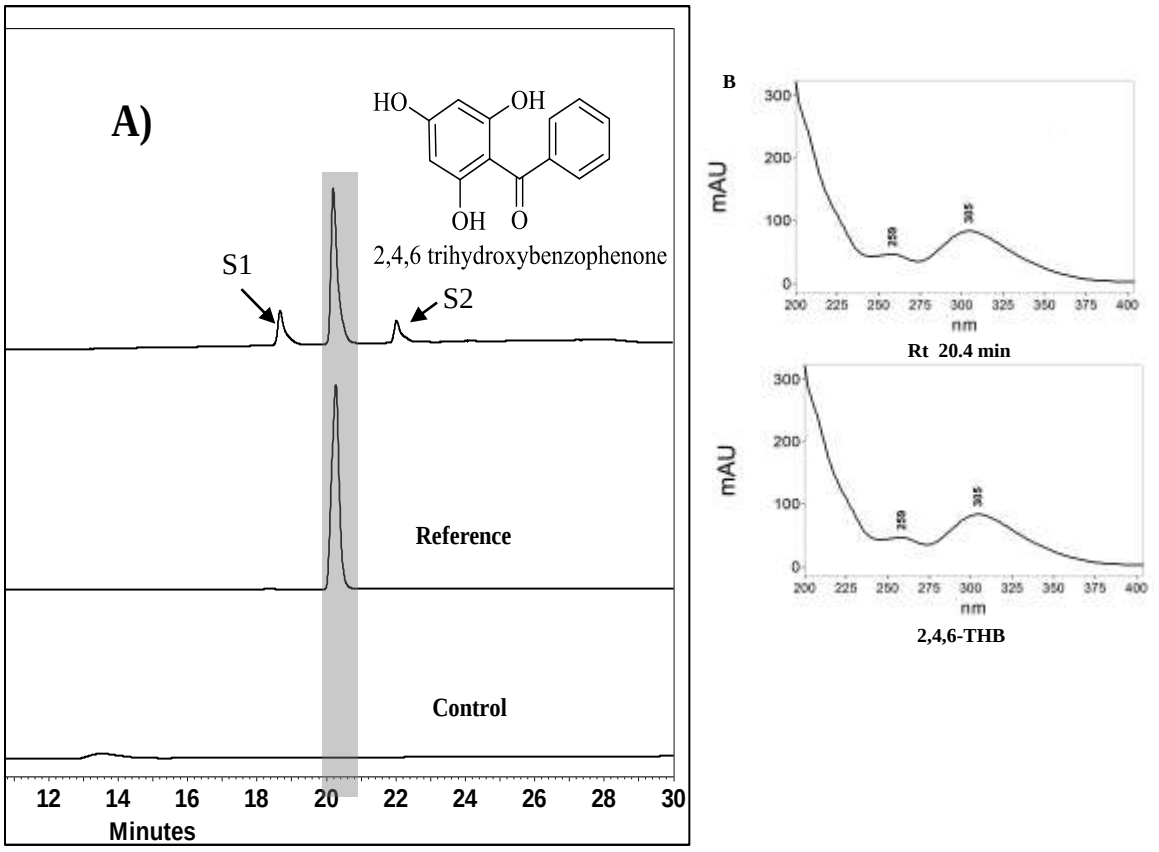

Figure 28. **A)** Stacked HPLC chromatograms of CeBPS and control assays (containing benzoyl-CoA) and the product reference. The enzymatic side products are tetraketide lactone (S1) and triketide lactone (S2). **B)** UV spectra of the enzymatic product and the authentic reference (2,4,6-THB).

2. 3-Hydroxybenzoyl-CoA (27.16 µM), 3-((3-hydroxybenzoyl)-oxy)benzoyl-CoA (11.9 µM), and 3-((3-hydroxybenzoyloxy)3-hydroxylbenzoyloxy)-benzoyl-CoA (10.3 µM) were also incubated in separate assays with malonyl-CoA as extender substrate. The two latter substrates were new and additional products upon synthesizing 3-hydroxybenzoyl-CoA (carried out by Dr. Benye Liu in our laboratory). HPLC analysis of the three chemically synthesized CoA esters and their UV spectra are documented in Appendix Fig. 72. Their LC-MS detection are presented in Appendix Fig 80, 81 and 82, as well as the ^{1}H and ^{13}C NMR data of 3-(3-hydroxybenzoyloxy)benzoyl-CoA in CD_3OD are presented in Appendix Table 5. The reactions with the three new CoA esters were accomplished as with benzoyl-CoA. At the same time samples for controls were incubated using heat-denatured enzyme. Surprisingly, all the three related CoA esters formed the same final product, which was detected as 2,3` ,4,6-tetrahydroxybenzophenone (2,3` ,4,6-THB), resulting from three stepwise condensations with malonyl-CoA. The R_t value was 16.5 min (Fig. 29 A). The UV spectra of the products had the identical characteristic absorption maxima at 305 and

259 nm, which matched those of the authentic 2,3` ,4,6-tetra-hydroxybenzophenone reference (Fig. 29 B).

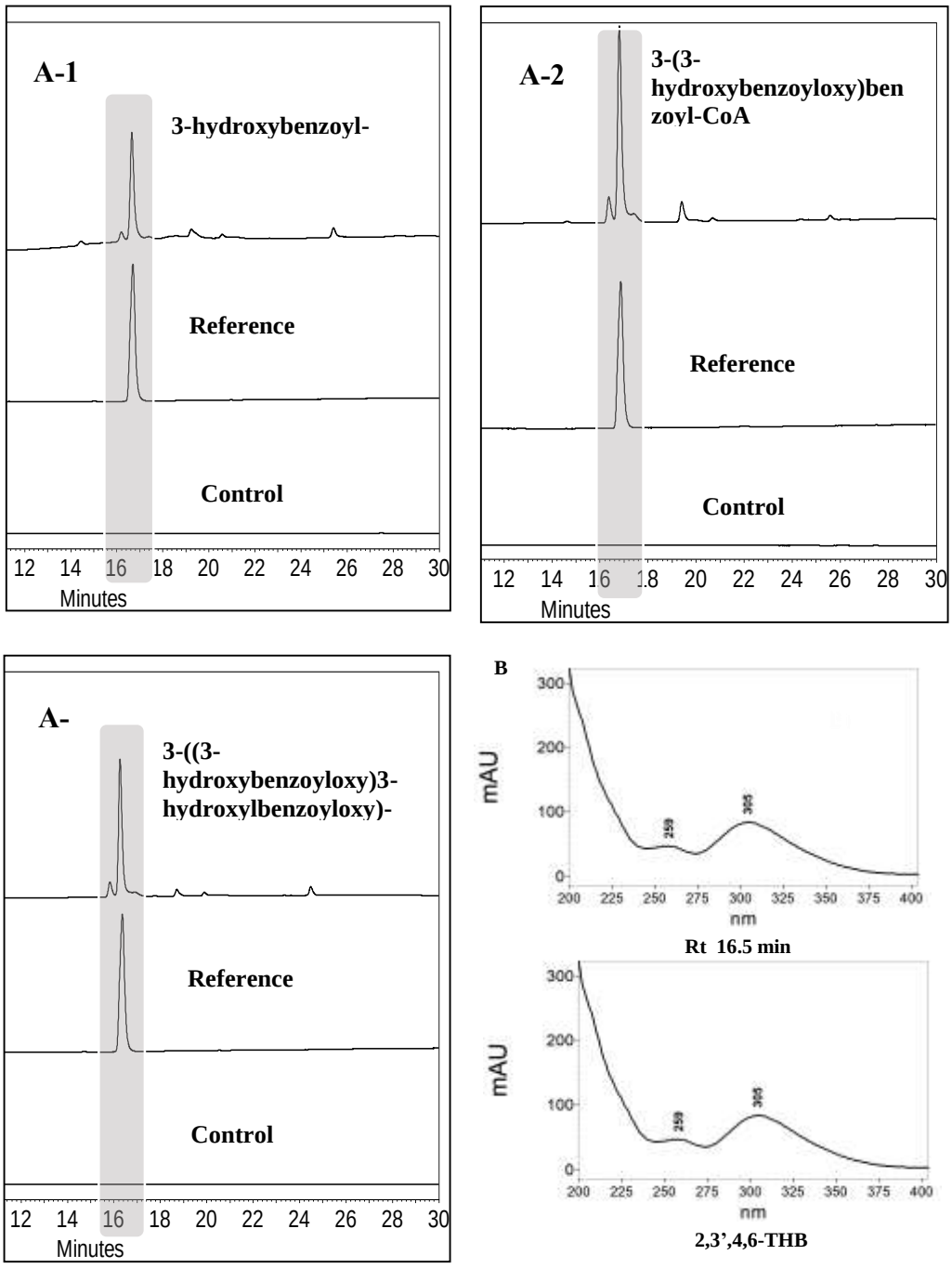

Figure 29. Stacked HPLC chromatograms of CeBPS and control assays and the product reference. The substrates were **(A-1)** 3-hydroxybenzoyl-CoA, **(A-2)** 3-((3-hydroxybenzoyl)-oxy)benzoyl-CoA, **(A-3)** 3-((3-hydroxybenzoyloxy)3-hydroxylbenzoyloxy)-benzoyl-CoA, **B)** UV spectra of the product and the authentic reference (2,3` ,4,6-THB).

3.1.3.2 *Swertia chirata* benzophenone synthase assay

Besides the newly clones CePBS, I was provided with a plasmid containing ScBPS, which was successfully cloned in our lab before (Agarwal 2013). The cDNA for ScBPS was obtained from root cultures of *S. chirata*, starting the cloning with degenerate primers derived from conserved regions of type III PKSs. The full-length cDNA encoded an ORF of 1179 bp. In this study, the activity of the purified enzyme was studied and the enzyme was characterized in parallel with CeBPS. CeBPS has 80.8 % identity with BPS from *S. chirata*.

The construct was inserted by *Nhe* I and *Kpn* I restriction sites and cloned in the pRSTB vector. To test the activity of ScBPS, purified protein (2 µg/assay) was incubated with the following starter substrates at 35°C for 10 min, with the extender substrate being malonyl-CoA at 37.5 µM.

- 3-Hydroxybenzoyl-CoA 27.16 µM, 3-((3-hydroxybenzoyl)-oxy)benzoyl-CoA 11.9 µM, and 3-((3-hydroxybenzoy)-oxy)oxybenzoyl-CoA 10.3 µM

The result was as with CeBPS. Incubation of ScBPS with the three related CoA esters 3-hydroxybenzoyl-CoA, 3-((3-hydroxybenzoyl)-oxy)benzoyl-CoA and 3-((3-hydroxybenzoyloxy)3-hydroxylbenzoyloxy)-benzoyl-CoA led to formation of the same product (2,3′,4,6-THB) at the R_t value 16.4 min, which matched with the authentic reference (Fig. 30). The product (2,3′,4,6-THB) was analysed by HPLC using gradient 1 (2.2.2.1) at 305 nm wavelength. The identical UV spectra of the products had the characteristic 2,3′,4,6-THB absorption maxima at 305 and 259 nm (Fig. 29 B). Control incubations were carried out without adding the potential starter substrate. The control incubations failed to yield any enzymatic product. The results are summarized in Fig. 31.

The UV spectra of the products had absorbance maxima at 305 and 259 nm, characteristic of 2,3′,4,6-THB (Fig. 29 B).

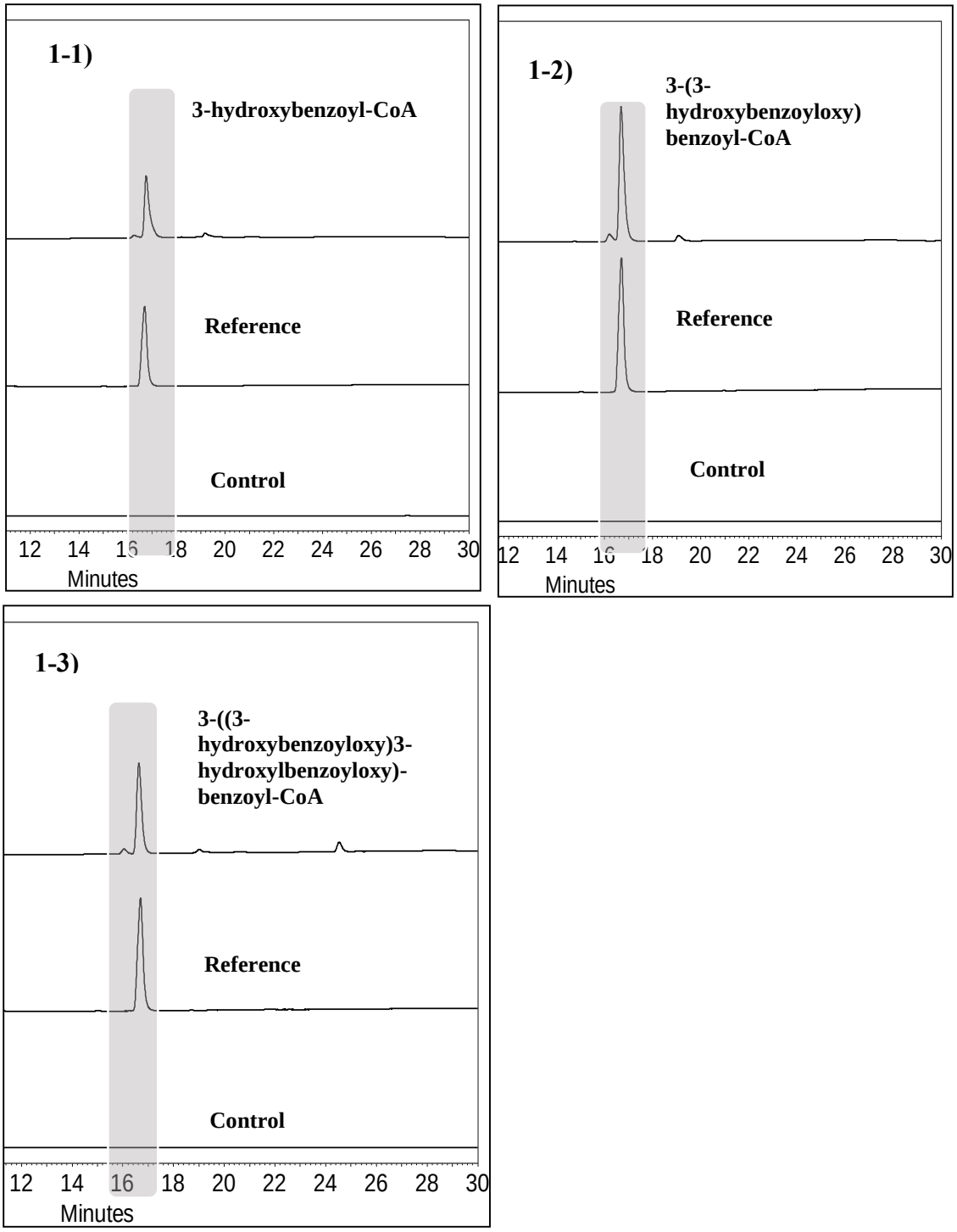

Figure 30. Stacked HPLC chromatograms of ScBPS and control assays and the product reference. The substrates were **(1-1)** 3-hydroxybenzoyl-CoA, **(1-2)** 3-((3-hydroxybenzoyl)-oxy)benzoyl-CoA, **(1-3)** 3-((3-hydroxybenzoyloxy)3-hydroxylbenzoyloxy)-benzoyl-CoA.

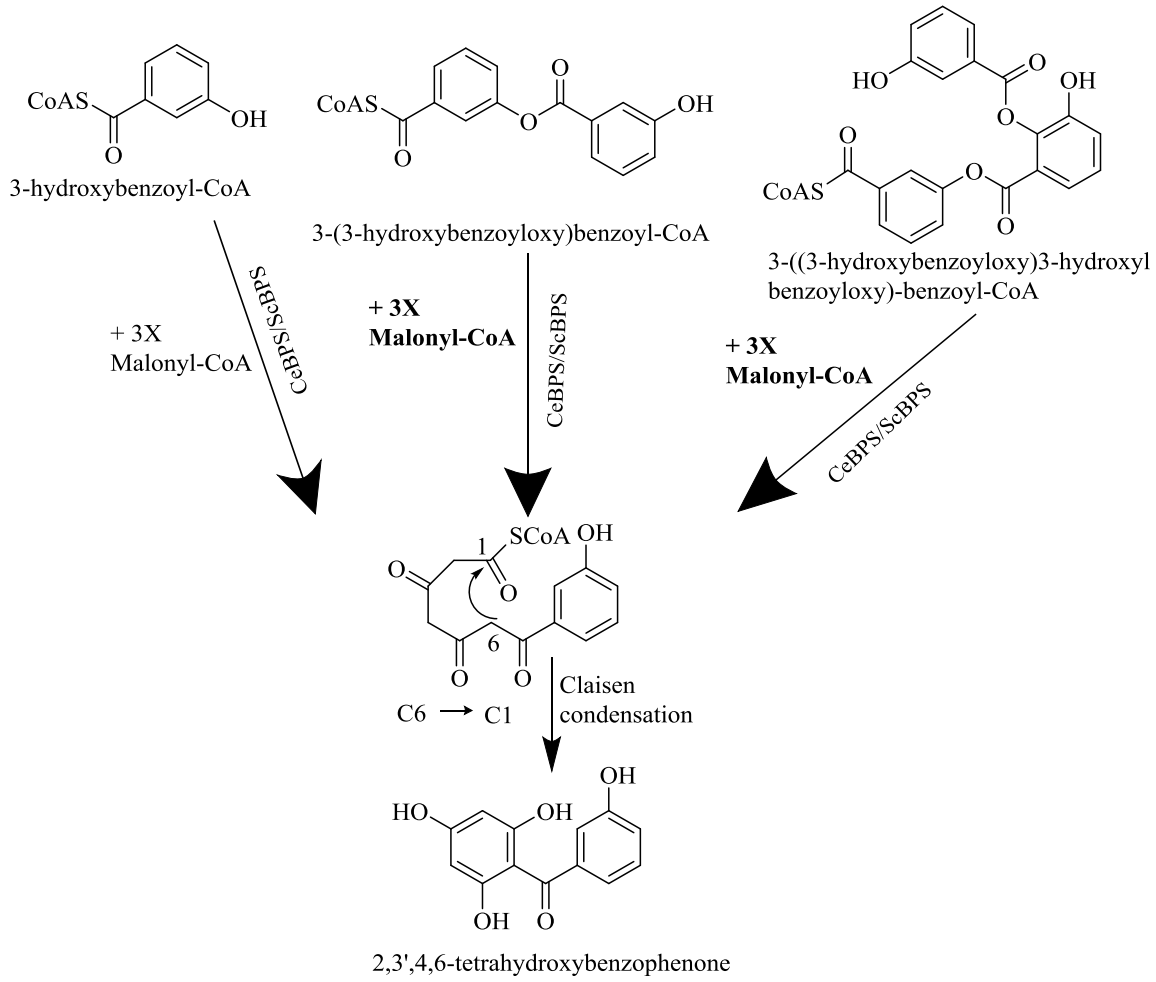

Figure 31. The three related substrates 3-hydroxybenzoyl-CoA, 3-(3-hydroxybenzoyloxy)benzoyl-CoA and 3-((3-hydroxybenzoyloxy)3-hydroxylbenzoyloxy)-benzoyl-CoA were converted by both CeBPS and ScBPS to the same product, 2,3` ,4,6-tetrahydroxybenzophenone.

ScBPS assay with benzoyl-CoA

Incubation with benzoyl-CoA resulted in the formation of a product at Rt 20.4 min. This product was identified by HPLC as 2,4,6-trihydroxybenzophenone (2,4,6-THB) (Fig. 32). Its UV spectrum showed the two characteristic absorption maxima at 305 and 259 nm, which matched those of the authentic reference (2,4,6-THB) (Fig. 28 B). Additionally formed side products were tetraketide lactone (S1) and triketide lactone (S2).

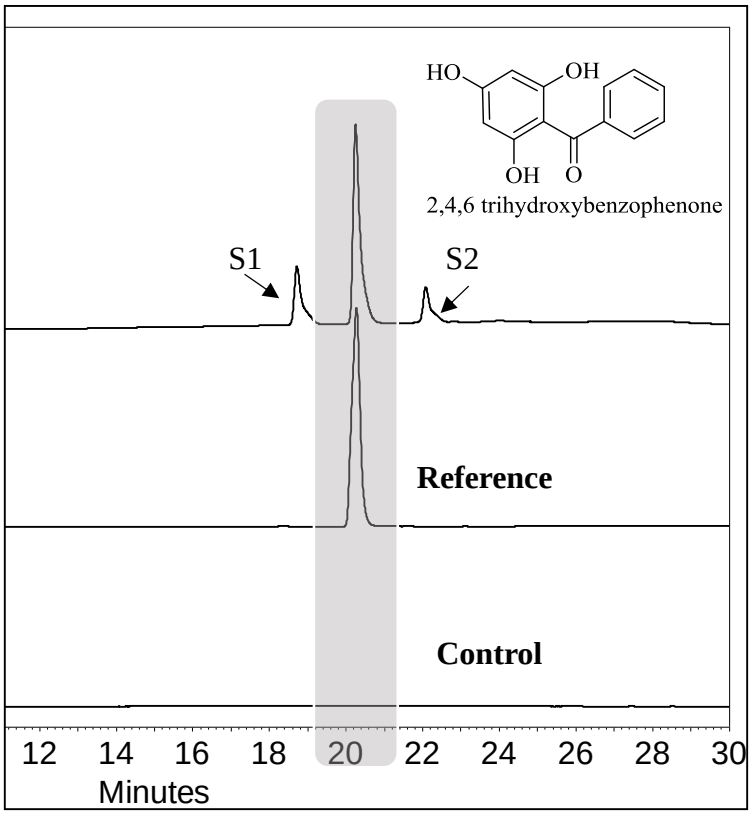

Figure 32. Stacked HPLC chromatograms of ScBPS and control assays (containing benzoyl-CoA) and the product reference.

3.1.4 Biochemical characterization of the recombinant BPSs of *Centaurium erythraea* and *Swertia chirata*

3.1.4.1 Enzyme stability

The activity of an enzyme is affected by freezing and thawing rates (Cao et al. 2003). To test at which rates the enzymes CeBPS and ScBPS conserve their activities when subjected to different storage conditions (0°C, 4°C, -20°C and -80°C), experiments were carried out as described in 2.2.1.7.1. CeBPS showed maximum activity when incubated freshly (after elution with elution buffer) with the three different CoA esters 3-(3-hydroxybenzoyloxy)benzoyl-CoA, 3-hydroxybenzoyl-CoA and benzoyl-CoA (Fig. 33). Although the activity was not expected to be affected by the various starter molecules, they were separately tested. The activity at 0°C reached around 50% of the starting activity with the three CoA esters 3-((3-hydroxybenzoyl)-oxy)benzoyl-CoA, 3-hydroxybenzoyl-CoA and benzoyl-CoA after 2 weeks (Fig. 33), however, the activity at 4°C, -20°C, and -80°C was decreased after one-day storage, then lost completely after one-week storage with the three CoA esters 3-(3-hydroxybenzoyloxy)benzoyl-CoA, 3-hydroxybenzoyl-CoA and benzoyl-CoA (Fig. 33). The conclusion was that fresh enzyme had to be used for all subsequent incubations. The activity of ScBPS was detected under the same conditions. The enzyme showed maximum activity when incubated directly after elution with elution buffer when incubated with the three

different CoA esters 3-((3-hydroxybenzoyl)-oxy)benzoyl-CoA, 3-hydroxybenzoyl-CoA and benzoyl-CoA (Fig. 34). The activity of the enzyme was significantly decreased in all storage conditions (0°C, 4°C, -20°C, and -80°C). An exception was 0°C when the activity reached 50% after one-day storage upon incubation with 3-((3-hydroxybenzoyl)-oxy)benzoyl-CoA (Fig. 34 A). As a conclusion, ScBPS had also to be used freshly after purification for all subsequent

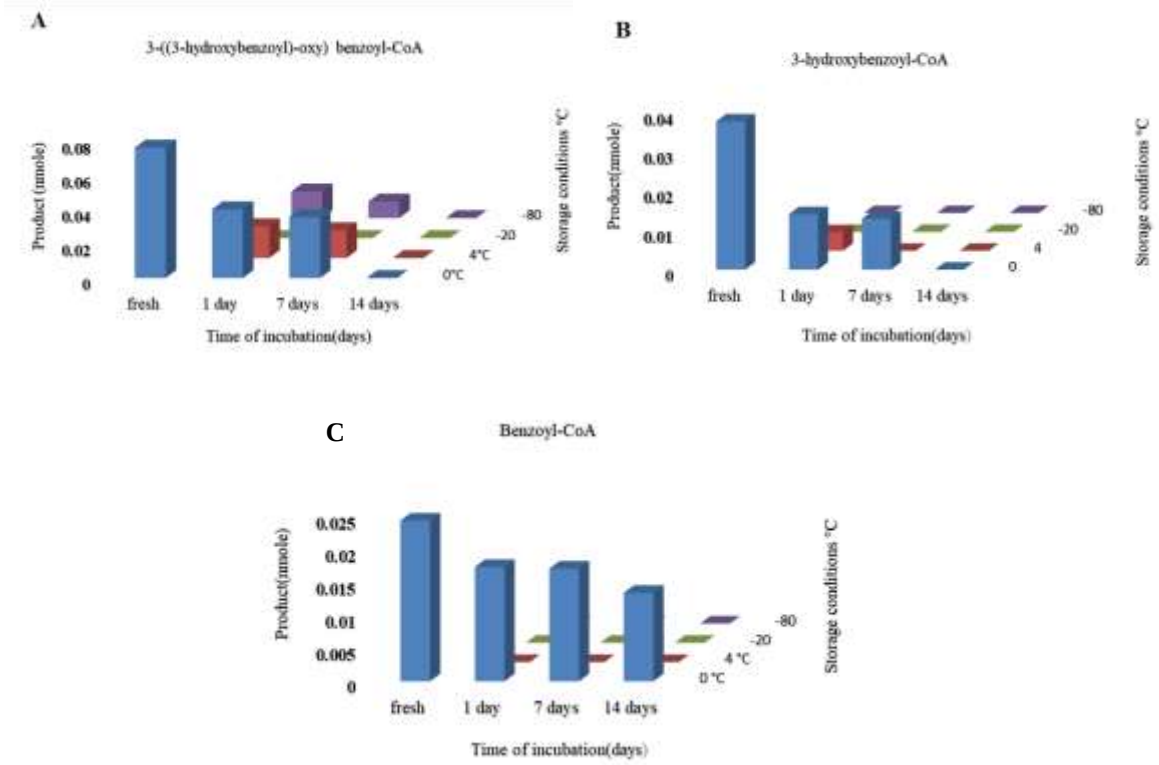

experiments.

Figure 33. Stability of CeBPS at 0, 4, -20, -80 °C, as tested with A) 3-(3-hydroxybenzoyloxy)benzoyl-CoA B) 3-hydroxybenzoyl-CoA and C) benzoyl-CoA. The three experiments can be considered as replicates.

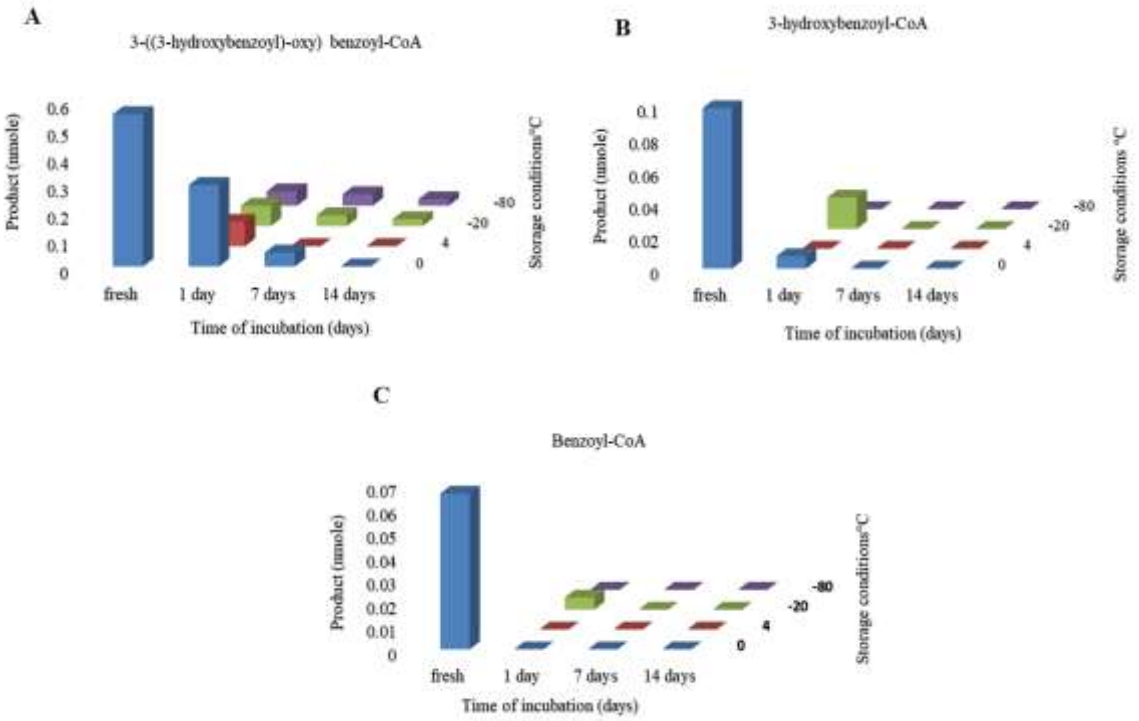

Figure 34. Stability of ScBPS at 0, 4, -20, -80 °C, as tested with A) 3-(3-hydroxybenzoyloxy)benzoyl-CoA B) 3-hydroxybenzoyl-CoA and C) benzoyl-CoA. The three experiments can be considered as replicates.

3.1.4.2 Determination of the optimum pH

The pH optimum is the point, where the enzyme has highest activity. Generally, enzymes are active and stable at different rates at varying pH values. At extreme values, denaturation and missfolding of the protein takes place, thus the pH value has a strong effect on the protein folding and activity. The dependence of CeBPS and ScBPS activity on pH was studied (Fig. 35). CeBPS and ScBPS had similar properties when compared to each other. The optimum pH for the CeBPS and ScBPS enzymes was determined to be 7 and 7 to 7.5, respectively. For subsequent characterization of both enzymes, the pH value 7 was defined.

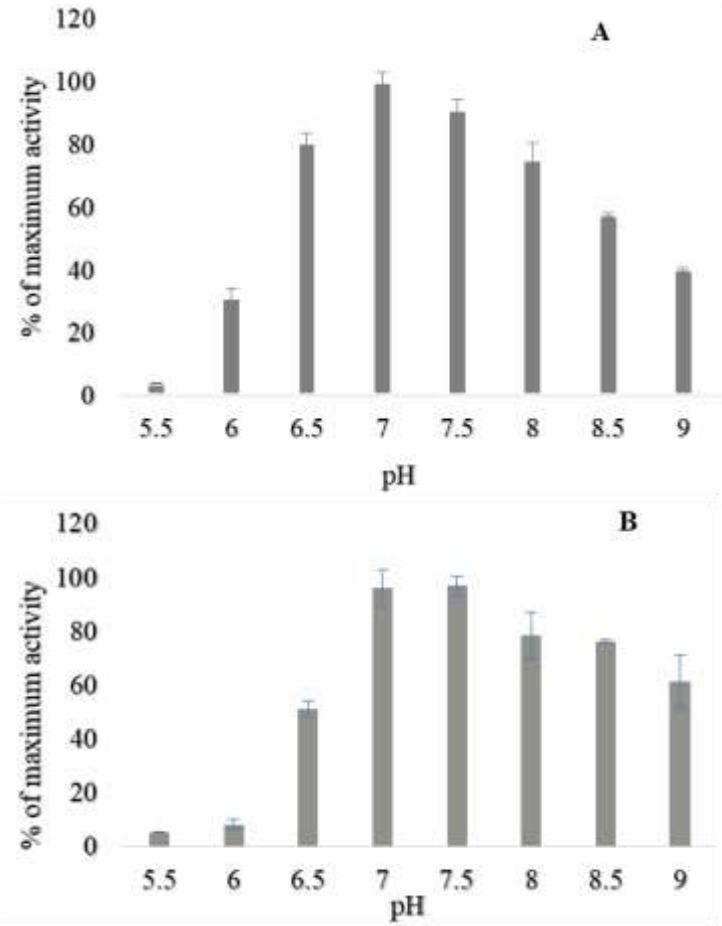

Figure 35. Effect of pH on CeBPS (A) and ScBPS activity (B). Data are means of two replicates.

3.1.4.3 Temperature optimum

Enzymes have the highest activity at a specific temperature, which is called the optimum temperature. Above and below this temperature, the activity of an enzyme decreases or is lost. The temperature is basically a critical factor for chemical reactions and the same is true for enzyme activity. At increasing temperature, molecules move faster and cause the frequency of collision to increase and enhance the activity of an enzyme until reaching the optimum. Further increasing the temperature causes more and more damage to the active sites of the proteins and their shapes. The substrates can no longer bind to the active site and the enzyme becomes inactive. When the temperature reaches higher than 60°C, most enzymes denature. Determination of the optimum temperature was carried out for both enzymes (CeBPS and ScBPS) by choosing varying temperatures as described (2.2.1.7.2). The temperature optimum of both enzymes was 35°C (Fig. 36).

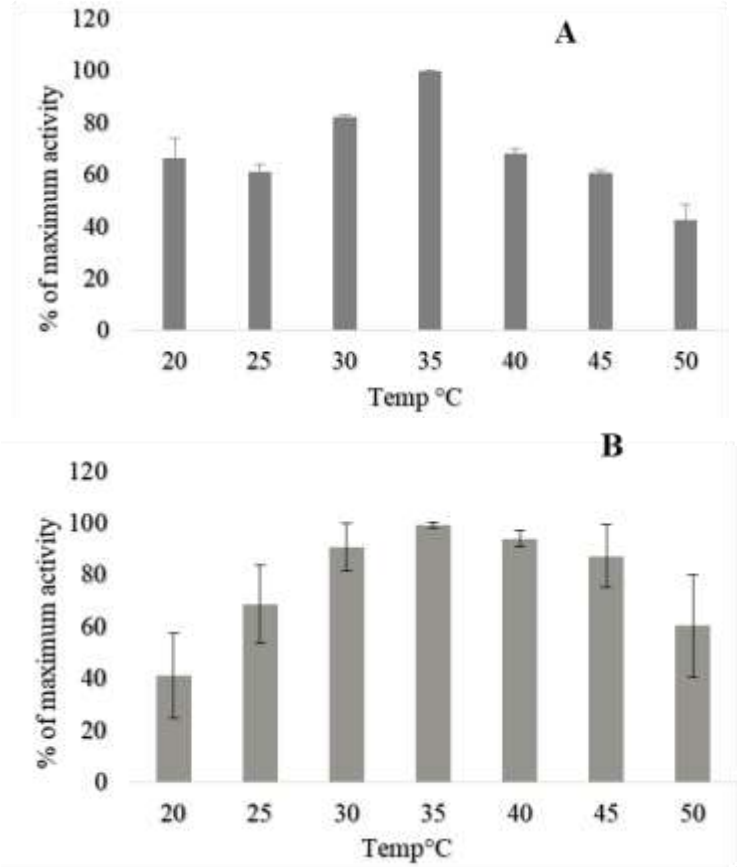

Figure 36. Effect of temperature on CeBPS (A) and ScBPS activity (B). Data are means of two replicates.

3.1.4.4 Linearity with protein concentration

Before determining the kinetic parameters of the enzymes, the effect of increasing protein concentrations on the amount of the enzymatic product over a specified period of time should also be estimated. For both enzymes tested, the accumulation of product was linear with the amount of protein per incubation up to 8 µg (Fig. 37).

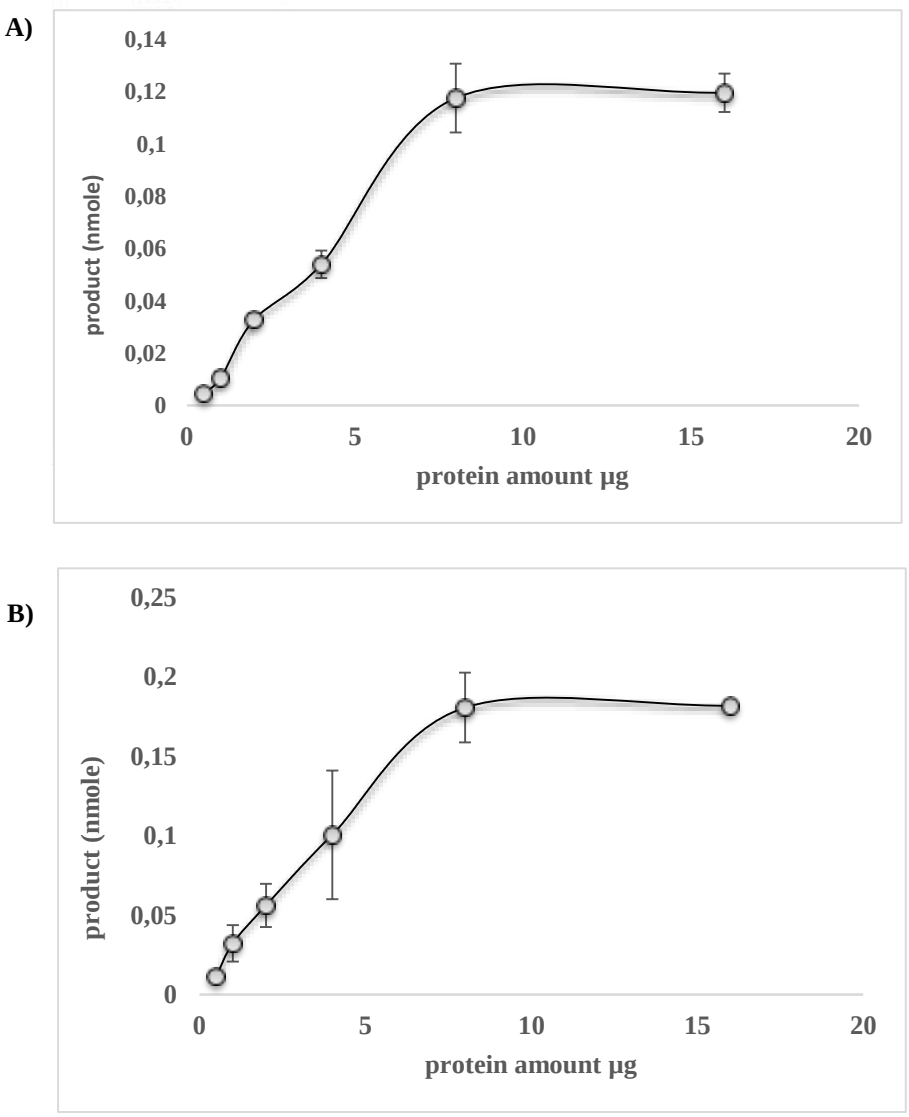

Figure 37. Dependency of CeBPS (A) and ScBPS activity (B) on the protein amount. Data are means of two replicates.

3.1.4.5 Linearity with incubation time

To detect the effect of reaction time on the enzyme activities, the reaction was carried out using the above optimum conditions at different time points (2.2.1.7.3). The accumulation of the product was linear up to 15 min in case of CeBPS (Fig. 38). The activity of ScBPS increased up to 20 min. Thus, 10 min and 15 min were defined as the time intervals for CeBPS and ScBPS incubations, respectively, and applied to the subsequent assays.

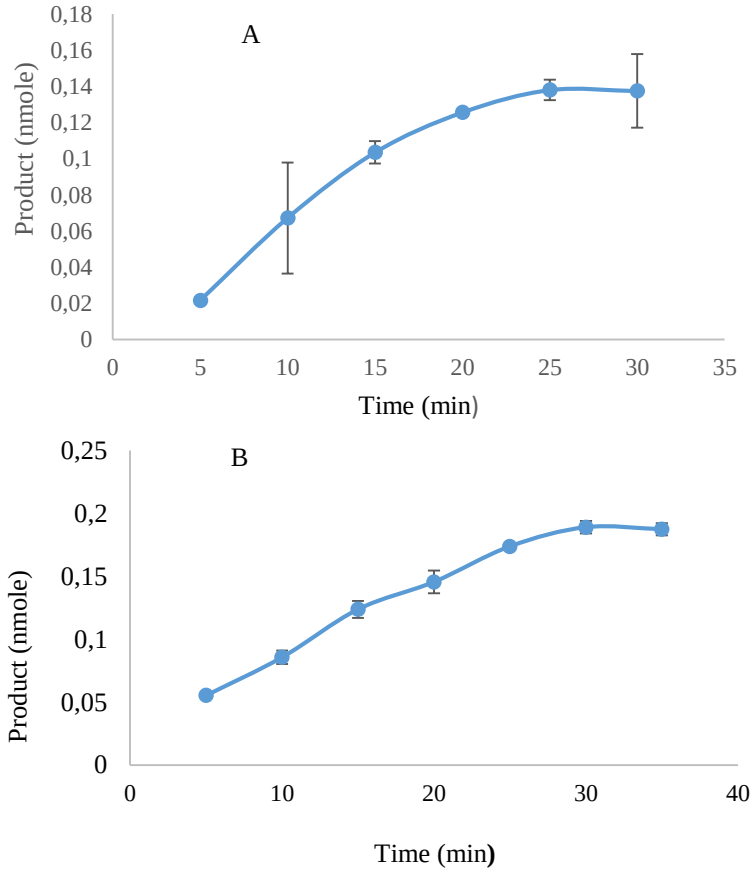

Figure 38. Effect of incubation time on CeBPS (A) and ScBPS activity (B). Data are means of two replicates.

3.1.4.6 Thiol (DTT) dependency

Dithiothreitol, also known as Cleland's agent, stabilizes free thiol groups of amino acids during the incubation and exposure to heating stress. The functional groups can form disulfide bonds, which affect the conformation and then the activity of the protein. Moreover, thiol groups are no longer available as catalytic groups (Alliegro 2000). To know the effect of varying DTT concentrations on the enzyme (CeBPS and ScBPS) activity, incubations were performed in the presence of 0, 10, 25, 50, 100, 200, 250, 500, and 1000 µM DTT. The results showed a gradual decrease rather than a recognizable enhancement of the activity of CeBPS, and ScBPS after addition of DTT (Fig. 39). Therefore, DTT was omitted in subsequent incubations of both BPSs.

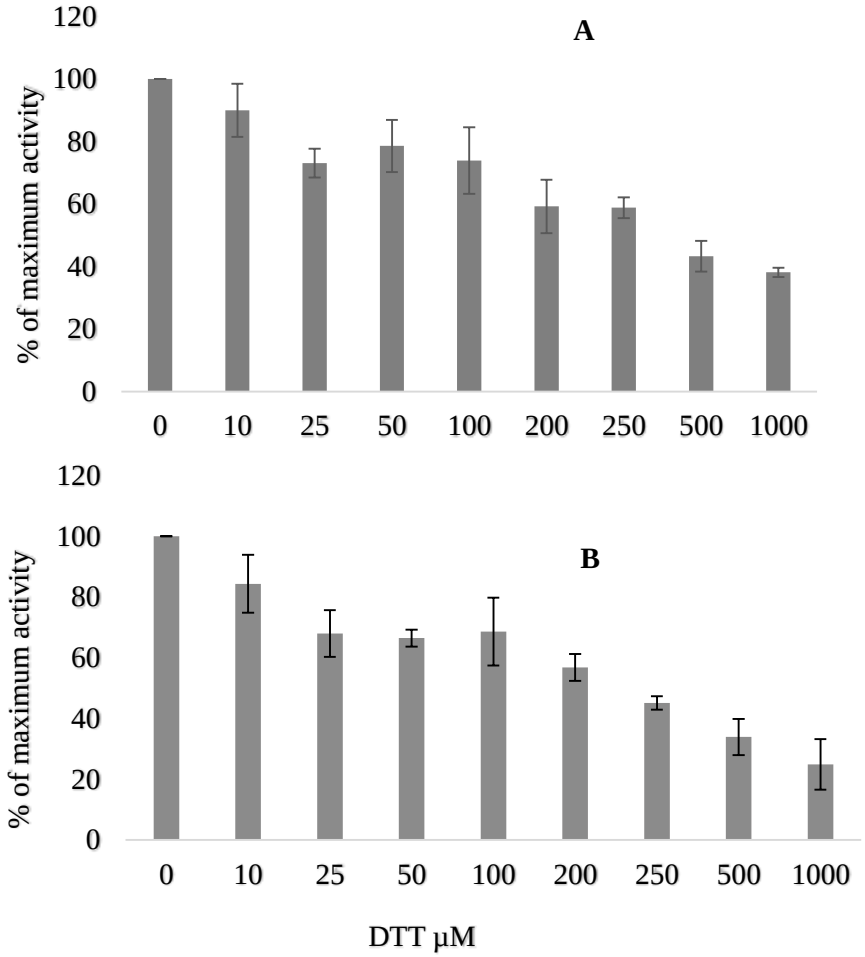

Figure 39. Effect of DTT on the CeBPS (A) and ScBPS activity (B). Data are means of two replicates.

3.1.4.7 Substrate specificity

For each enzyme, there may be more than one preferred substrate which form final products. The affinity of the enzyme for a substrate depends on the conformational structure of the active site cavity. Both CeBPS and ScBPS were tested under the respective optimum assay conditions with a series of potential substrates (Fig. 40) in the presence of malonyl-CoA. As a result (Fig. 41), both enzymes showed similar substrate specificities, thus preferring similar molecular sizes of the substrates and substitution patterns. With decreasing degree of priority, both enzymes accepted 3-(3-hydroxybenzoyloxy)benzoyl-CoA, 3-((3-hydroxybenzoyloxy)3-hydroxylbenzoyloxy)-benzoyl-CoA and 3-hydroxybenzoyl-CoA. In all three reactions catalyzed by CeBPS and ScBPS, a tetraketide intermediate is formed, followed by the CHS-cyclization mechanism (C1 to C6 Claisen condensation), and the final product was the same in all incubations (2,3` ,4,6-THB). In addition, a substrate similar to benzoyl-CoA led to a high degree of activity. Cinnamoyl-CoA was accepted by both BPSs with high catalytic activity. However, there was only production of a triketide intermediate, followed by keto-enol C5-oxy to C1 lactonization, and styrylpyrone was the final product (Fig. 42), as detailed below.

Notably, 4-coumaroyl-CoA, 2-coumaroyl-CoA, 3-coumaroyl-CoA, dihydro-cinnamoyl-CoA and dihydro-4-coumaroyl-CoA were accepted by neither enzyme. Both BPSs also accepted benzoyl-CoA and 2,4,6-THB was the product, resulting from the CHS-cyclization mechanism C1 to C6 Claisen condensation. In contrast, 2-hydroxybenzoyl-CoA and 4-hydroxybenzoyl-CoA were not accepted by the BPSs. Further CoA esters were tested, but accepted by neither enzyme, e.g. acetyl-CoA, caffeoyl-CoA, feruloyl-CoA and *N*-methylanthraniloyl-CoA (Fig. 41).

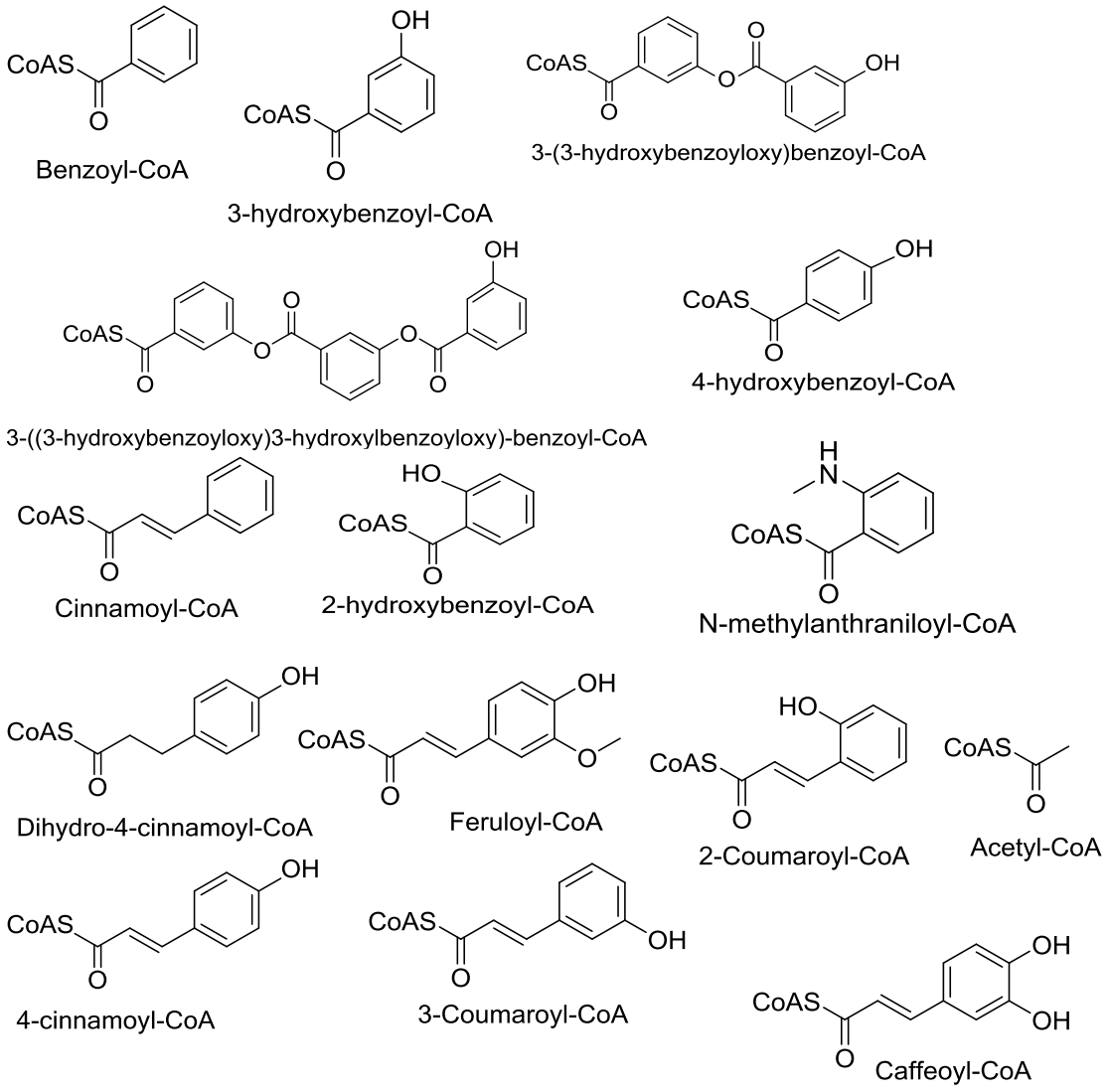

Figure 40. Compounds tested as potential substrates for CeBPS and ScBPS.

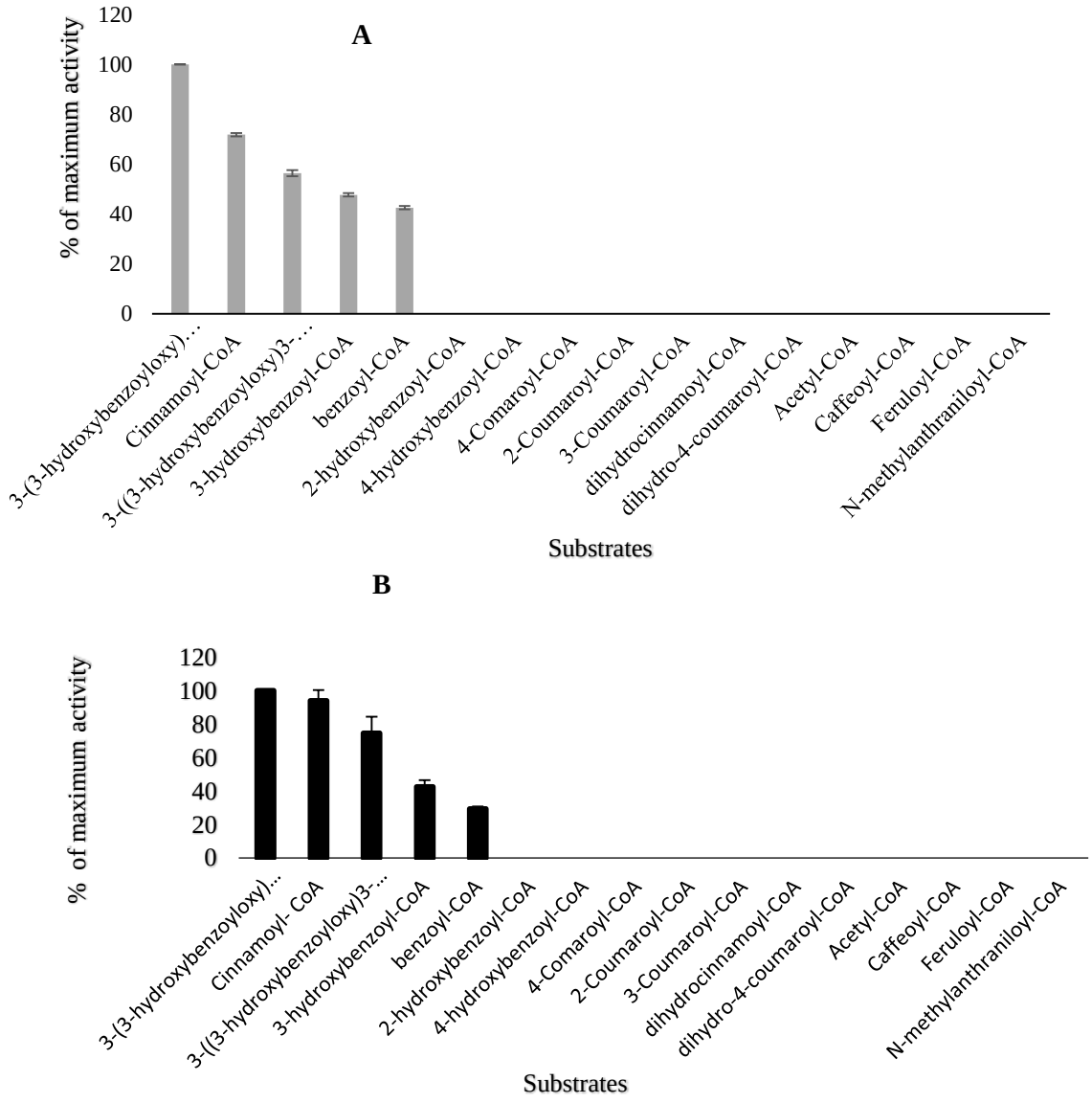

Figure 41. Substrate specificity of CeBPS (A) and ScBPS (B). Data are means of three replicates ± SD.

- **CeBPS and ScBPS activity with cinnamoyl-CoA**

The incubation of the enzymes with cinnamoyl-CoA (26.5 µM) for 10 min at 35°C was followed by stopping the reaction and extracting the products with ethyl acetate, as previously described (2.2.1.6). Both enzymes (CeBPS and ScBPS) allowed only a condensation with 2 molecules of malonyl-CoA to form the triketide lactone (styrylpyrone) (Fig. 42). The product was injected to HPLC and analyzed at 347 nm wavelength (Fig. 43). Since we lacked an authentic reference, we used demethoxyyangonine as a reference to compare its UV spectrum

with that of the product formed. Incubation with denatured proteins failed to show any activity in HPLC chromatograms. The UV spectrum of the product had characteristic absorption maxima at 254 and 347 nm, whereas the UV spectrum of the reference had characteristic absorption maxima at 256 and 342 nm, as shown in Fig. 44. Then the product was supported by electrospray ionization-mass spectrometry (ESI MS/MS) by direct spray infusion. The mass spectrometric analysis was carried out through 'Positive full-scan mode' and the MS/MS fragment pattern (EPI+) showed a molecular ion peak $[M+H]^+$ at 215 (Fig. 45)..

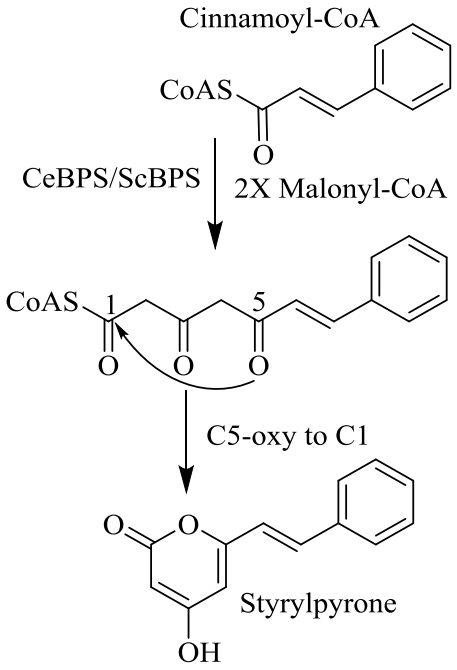

Figure 42. Biosynthesis of styrylpyrone by *C. erythraea* and *S. chirata* BPSs

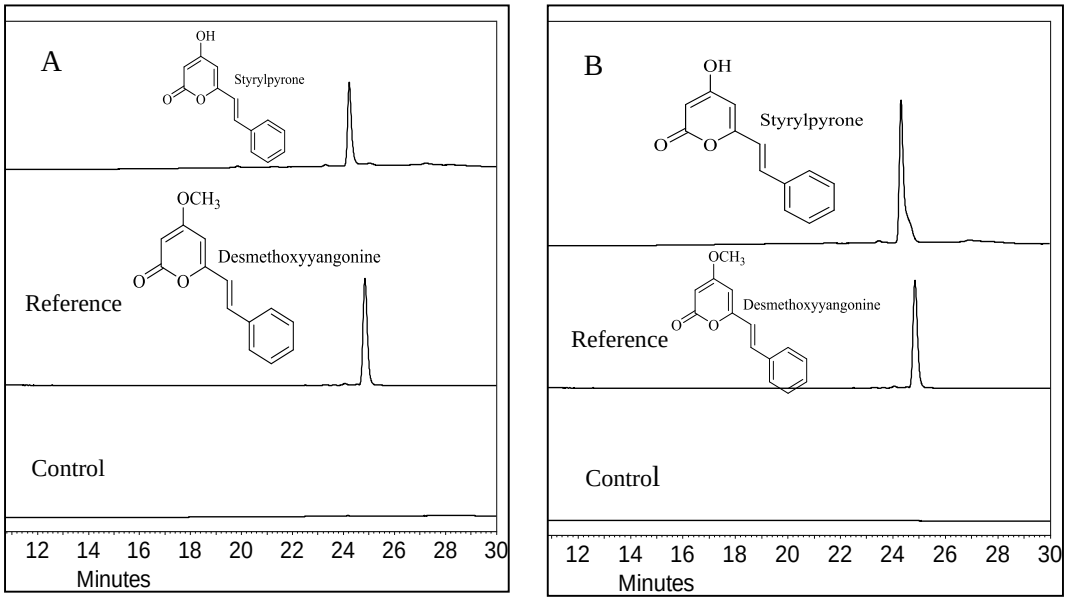

Figure 43. Stacked HPLC chromatograms of CeBPS (A) and ScBPS (B) and control assays and the product reference.

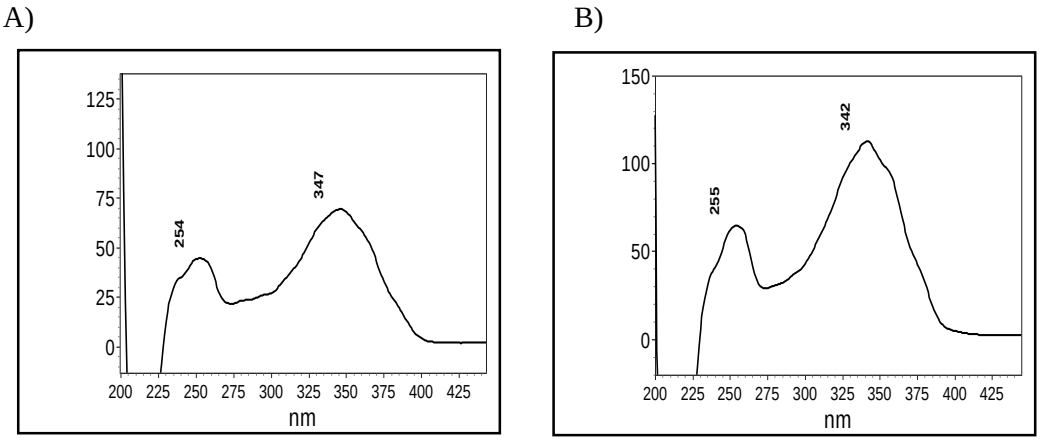

Figure 44. UV spectra of A) the cinnamoy-CoA product (styrylpyrone) and B) the reference compound demethoxyyangonine.

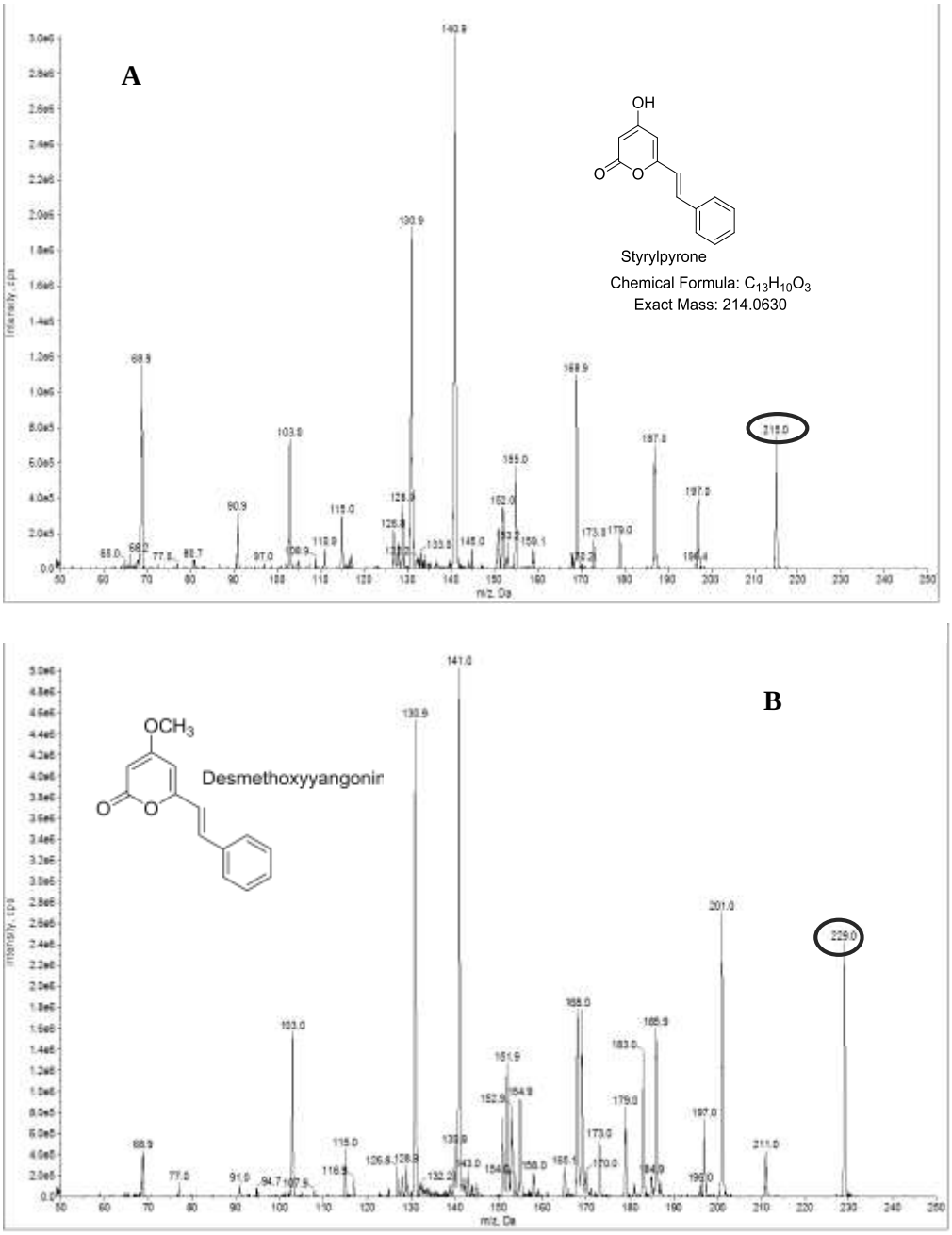

Figure 45. MS/MS fragment patterns (EPI^+) of enzymatic styrylpyrone (A) and authentic demethoxyyangonine (B).

3.1.4.8 Kinetic parameters of recombinant CeBPS and ScBPS

At the optimum conditions for CeBPS (pH 7, 35°C, 10 min, and 5 µg purified fresh protein) and for ScBPS (pH 7, 35°C, 15 min, and 7.5 µg purified fresh protein), the kinetic constants for 3-(3-hydroxybenzoyloxy)benzoyl-CoA, 3-((3-hydroxybenzoyloxy)3-hydroxylbenzoyloxy)-benzoyl-CoA, cinnamoyl-CoA, 3-hydroxybenzoyl-CoA, and benzoyl-

CoA were determined. The important characterizations (K_m, V_{max}, K_{cat}, K_{cat}/K_m) for the five starter substrates were measured in two independent series of experiments. This kinetic characterization helps find out the preferred substrate for each enzyme. The increases in reaction rate with increasing concentrations of substrates obeyed Michaelis-Menten kinetics. The Lineweaver-Burk plot is a linear representation of the Michaelis-Menten equation and commonly used to determine the kinetic parameters of an enzyme. It is a plot of the reciprocal of the enzymatic reaction velocity (1/v) versus the reciprocal of the substrate concentration (1/[S]).

The Michaelis constant (**K_m**) is the substrate concentration for half-maximal velocity. K_m reflects the enzyme affinity or efficiency to choose a substrate and to bind it. If the K_m value is low, the enzyme has a high affinity for the substrate.

The catalytic constant (K_{cat}) is the turnover number, which reflects the number of substrates converted to products inside the active site of the enzyme per second.

The catalytic efficiency (K_{cat}/K_m) indicates the substrate binding and catalytic events in the active site of the enzyme. Based on this important data, one can conclude the best substrate under the preferred conditions of reaction. The parameter can be used to compare between utilization of different substrates by one enzyme and to compare the catalytic efficiency between different enzymes. Based on all aforementioned, we determined the best substrate for CeBPS and ScBPS. The summaries of the kinetic data for the two enzymes are presented in Tables 2 and 3.

Table 2. Kinetic parameters of *Centaurium erythraea* benzophenone synthase (CeBPS) with five substrates and malonyl-CoA. Data are average values of two determinations ± SD.

Enzyme	Calculated subunit mass (Da)	Substrate	K_m (µM)	V_{max} (pkat mg^{-1})	K_{cat} (min^{-1})	K_{cat}/K_m (min^{-1} M^{-1})
CeBPS	42308.85	3-(3-hydroxybenzoyloxy) benzoyl-CoA	8 ± 1.0	247 ± 13.4	1.3	162500
		Malonyl-CoA	54 ± 8.4	310 ± 34.6	1.5	27777
		Cinnamoyl-CoA	6.5 ± 0.5	193 ± 36	0.99	145925
		Malonyl-CoA	10 ± 0.7	273 ± 9.9	1.4	133637
		Benzoyl-CoA	63 ± 5.7	100 ± 8.14	0.54	8075
		Malonyl-CoA	82 ± 11	120 ± 13.4	0.6	7394
		3-hydroxybenzoyl-CoA	47 ± 0.44	63 ± 0.16	0.4	8421
		Malonyl-CoA	30 ± 5.6	72 ± 2.1	0.4	12172
		3-((3-hydroxybenzoyloxy)3-hydroxylbenzoyloxy)-benzoyl-CoA	16 ± 0.21	194 ± 0.63	1.0	62500
		Malonyl-CoA	46 ± 0.14	207 ± 1.41	1.0	22668

CeBPS has highest affinity for 3-(3-hydroxybenzoyloxy)benzoyl-CoA and cinnamoyl-CoA. The K_m values were similar and the conversion of 3-(3-hydroxybenzoyloxy)benzoyl-CoA was catalyzed slightly more efficiently than that of cinnamoyl-CoA (Table. 2). So, 3-(3-hydroxybenzoyloxy)benzoyl-CoA is the best substrate, as reflected by the K_{cat}/K_m value. The catalytic efficiency with 3-(3-hydroxybenzoyloxy)benzoyl-CoA is 2.6, 19, and 20 fold more than those with 3-((3-hydroxybenzoyloxy)3-hydroxylbenzoyloxy)-benzoyl-CoA, 3-hydroxybenzoyl-CoA and benzoyl-CoA, respectively (Table. 2).

Table 3. Kinetic parameters of *Swertia chirata* benzophenone synthase (ScBPS) with five substrates and malonyl-CoA. Data are average values of two determinations ± SD.

Enzyme	Calculated subunit mass (Da)	Substrate	K_m (µM)	V_{max} (pkat mg^{-1})	K_{cat} (min^{-1})	K_{cat}/K_m ($min^{-1}.M^{-1}$)
ScBPS	42703.04	3-(3-hydroxybenzoyloxy) benzoyl-CoA	13.5 ± 2.8	316 ± 36	1.6	122300
		Malonyl-CoA	73 ± 14	330 ± 57	1.7	23949
		Cinnamoyl-CoA	31 ± 7	344 ± 46	1.7	56444
		Malonyl-CoA	17 ± 3.5	276 ± 36	1.4	80833
		Benzoyl-CoA	88 ± 2.1	168 ± 7.7	0.9	9598
		Malonyl-CoA	71.8 ± 0.14	164 ± 16.9	0.8	11698
		3-hydroxybenzoyl-CoA	56 ± 1.4	276 ± 4.2	1.4	25008
		Malonyl-CoA	64 ± 5	206 ± 12	1.1	15926
		3-((3-hydroxybenzoyloxy)3-hydroxylbenzoyloxy)-benzoyl-CoA	26 ± 9	2401 ± 14	1.2	49394
		Malonyl-CoA	40.5 ± 7.7	273 ± 13	1.3	33789

ScBPS has the highest affinity for 3-(3-hydroxybenzoyloxy)benzoyl-CoA, the K_m value is 13. The catalytic efficiency (K_{cat}/K_m) with 3-(3-hydroxybenzoyloxy)benzoyl-CoA is 2.1, 2.4, 4.8, and 13 times more than with cinnamoyl-CoA, 3-(3-hydroxybenzoyloxy)3-hydroxylbenzoyloxybenzoyl-CoA, 3-hydroxybenzoyl-CoA and benzoyl-CoA, respectively (Table. 3). This means that 3-(3-hydroxybenzoyloxy)benzoyl-CoA is also the best substrate for ScBPS.

3.1.4.8.1 Graphical representation of enzyme kinetics for CeBPS through Michaelis-Menten and Lineweaver-Burk plots

Only one example of graphical representation is shown here, whereas those for the other four substrates are documented in Appendix (7.3.1).

- **3-(3-hydroxybenzoyloxy)benzoyl-CoA**

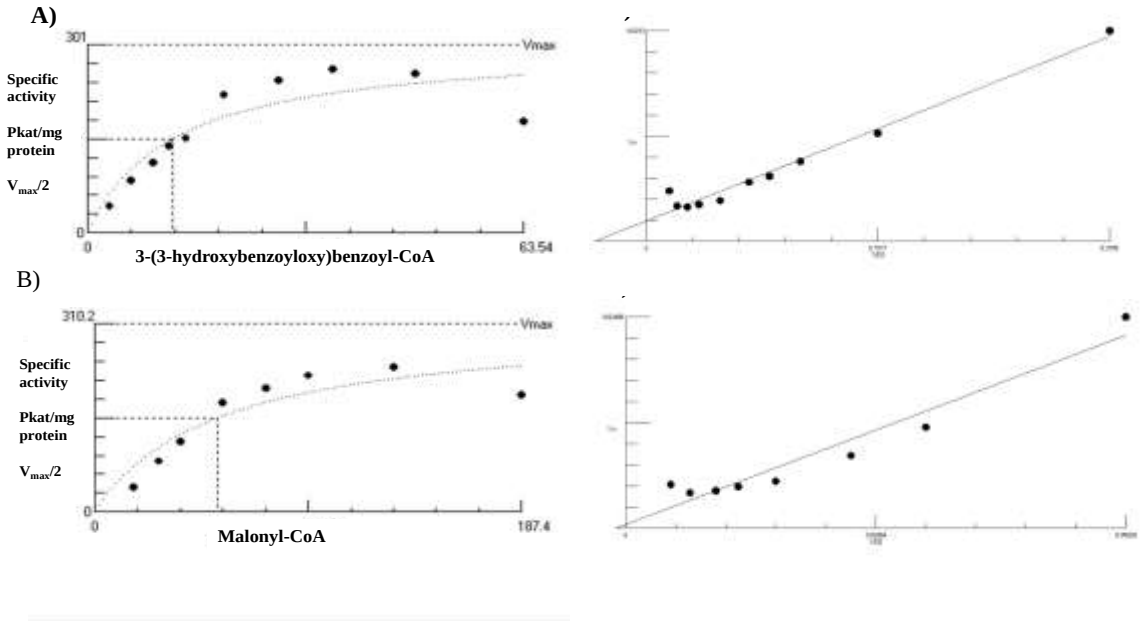

Figure 46. Graphical representation of enzyme kinetics for CeBPS through Michaelis-Menten and Lineweaver-Burk plots. A) 3-(3-hydroxybenzoyloxy)benzoyl-CoA, B) Malonyl-CoA.

3.1.4.8.2 Graphical representation of enzyme kinetics for ScBPS through Michaelis-Menten and Lineweaver-Burk plots

Only one example of graphical representation is shown here, whereas those for the other four substrates are documented in Appendix (7.3.2).

❖ **3-(3-hydroxybenzoyloxy)benzoyl-CoA**

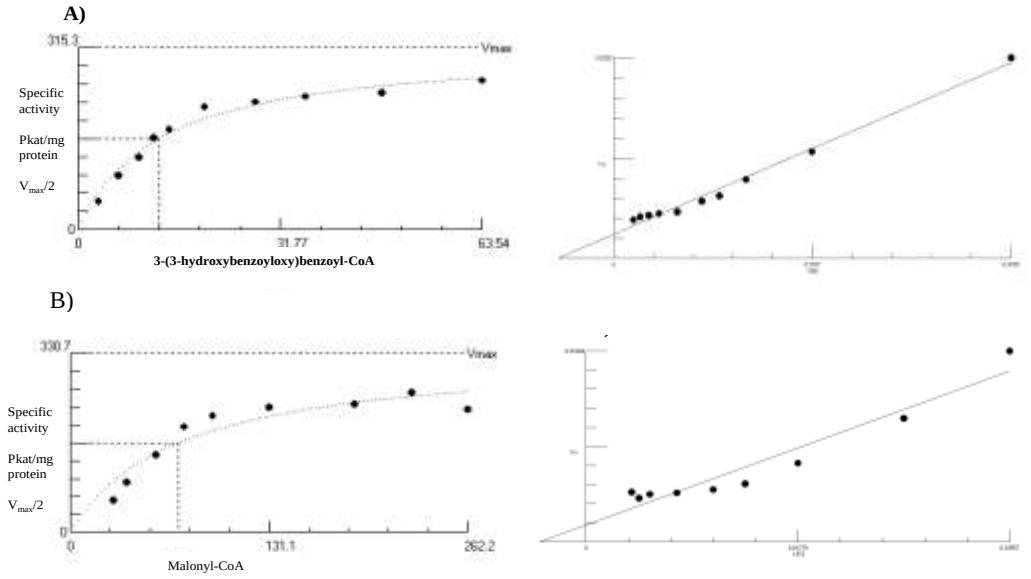

Figure 47. Graphical representation of enzyme kinetics for ScBPS through Michaelis-Menten and Lineweaver-Burk plots. A) 3-(3-hydroxybenzoyloxy)benzoyl-CoA, B) Malonyl-CoA.

3.1.5 Semiquantitative RT-PCR

Expression of the *CeBPS* gene was analyzed in addition to that of *Ce 18s rRNA*. Ce 18s rRNA served as a control to ensure equal RNA levels and to normalize the RT-PCR results. The samples were prepared and the experiment was carried out as described (2.2.3.4.5). As shown in Fig. 52, the expression of *CeBPS* was not clearly increased after a specific time interval of induction by yeast extract addition. The studied time points (3, 6, 9, 15, 20, 24, 30 h) showed high variations at the level of transcript amplification (Fig. 48). Principally, one would expect *CeBPs* to be a rapidly and highly transcribed gene in response to induction. Therefore, the following experiments focused on elicitor-induced changes in the metabolite profiles.

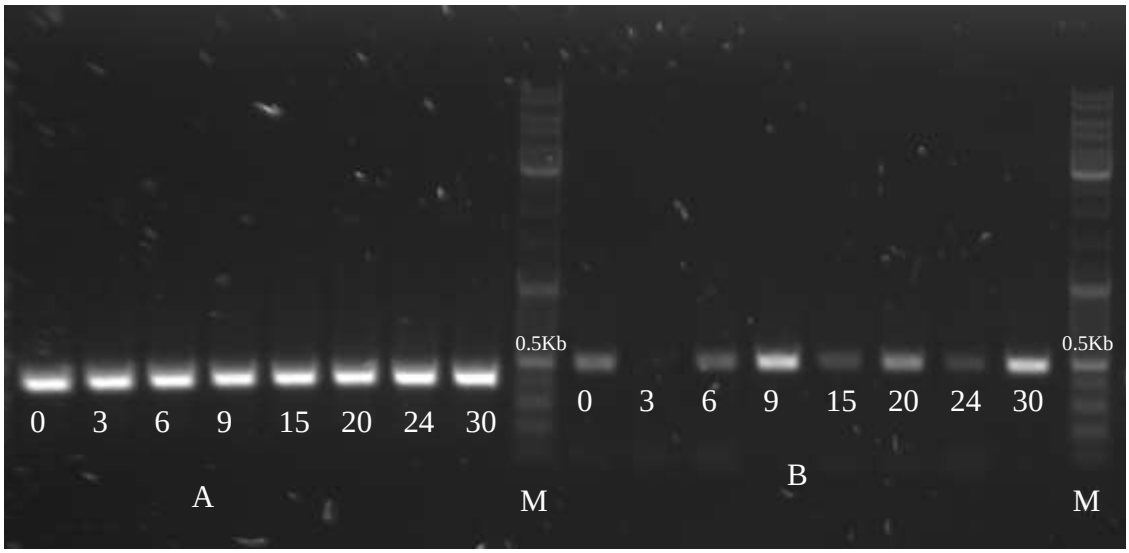

Figure 48. Semiquantitative RT-PCR analysis of *18S Ce rRNA* (A) and *CeBPS* expression (B). Numbers indicate hours after elicitation.

3.2 *In vitro* cultures of *C. erythraea* and *S. chirata*

3.2.1 Root cultures of *S. chirata*

Three different types of root cultures (roots from either shoots, callus or leaves) were established in our laboratory, as described previously (Agarwal 2013). Two earlier studies in our lab aimed to detect the accumulation of xanthones and amarogentin in *in vitro* roots of *S. chirata* (Agarwal 2013; Singh 2014). The roots of *S. chirata* (Fig. 13) were used in this work to study the growth pattern of root cultures. In addition, trials were performed to clone a full-length gene of biphenylcarboxylate synthase from the root cultures. To study the growth curve of *S. chirata* root cultures, about 0.04 g/DW was used as starting mass for growth in ½ MS medium in the dark at 80 rpm. The samples were harvested over a period of 53 days (Fig. 49). In the first three weeks, no notable increase in biomass was detected. Afterwards, active growth of the roots was observed, showing a maximum biomass production (0.69 g DW) at 42 days. After this time point (plateau phase), no change in the biomass of the root cultures was observed. From 53 days on, the cultures began to consume all the medium and to lose vitality. The root color became dark brown to black. The initial mass of the roots was enhanced more than 16-fold, giving a root biomass of 0.69 g dry weight (Fig. 49).

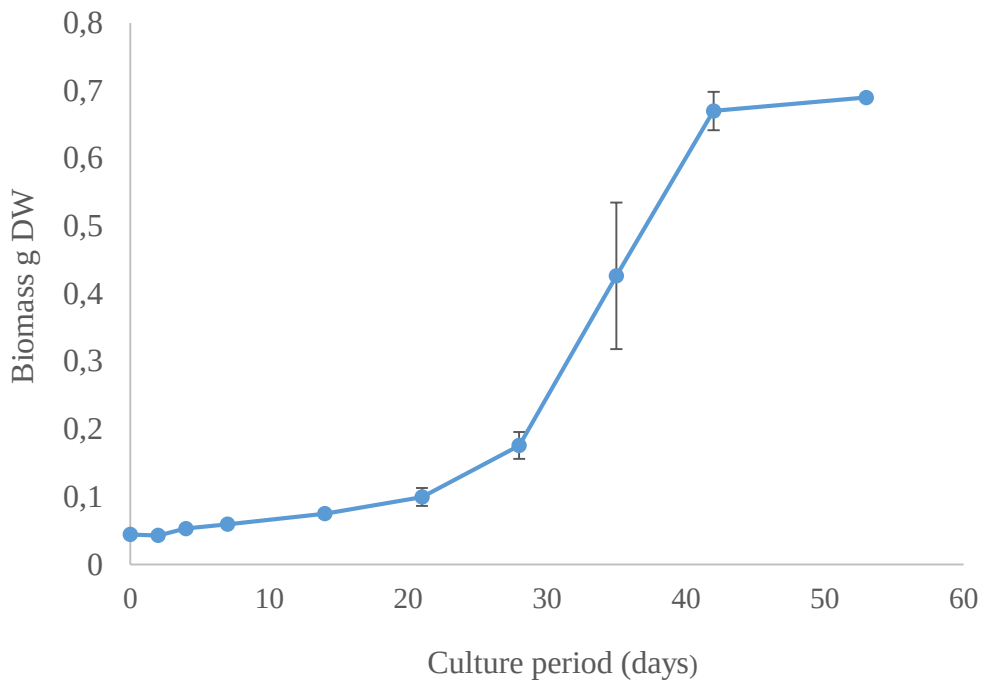

Figure 49. Growth curve of *Swertia chirata* root cultures over a 53-day growth period.

3.2.2 Cell suspension cultures of *C. erythraea*

3.2.2.1 Analysis of metabolites from cell cultures of *C. erythraea* (Ce_St)

Two lines of *C. erythraea* cell cultures were available, which originated from two different proveniences, i.e. *C. erythraea* Stuttgart (Ce_St) and *C. erythraea* Karlsruhe (Ce_Kr), established previously in our laboratory by Dr. Mariam Gaid. We started with the analysis of Ce_St.

The metabolites were extracted from both cells and medium, as described (2.2.1.2.1 and 2.2.1.2.2). The samples were analyzed using an Agilent HPLC and the gradient 3 (2.2.2.1). The chromatograms shown in Fig. 50 were obtained after a lot of comparing at different wavelengths. As shown in A), the cell extract did not show any difference in the metabolites after induction by MeJ (3) or YE (4), as compared with the control samples (1 and 2). However, the medium extract showed two unprecedented peaks. The first peak was induced by MeJ, as detected at wavelength 319 nm and Rt = 25.8 min (Fig. 51 A). The second peak was induced by YE, as detected at wavelength 289 nm and Rt = 19.3 min (Fig. 51 B). The two induced compound peaks were only observed in medium extract but not in the cell extract.

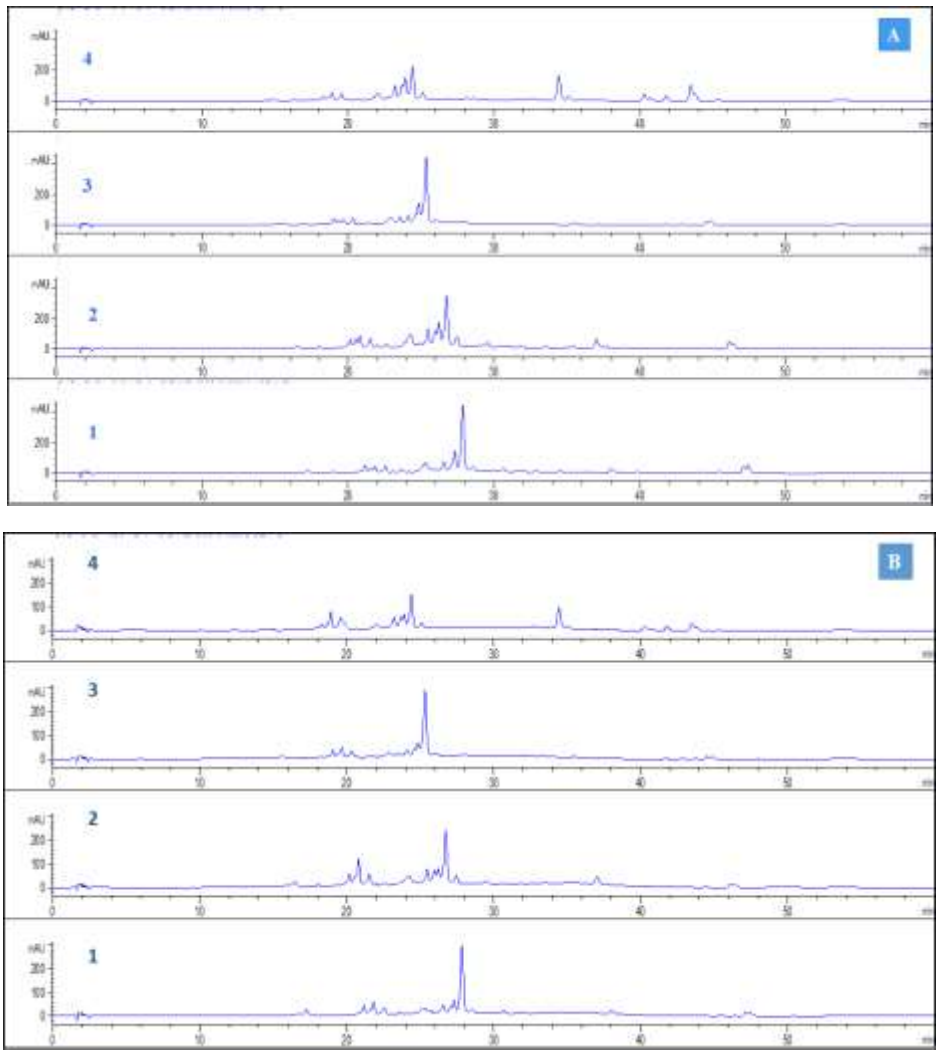

Figure 50. Chromatograms representing the metabolite profile of *C. erythraea* **cell** extracts at wavelengths of **319** nm (A) and **289** nm (B) for 1) untreated cells, 2) ethanol, 3) methyl jasmonate, 4) yeast extract.

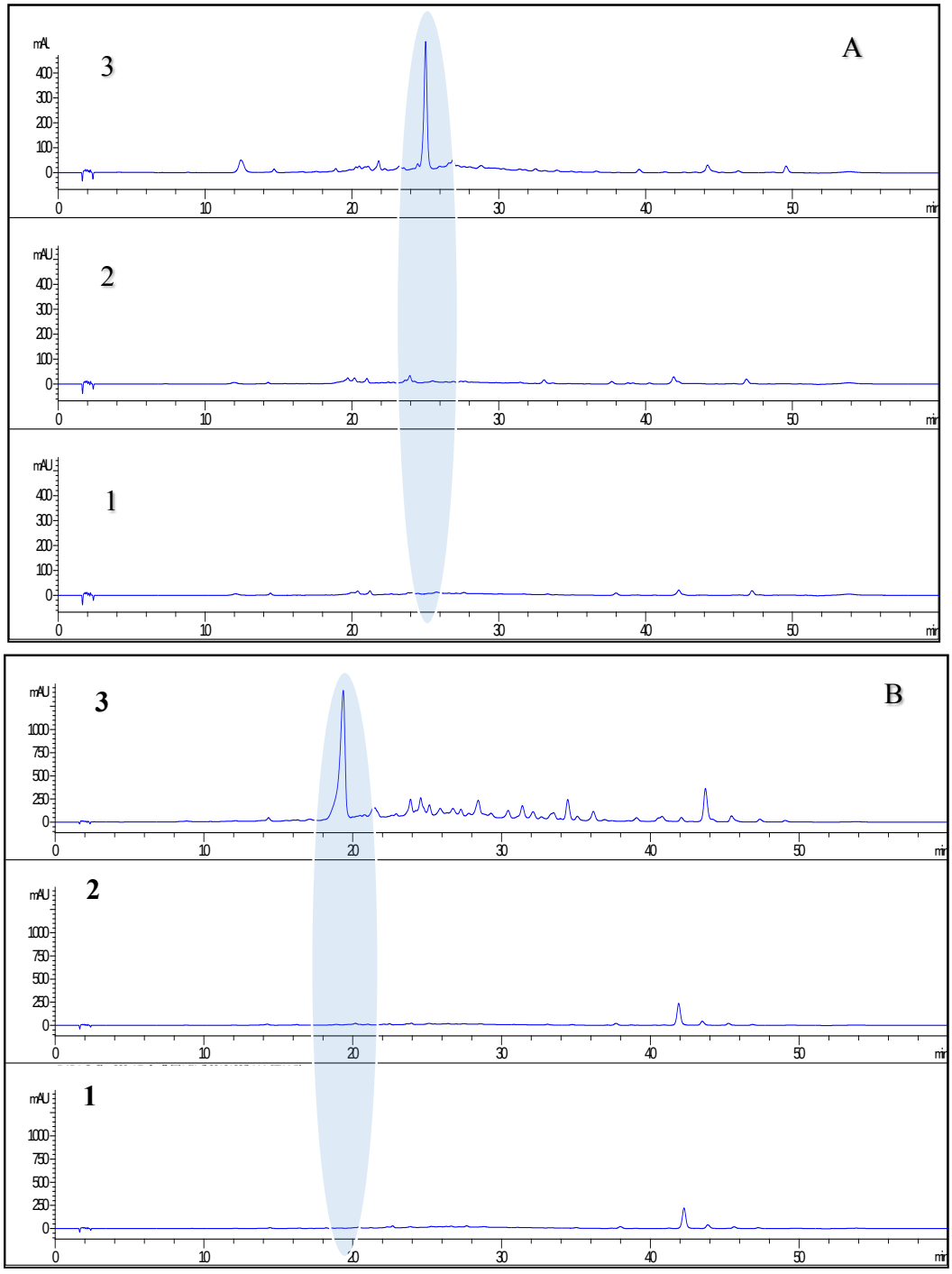

Figure 51. HPLC chromatogram representing the metabolite profile of *C. erythraea* **medium** extracts at wavelengths of either **319** nm (A) for 1) untreated medium, 2) ethanol, 3) MeJ or **289** nm (B) for 1) untreated medium, 2) H_2O, 3) YE.

3.2.2.1.1 Spectral analysis of two induced compounds

3.2.2.1.1.1 UV spectral analysis

The UV spectrum of the MeJ-induced compound had maxima at 250 and 356 nm. The YE-induced compound had a maximum at 289 nm (Fig. 52). The two induced compounds were detected for the first time in the medium of cell cultures of *C. erythraea*. However, they do not exhibit a characteristic xanthone spectrum.

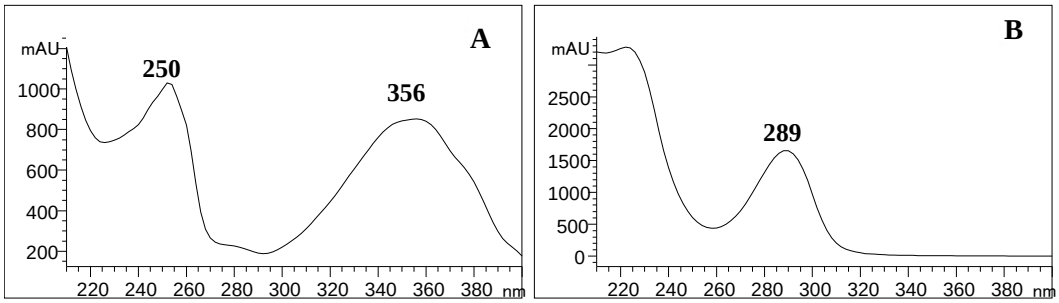

Figure 52. UV spectra of the compounds excreted into the medium after MeJ induction (A) and YE induction (B).

3.2.2.1.1.2 Mass spectrometric analysis

The induced compounds were analyzed by electrospray ionization-mass spectrometry (ESI MS/MS) via direct spray infusion. Mass spectrometric analysis was carried out through 'Positive full-scan mode'. The MS/MS fragment pattern (EPI+) of the compound after MeJ showed a molecular ion peak $(M+H)^+$ at m/z 421, while the induced compound after YE showed a molecular ion peak $(M+H)^+$ at m/z 225, as shown in Fig. 53.

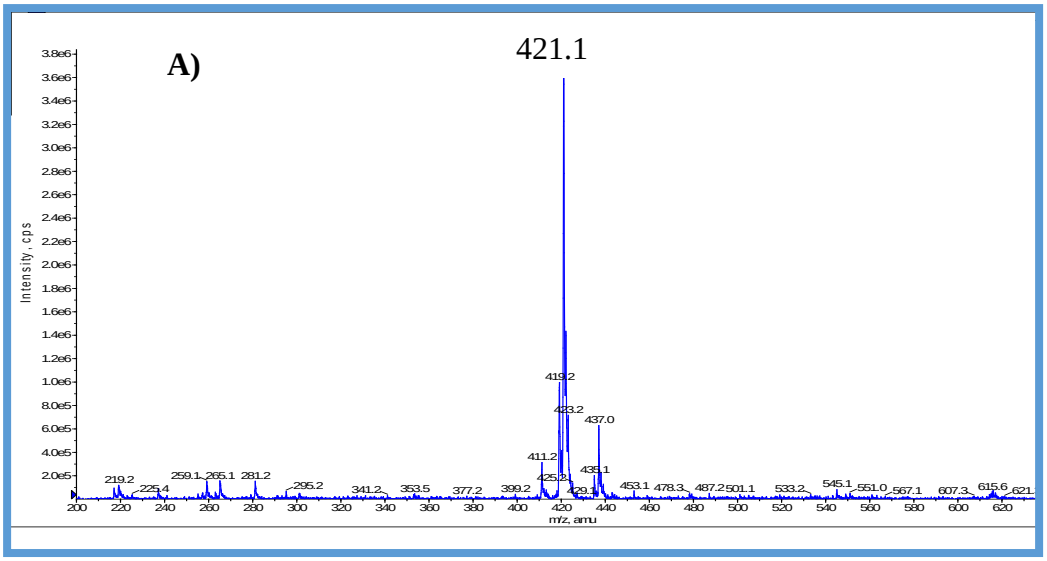

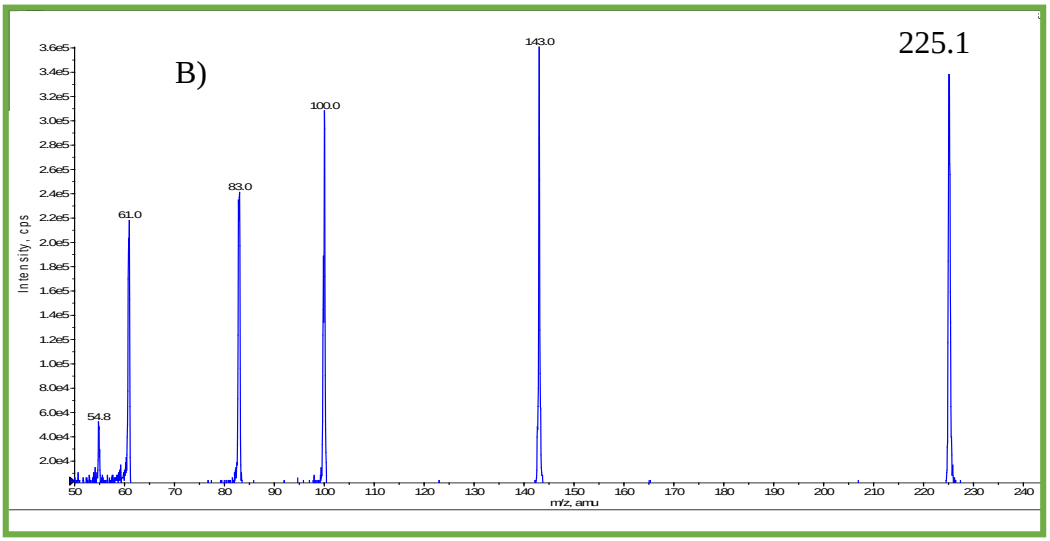

Figure 53. MS/MS fragment patterns (EPI+) of the MeJ (A) and the YE induced compounds (B).

3.2.2.2 Analysis of metabolites from cell cultures of *C. erythraea* (Ce_Kr)

The above-described cell cultures of *C. erythraea* (Ce_St) showed a clear result, because two induced peaks were observed in medium extract, whereas the cells themselves lacked to change at the metabolite level post-elicitation with YE and MeJ. A second analysis of metabolites was carried out with a different batch of cell suspension cultures of *C. erythraea* (Ce_Kr). Firstly, we analyzed the metabolites pre-induction, for which samples were collected from the cell suspension cultures at all growth days. The samples were analyzed by HPLC (VWR-Hitachi) using the gradient 2 (2.2.2.1). The metabolite extract showed the presence of five peaks, which were detected at all growth days (Fig. 54).

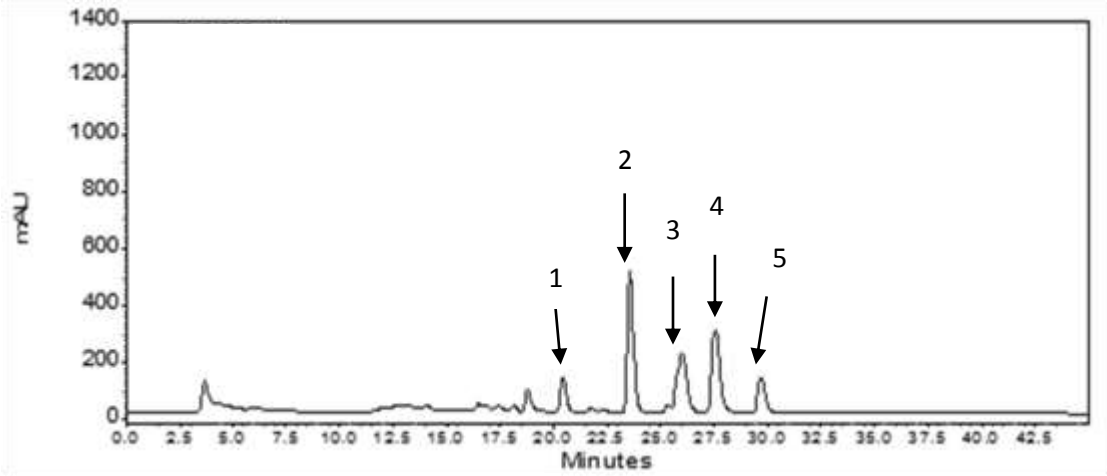

Figure 54. HPLC chromatogram representing the metabolite profile of *C. erythraea* (Ce_Kr) untreated cells with five major peaks.

3.2.2.2.1 UV spectroscopic analysis of five major constituents

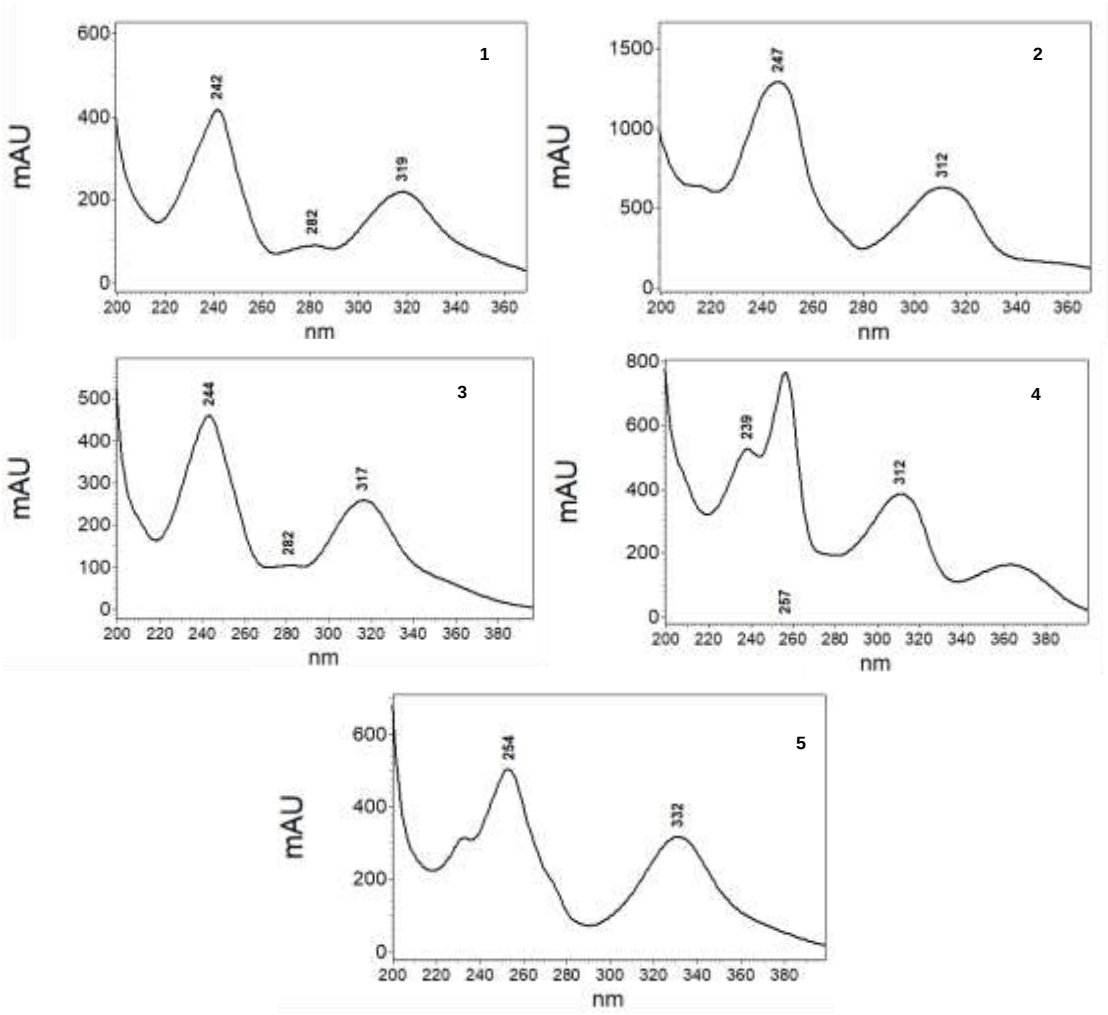

Figure 55. UV spectra of the five major constituents detected in cell cultures of *C. erythraea.*

The above UV spectra showed characteristic absorption maxima, which matched those of authentic xanthones available in our laboratory **1)**: tetrahydroxyxanthone derivative, **2)** 1,5-dihydroxy-3-methoxyxanthone, **3)** pentamethoxyxanthone, **4)** 1-hydroxy-3,5-dimethoxyxanthone and **5)** 3,5,8-trimethoxyxanthone.

3.2.2.2.2 Total xanthone accumulation after induction by yeast extract

At different time points (0, 2, 4, 6, 8, 10, 24, 48, 72, 96 h) post-induction by yeast extract (3g/l), samples were collected for determination of the total xanthone content, as described (2.2.1.2.4). At all time points of induction, we confirmed the presence of the five peaks for xanthones (Fig. 54). We included them in the calculation of total xanthones, which accumulated in the cultures post-induction. Fig. 56 shows that there is decrease rather than increase in xanthones in cell cutures of *C. erythraea* (Ce_Kr) post-induction by YE, compared with the control sample (0 h).

.

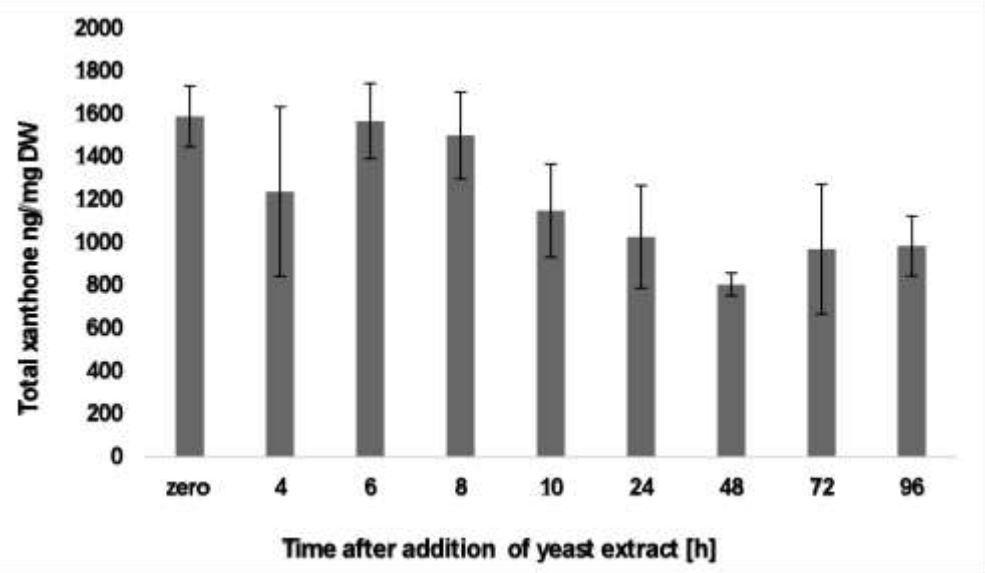

Figure 56. Total xanthone content post-induction by yeast extract.

Previously, cell suspension cultures of *C. erythraea* and *C. littorale* were found to show a clear response to MeJ and YE induction. MeJ treatment induced 1-hydroxy-3,5,6,7-tetramethoxyxanthone, while YE treatment induced 1,5-dihydroxy-3-methoxyxanthone (Beerhues and Berger 1995).

3.2.2.2.3 Cell and medium extraction after treatment with methyl jasmonate

The effect of MeJ was also studied in this type of cell cultures. The metabolites were extracted from both the cells and the medium, as described (2.2.1.2.1 and 2.2.1.2.2). The samples were analyzed by HPLC (VWR-Hitachi), using the gradient 2 (2.2.2.1). The results observed with this type of suspension cultures of *C. erythraea* (Ce_Kr) were compared to those with cell suspension cultures of *C. erythraea* (Ce_St). The cell and medium extracts showed no response after treatment by MeJ, as shown in Fig. 57. In contrast, suspension cultures of *C. erythraea* (Ce_St) showed the presence of a peak post-induction by MeJ and this peak was observed in medium extract (Fig. 51 A).

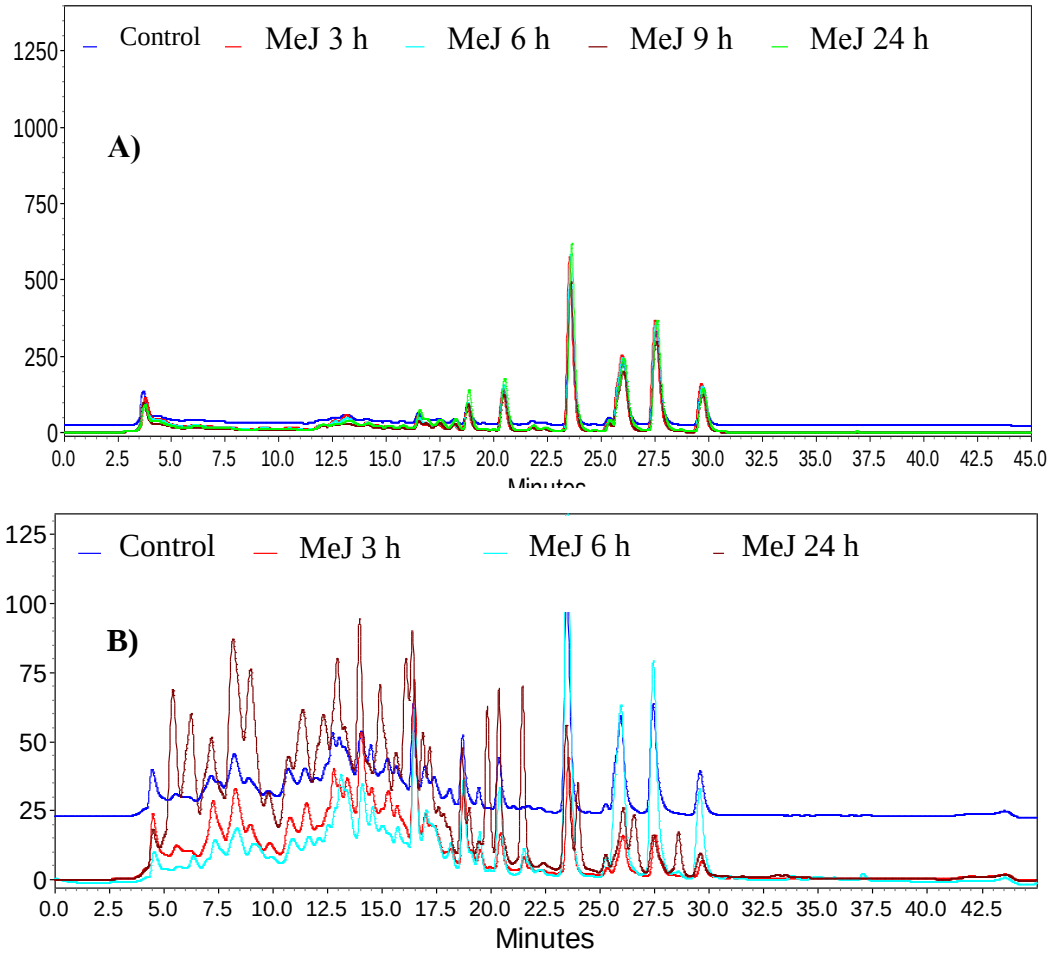

Figure 57. Chromatograms representing the metabolite profiles of *C. erythraea* (Ce_Kr) cell cultures post-induction by MeJ. (A) Cell extract, (B) Medium extract.

3.2.2.2.4 Cells and medium extraction after induction by yeast extract

Cell suspension cultures of *C. erythraea* (Ce_Kr) were treated with YE as described (2.2.1.1). The metabolites were extracted from both the cells and the medium as described (2.2.1.2.1 and 2.2.1.2.2). The samples were analyzed by HPLC (VWR-Hitachi), using the gradient 2 (2.2.2.1). The extract from cells showed no difference post-induction by YE at 3, 6, 9, and 24 h (Fig. 58). However, the medium extract contained the same induced compound that was detected above in medium extract from *C. erythraea* (Ce_St) (Fig. 51 B). The compound was detected after 6 and 9 h and declined afterwards, as shown in Fig. 59**.**

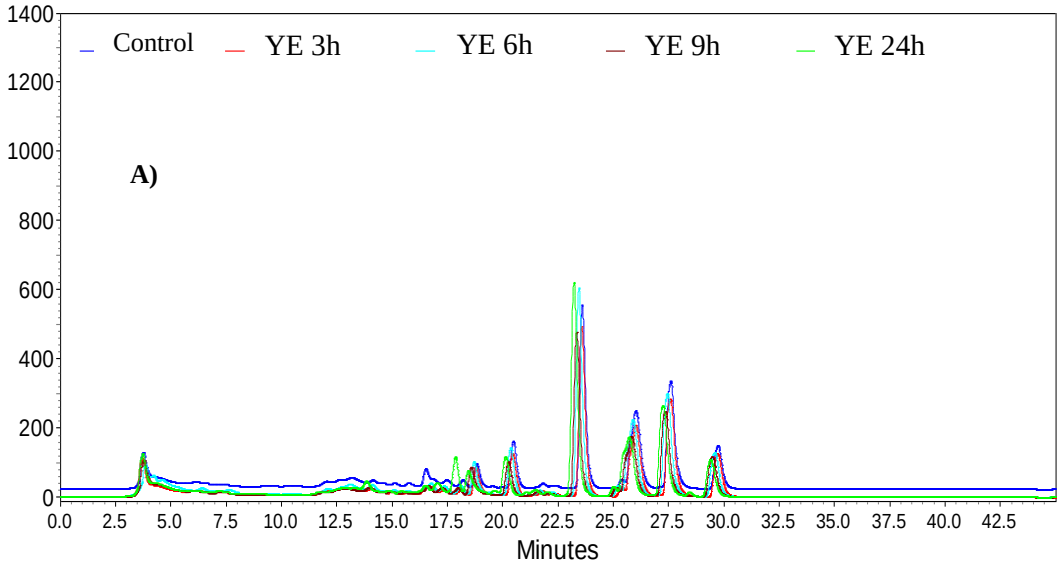

Figure 58. HPLC chromatograms of cell extract metabolites after treatment with YE.

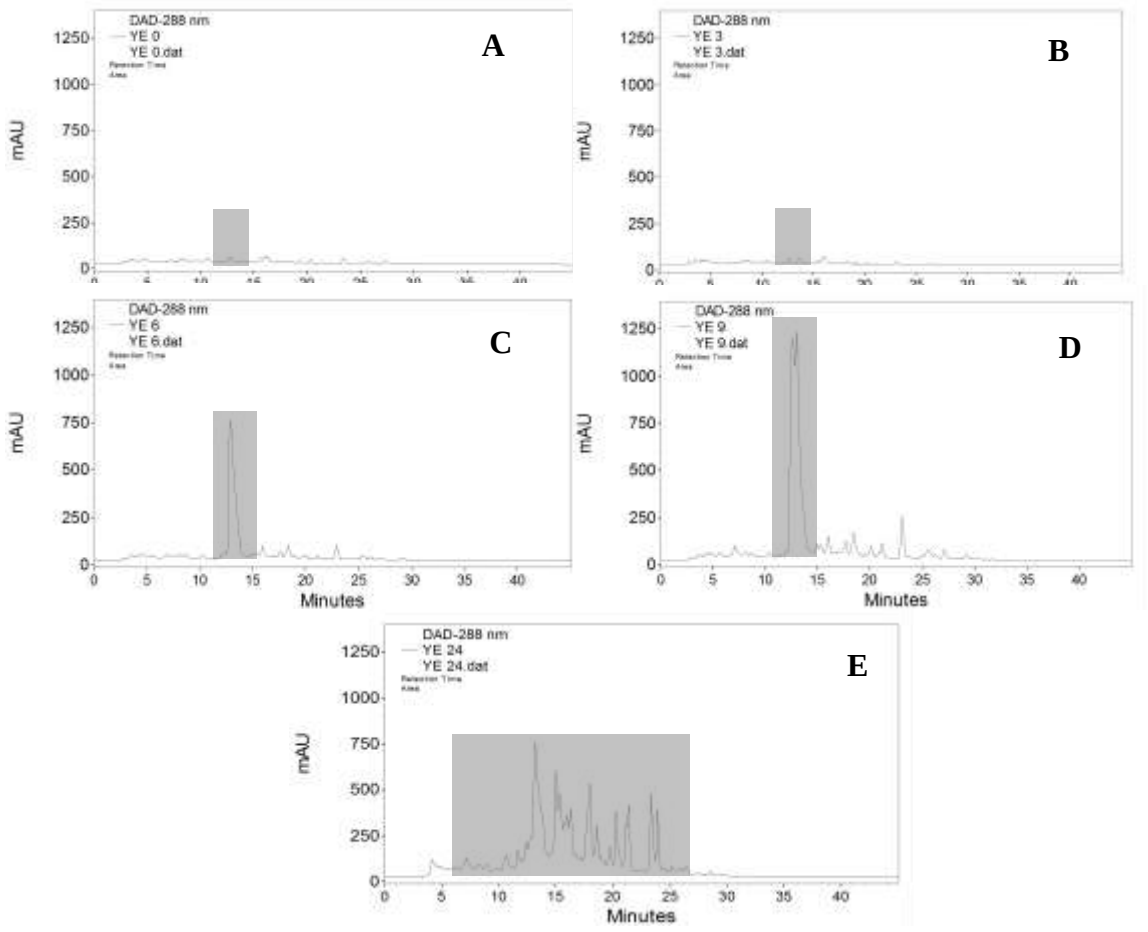

Figure 59. HPLC chromatograms representing the metabolite profiles of medium from yeast extract-treated *C. erythraea* (Ce_Kr) cell cultures. A) Control. B) 3 h. C) 6 h. D) 9 h. E) 24 h.

As a conclusion, two batches of cell suspension cultures originating from two different *C. erythraea* proveniences (Ce_St and Ce_Kr) showed identical response to treatment with YE after analysis of the metabolites. However, the peak detected post-induction with MeJ in medium extract of *C. erythraea* (Ce_St) (wavelength 319 nm, 25.8 min) was not observed in medium extract of *C. erythraea* (Ce_Kr).

3.3 Molecular cloning of biphenylcarboxylate synthase (BICS)

3.3.1 Isolation of total genomic DNA

Genomic DNA was isolated from root cultures of *S. chirata* as described (2.2.3.1.2). Genomic DNA from the leaf of *G. lutea* was also available in our lab and used as a template for PCR-amplification of a putative BICS sequence.

3.3.2 PCR with gene-specific primers to fish out the 5` end of fragment 2

The motivation was to clone the full-length sequence for biphenylcarboxylate synthase (BICS) from Gentianaceae (*G. lutea* or/and *S. chirata*). A first step, i.e. cloning of fragment 2, was achieved by Swiddan (2010), who cloned the following putative part of the gene with ~741 bp from *G. lutea*

Nucleotide sequence of fragment 2 (Swiddan 2010)

```
5′CAACAAAGGTGCACGAGTTCTTATTGTTTGCTCGGAGATCATCGGACT
TACTTTCCGGGGACCGAGCGAAACAGATTTAGATGGTCTAGTCGGACAGG
CCTTATTTGCAGATGGCGCTGCATCGTTGGTAGTCGGTTCAKACCCCATC
CCAGGATTAGAAAAGCCTGTGTTTGAGATTGTTTCAGCTGCCCAAACTTT
TATTCCAGAGAGTCATGGTTCCATTACCGGTGATCTTCGTGAGGCTGGCC
TTATTGTCAAGCTAAGTAAAAATGTTCCAAAGTTTTTCGGAGAGAATATT
GATAAGTGCTTGGATGAGGCCTTTCAACCTCTGGGGATTACTGATTGGAA
TTCCATTTTCTGGATTGCACACCCTGGTGGGGCGTTGATTTTGGACAAAG
TGGAACAAAAGTTAGGCCTACATCCTAAGAAGCTAAGAGCTACAAGACAT
ATATTAAGTGAGTATGGAAACATGTCAAGTGTTTGTGTGTTTTTCATACT
TGATGAAGTCAGAAAGTATTCAATCAAGAATGGATTTAGCACTACTGGAG
AAGGGCTAGAATGGGGTGTGCTCTTCGGTTTGGGTCCTGGCCTAACTGTT
GAAACTGTTGTTTTACGCAGTGTAGCAATTTAAGTTACTACTGTGTTTCT
TGATTCACAGAAWGCATGTTAGGKGTGATYSCCATCTTCTTCTTATTATT
TAATTATGTGTTTGTAATGGTGATCAAATAATTGCATGGTCCAAAAAAAA
AAAAAAAAAAAAAAAAAAA-3′
```

3.3.2.1.1 Primer design

The cloned part of the gene had 73% identity with CHS in BLAST (Basic Local Alignment Search Tool). It lacked about 600 bp toward the 5` end to get the full-length. Starting from fragment 2, three primers were designed: GL2_F, GL2_R1, and GL2_R2. The other two primers were derived from the full length of putative BICS of *G. acaulis* present in the data bank: GL2_3 *Kpn* I and GL2_5 *Nhe* I (2.1.7.5).

3.3.2.1.2 PCR amplification for BICS cloning

Two genomic DNA pools from separate species were used in PCR amplification as templates. The two primers GL2_3 *Kpn* I and GL2_5 *Nhe* I were used first. As a result, the amplification was successful with *G. lutea* genomic DNA in the first trial, while the PCR amplification failed with *S. chirata* genomic DNA, despite repeated trials (Fig. 60 A). The other trial was performed by using genomic DNA of *S. chirata* as a template with the two primers GL2_F and GL2_3 *Kpn* I in the first and the second amplification rounds. However, it failed to give the desired band (Fig. 60 B).

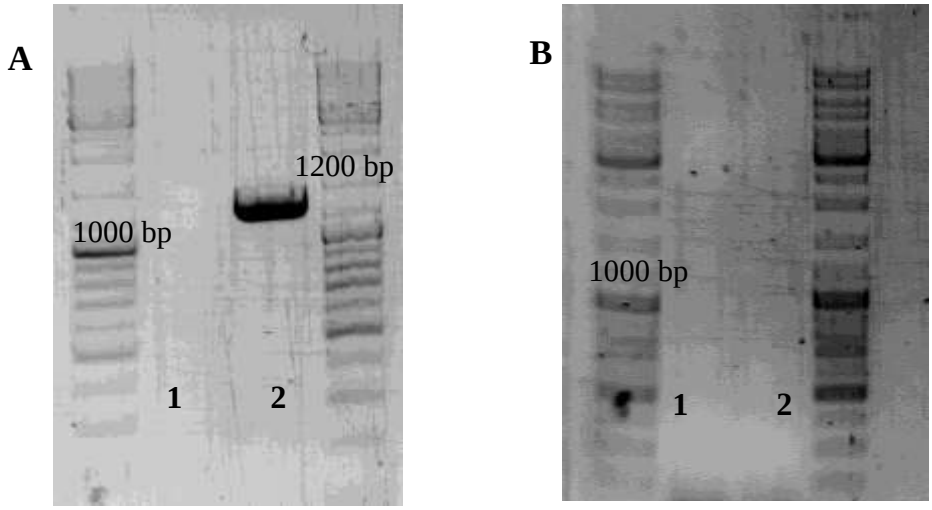

Figure 60. (A) PCR amplification using genomic DNA of *S. chirata* as template (lane **1**) and genomic DNA of *G. lutea* as template (lane **2**), both with the GL2_3 *Kpn* I and GL2_5 *Nhe* I primers. (B) PCR amplification using genomic DNA of *S. chirata* as template with the GL2_F and GL2_3 *Kpn* I primers in the first and second amplifications.

Assembling the GL2BICS contig using SeqMan software of DNA Star

The extracted DNA band from the gel was ligated to the expression vector pRSETB. The important step was to analyze the sequence to contain the right insert. The constructed plasmid was sequenced. Then both sequences (fragment 2 and this fragment received after sequencing) were assembled using SeqMan software Lasergene. After analysis, we found the overlapping region and got contig 1 (1280bp), but it contained introns. For this reason, we designed two primers (GL2_cutintron _F and GL2_cutintron_R) to remove the introns. The primers were designed according to the sequencing results (2.1.7.5). Re-amplification of the plasmid, which contains the introns, was done with two primers. The result is shown in Fig. 69.

Figure 61. Re-amplification of the plasmid with GL2_cutintron_F and GL2_cutintron_R.

3.3.3 Analysis of the putative GL2BICS amino acid sequence

Having established the new plasmid provided with the right gene, it turned out to be a continuous open reading frame from the start codon ATG to the stop codon TAA (1170 bp). The calculated molecular mass of the derived protein was 42.7 kDa, due to 389 amino acids (Appendix 2). On BLASTing the sequence in the NCBI databank, it showed a maximum of 74% identity with available sequences, mostly chalcone synthases (Fig. 62)

chalcone synthase [Apocynum venetum]
Sequence ID: AJM90013.1 Length: 389 Number of Matches: 1

Range 1: 1 to 389 GenPept Graphics ▼ Next Match ▲ Previous Match

Score	Expect	Method	Identities	Positives	Gaps	Frame
619 bits(1595)	0.0	Compositional matrix adjust.	286/389(74%)	337/389(86%)	0/389(0%)	+1

```
Query  1     MMTEKELRRPERADGLATVFAIGTASPPNFVEQISYADYYFKVTNSEHMIELKEKFKRIC  180
             M++ +++RR +RA+G ATV AIGTA+PPN VEQ +Y DYYF+VTNSEH  ELKEKFKR+C
Sbjct  1     MVSVEDVRRAQRAEGPATVMAIGTATPPNCVEQSTYPDYYFRVTNSEHKTELKEKFKRMC  60

Query  181   EKSMIRKRHMFLTEEILKENPSICASAAPSLDDRQNILVVEVPKLGKEAAEKAINEWGQP  360
             EKSMI+KR+M+LTEEILKENP++CA  APSLD RQ+++VVE+PKLGKEAA+KAI EWGQP
Sbjct  61    EKSMIKKRYMYLTEEILKENPNVCAYMAPSLDARQDMVVVEIPKLGKEAAQKAIKEWGQP  120

Query  361   KSKITHLIFCTISGVDMPGADYQLTRLLGLNPSVNRLMLYLMGCFGGGTVLRLAKDIAEN  540
             KSKITHL+FCT SGVDMPGADYQLT+LLGL PSV RLM+Y  GCF GGTVLRLAKD+AEN
Sbjct  121   KSKITHLVFCTTSGVDMPGADYQLTKLLGLRPSVKRLMMYQQGCFAGGTVLRLAKDLAEN  180

Query  541   NKGARVLIVCSEIIGLTFRGPSETDLDGLVGQALFADGAASLVXXSDPIPGLEKPVFEIV  720
             NKGARVL+VCSEI  +TFRGP++T LD LVGQALF DGAA+++  SDPIP +E+P+FE+V
Sbjct  181   NKGARVLVVCSEITAVTFRGPTDTQLDSLVGQALFGDGAAAVIVGSDPIPEVERPLFELV  240

Query  721   SAAQTFIPESHGSITGDLREAGLIVKLSKNVPKFFGENIDKCLDEAFQPLGITDWNSIFW  900
             SAAQT +P+SHG+I G LRE GL   L K+VP    +NI K LDEAFQPLGI+DWNS+FW
Sbjct  241   SAAQTILPDSHGAIDGHLREVGLTSHLLKDVPGLISKNIGKALDEAFQPLGISDWNSLFW  300

Query  901   IAHPGGALILDKVEQKLGLHPKKLRATRHILSEYGNMSSVCVFFILDEVRKYSIKNGFST  1080
             IAHPGG  ILD+VE+KL L P+KLR+TRH+LSEYGNMSS CV FILDE+RK S KNG ST
Sbjct  301   IAHPGGPAILDQVEEKLALKPEKLRSTRHVLSEYGNMSSACVLFILDEMRKSSAKNGLST  360

Query  1081  TCEGLEWGVLFGLGPGLTVETVVLRSVAI  1167
             TCEGLEWGVLFG GPGLTVETVVL SV++
Sbjct  361   TCEGLEWGVLFGFGPGLTVETVVLHSVSV  389
```

Figure 62. Comparison of Gl2BICS with the best match in the databank, a CHS.

On performing NCBI-BLAST for the *Gl2BICS* gene, most hits were *CHSs* with ~74% identity, which was not high enough to predict that GL2BICS would be a CHS. Therefore, it was interesting to study its alignment with the other PKSs from the databank. An alignment was obtained using MegAlign software (Fig. 63). Note that putative BICS from *G. lutea* (number 1) shared a maximum of 96.1% identity with putative BICS from *G. acaulis* (number 3). This was a promising result and initiated to hypothesize that the GL2BICS protein might have a function of BICS.

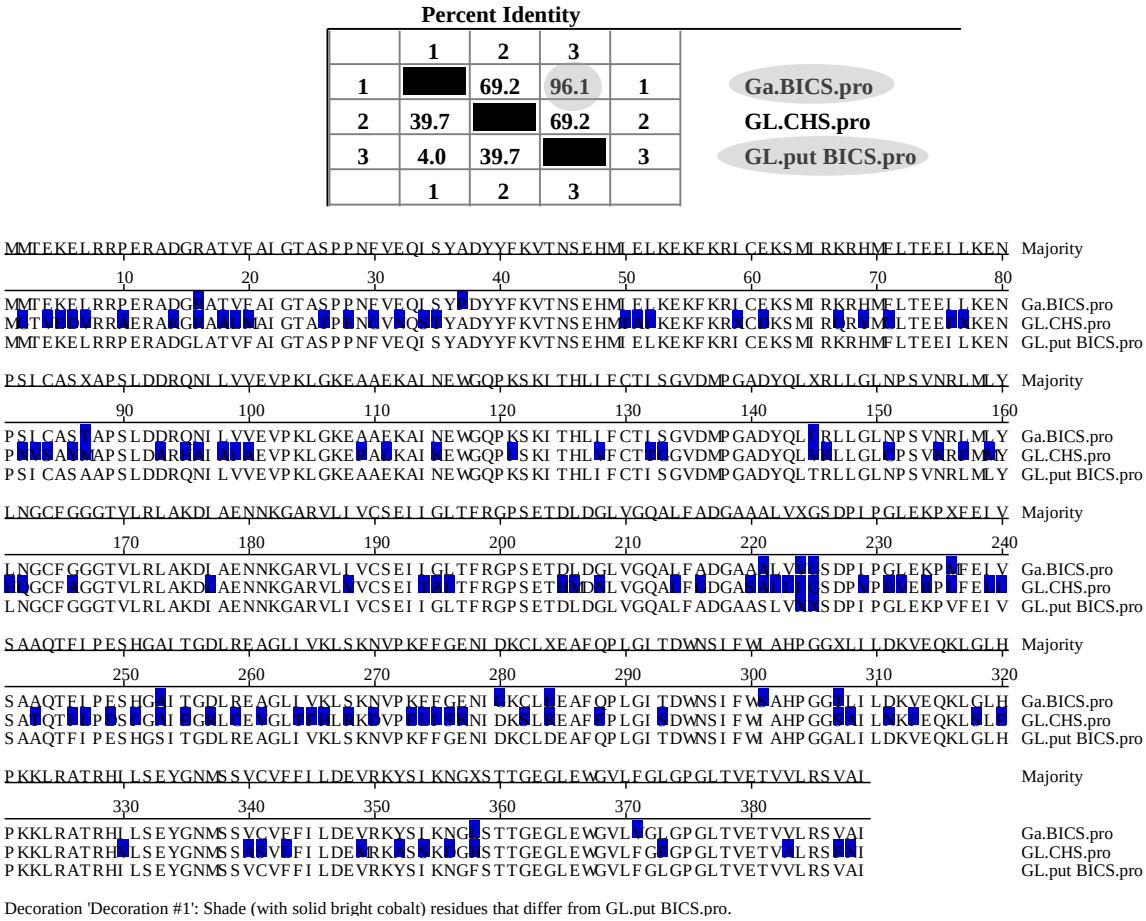

Figure 63. Amino acid alignment of *G. lutea* (Gl.putBICS) with *G. acauris* (Ga.BICS) and *G. lutea* chalchone synthase (Gl.CHS).

3.3.4 Expression of the GL2BICS ORF in *E. coli*

To induce the production of the recombinant protein, IPTG was added. The cloned target sequence (putative BICS) was successfully expressed in the *E. coli* BL21 strain. The efficiency of the expression was detected by SDS-PAGE (Fig. 64). The size of the expressed protein (pure sample) matched the calculated subunit size of 42.7 kDa.

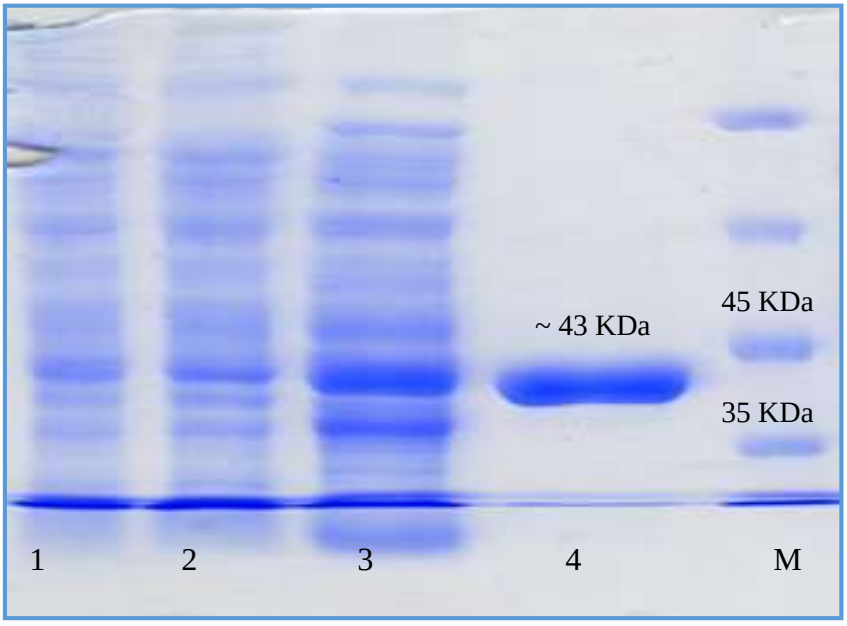

Figure 64. SDS-PAGE (12%) of fractions containing Gl2BICS protein after the following purification steps, steps. 1: pre-induction. 2: post-induction. 3: pellet. 4: pure protein.

3.3.5 *Gentiana lutea* biphenylcarboxylate synthase (GLBICS) assay

Since we cloned a full-length cDNA with an ORF of 1170 bp from *G. lutea*, which shared a high percentage of identity with putative *G. acaulis* BICS (96.1%), we were interested in the enzymatic activity. The activity of the pure recombinant protein (GL2BICS) was checked using the standard substrates 3-hydroxybenzoyl-CoA and benzoyl-CoA as starter substrates and malonyl-CoA as extender substrate in a standard incubation (2.2.1.6). Products were analyzed by HPLC using gradient 1 (2.2.2.1). Samples for control were incubated without adding the starter substrate. Several attempts were carried out, however, no enzymatic activity was detected.

4 Discussion

4.1 The physiological starter substrate in the Gentianaceae family

In xanthone biosynthesis, the preferred starter molecule is either 3-hydroxybenzoyl-CoA or benzoyl-CoA. Sequential chain elongation with three molecules of malonyl-CoA yields an intermediate benzophenone, as proved in cell cultures of *C. erythraea* and *H. androsaemum* (Beerhues 1996; Schmidt and Beerhues 1997). In Gentianaceae, the physiological starter substrate is 3-hydroxybenzoic acid, which originates from a different pathway compared to other xanthone-producing families. In Gentianaceae, it appears to originate directly from the shikimate pathway, which was confirmed by two studies. A first study was carried out with cell cultures of *C. erythraea* by Abd El-Mawla et al. (2001). The results showed the lack of incorporation of cinnamic acid into xanthones in a radiolabeled precursor feeding experiment, indicating that 3-hydroxybenzoic acid formation was through a phenylalanine-independent pathway. Furthermore, in cell cultures of *C. erythraea* benzoic acid was a poor substrate for 3-hydroxybenzoat:CoA ligase but 3-hydroxybenzoic acid was the best one. Thus, in this species 3-hydroxybenzoic acid appears to be the sole physiological substrate (Barillas and Beerhues 1997). Benzoic acid is a rare starter substrate for PKSs type III, although it is the preferred starter substrate for xanthone biosynthesis in Hypericaceae (Beerhues and Liu 2009).

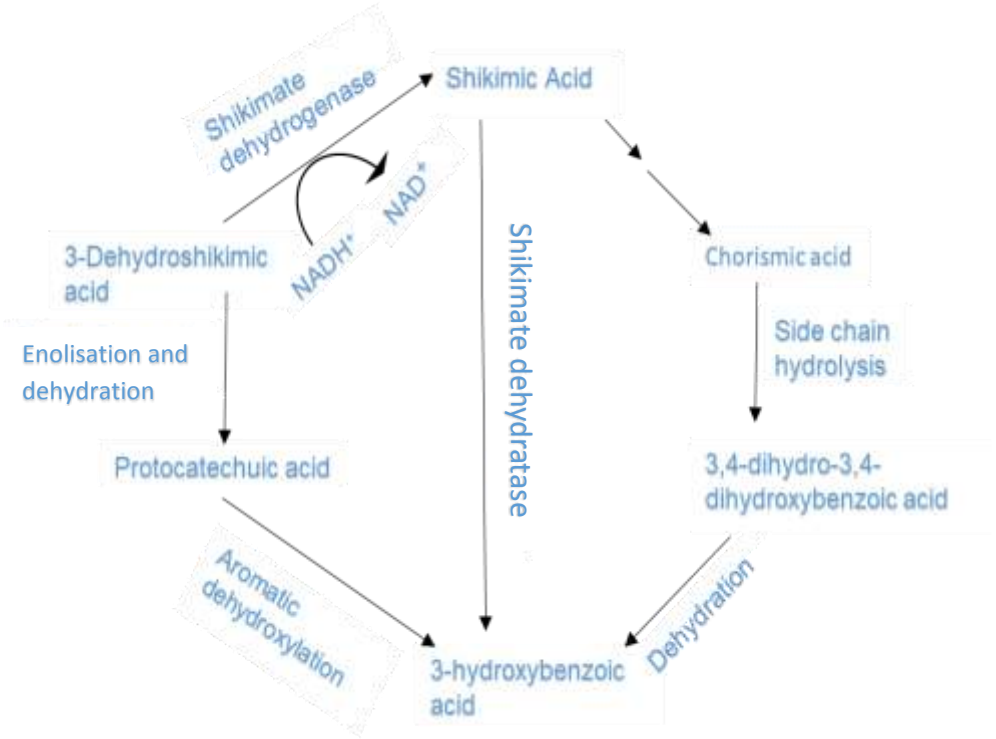

Figure 65. Intermediates of the shikimate pathway as potential precursors of 3-hydroxybenzoic acid (Abd El-Mawla et al. 2001).

A second study was carried out by Wang et al. (2003). This study showed that the starter unit for 1,3,5,8-tetrahydroxyxanthone biosynthesis in root cultures of *Swertia chirata* was 3-hydroxybenzoyl-CoA, which originated from an early shikimate pathway intermediate and not from cinnamic acid, benzoic acid or phenylalanine. Also, phenylalanine ammonia-lyase (PAL) activity in cell cultures of *C. erythraea* agreed with this observation, because no change in this activity occurred post-induction with methyl jasmonate (Abd El-Mawla et al. 2001; Beerhues and Berger 1995). 3-Hydroxybenzoic acid is then converted to its CoA-ester by 3-hydroxy benzoate CoA ligase, which was separated from *p*-coumarate:CoA ligase by fractionated ammonium sulphate precipitation and hydrophobic interaction chromatography (Barillas and Beerhues 1997; Singh 2014). 3-Hydroxybenzoyl-CoA then enters either xanthone or amarogentin biosynthesis by BPS and BICS, respectively. Very limited physiological function of 3-hydroxybenzoic acid has been reported. In some secoiridoides, a 3-hydroxybenzoyl residue occurrs (van der Sluis and Labadie 1981), and it was detected in a tropane alkaloid from *Cochlearea aretica* (Liebisch et al. 1973).

4.2 3-Hydroxybenzoyl-CoA synthesis

Previously, 3-hydroxybenzoyl-CoA was synthesized via the *N*-hydroxy-succinimide ester of 3-hydroxybenzoic acid, followed by transesterification with CoA (Beerhues 1996). To synthesize 3-hydroxybenzoyl-CoA, a new alternative attempt has recently been achieved to overcome the problems faced in the method carried out in our lab by Singh (2014). The product was an undesirable (impure) compound after storage at -20°C for a longer time. Therefore, a new batch of 3-hydroxybenzoyl-CoA was synthesized (Liu, 2016, unpublished) by using the 'modified imidazolide method'. The synthesized product was used in the present work for biochemical characterizations and studies of the kinetic parameters of the newly cloned enzymes CeBPS and ScBPS. In addition, the synthetic procedure and subsequent purification yielded two novel related CoA esters from different fractions: 3-(3-hydroxybenzoyloxy)benzoyl-CoA and 3-((3-hydroxybenzoyloxy)3-hydroxylbenzoyloxy)-benzoyl-CoA. The analysis of all fractions was carried out by UV spectroscopy, mass spectrometry and, for 3-(3-hydroxybenzoyloxy) benzoyl-CoA, also by ^{1}H-NMR spectroscopy (Table. 5). The two new CoA esters were previously not detected in plant cell cultures.

4.3 Plant type III polyketide synthases

Type III PKSs are of simple structure. They are small homodimeric proteins of approximately 40-45 kDa with a conserved region in the active site. Through structural insight into the reaction mechanism of *M. sativa* CHS the existence of three interconnected cavities were detected: CoA binding pocket, coumaroyl-binding pocket and cyclization pocket (Austin and Noel 2003). Type III PKSs give rise to a diversity of secondary metabolites by varying the starter molecules ranging from aliphatic to aromatic CoA esters and from smaller molecules (acetyl-CoA) to bulky molecules (*p*-coumaroyl-CoA) and from polar (malonyl-CoA) to nonpolar (isovaleroyl-CoA). This leads to extraordinary functions and thereby chemical diversification (Austin and Noel 2003; Flores-Sanchez and Verpoorte 2009). This remarkable variety is further increased by differences in the number of acetyl addition (1 to 7) and the

mechanism of ring formation used to form the final product (Claisen condensation, aldol condensation, or heterocyclic lactone formation) (Austin and Noel 2003; Schröder 1999). A large number of *CHS* genes and a lot of new members of the plant type III PKSs were cloned and characterized with novel and unexpected activities. These findings confirm the important role of type III PKSs in generating a wealth of substantially variable molecules by contributing to the biosynthesis of many classes of plant secondary metabolites (Abe 2010; Duckworth 2012). Benzophenone synthase is a type III PKS and the first two full-length cDNAs cloned from cell cultures of *C. erythraea* were inactive as BPS, in spite of the presence of the conserved catalytic triad (Cys^{164}-His^{303}-Asn^{336}) (Liu and Beerhues, unpublished results). On the other hand, two cDNAs encoding BPS and BIS were successfully cloned from cell suspension cultures of *H. androsaemum* and *S. aucuparia*, respectively. Both used benzoyl-CoA as starter substrate but formed 2,4,6-trihydroxybenzophenone and 3,5-dihydroxybiphenyl, respectively. Both were inactive with CoA-linked cinnamic acids, which mostly serve as starter substrates for chalcone synthases and stilbene synthases (Liu et al. 2003; Liu et al. 2007). In the last years, two cDNAs were successfully cloned from *C. erythraea* cell cultures in our laboratory. One of them was inactive (CePKSI), but the second one was functional as phenylpyrone synthase (CePPS) (Agarwal 2013). Recently, a cDNA encoding PPS (ScPKS1) and a cDNA encoding putative BPS (ScPKS2) have been cloned from root cultures of *S. chirata* (Agarwal 2013).

4.3.1 Benzophenone synthases from *Centaurium erythraea* and *Swertia chirata*

It is interesting to work on the molecular aspects of xanthone biosynthesis in *C. erythraea* and *S. chirata*, because there have been various types of studies on the metabolite profile and the detection of different types of xanthones (Aberham et al. 2011; Bajpai et al. 1991; Ghosal et al. 1973a; Scharnhop 2008; Valentão et al. 2001). *In vitro* studies have shown the accumulation of xanthones in cell suspension cultures of *C. erythraea* before and after treatment with elicitors (Beerhues and Berger 1994; 1995). In addition, two studies were carried out with root cultures of *S. chirata* and various xanthones and amarogentin were detected (Agarwal 2013; Singh 2014). The activity of benzophenone synthase was detected for the first time in cell-free extracts of cultured cells of *C. erythraea* (Beerhues 1996). The incubation of synthesized 3-hydroxybenzoyl-CoA with malonyl-CoA and desalted crude protein extract from 5-d old cells showed the formation of 2,3` ,4,6-THB .

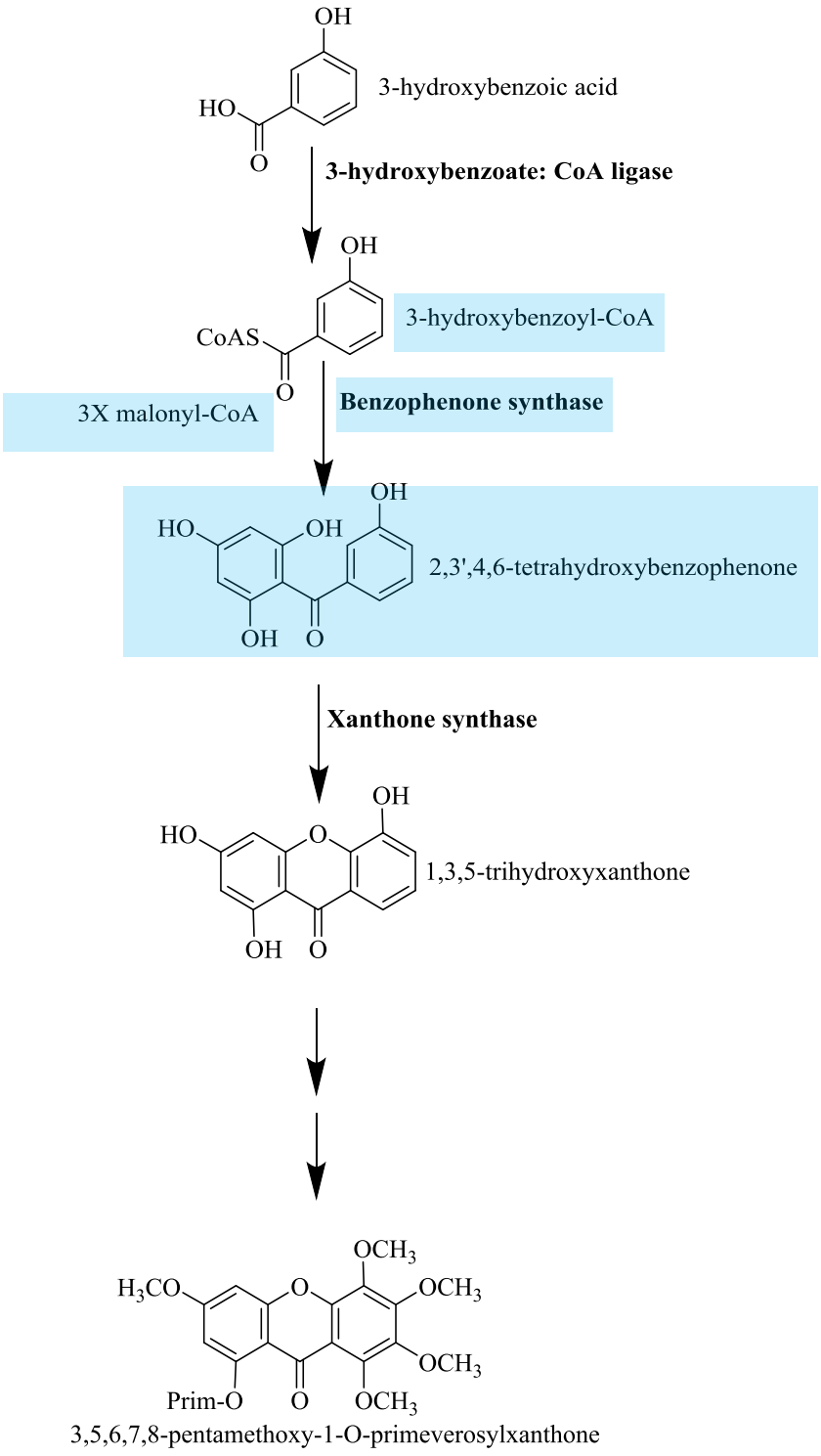

Figure 66. Proposed xanthone biosynthesis pathway in cell cultures of *Centaurium erythraea* (Peters et al. 1997)

Feeding experiments with intact plants of *Gentiana lutea* and *Garcinia mangostana* have demonstrated that 2,3` ,4,6-THB is an intermediate in xanthone biosynthesis (Peters et al. 1997). Furthermore, formation of 2,4,6-THB was found upon incubation of crude protein

extract with benzoyl-CoA and malonyl-CoA. Thus, benzophenone synthase is the enzyme catalyzing the central step in xanthone biosynthesis by the formation of the C_{13} skeletone, i.e an intermediate benzophenone (Fig. 66). The majority of xanthones are distributed between two plant families, Gentianaceae and Hypericaceae. Oxygenated xanthones are common in both families but more highly oxygenated xanthones are found in Gentianaceae, while prenylated xanthones are widely distributed in Hypericaceae (Bennett and Lee 1989). As mentioned above, some attempts were carried out at the molecular level but failed to clone active benzophenone synthase from cell suspension cultures of *C. erythraea*. This was motivating us to proceed in cloning BPS from these cell cultures, which finally succeeded. The full-length cDNA contained a 1170 bp open-reading frame (ORF) with a GC content of 50.17 % and an AT percentage of 49.83 %. This cDNA encoding a 42.3 kDa protein was heterologously expressed as a His_6-tagged protein consisting of 389 amino acids and having a *pI* of 6.269. The similarity of the CeBPS sequence with the putative ScBPS reached 82.8%. ScBPS has recently been cloned from root cultures of *S. chirata*. ScBPS was heterologously expressed as a N-terminally His_6-tagged protein. The ORF encodes a 42.7 kDa protein that contained 392 amino acids with a *pI* of 6.001. The GC percentage was 45.38% and the percentage of AT was 54.28 % (Agarwal 2013). It was interesting to work on two new BPSs from Gentianaceae, which had novel properties. At the level of amino acid sequence, general comparisons were achieved between the two recent benzophenone synthases CeBPS and ScBPS.

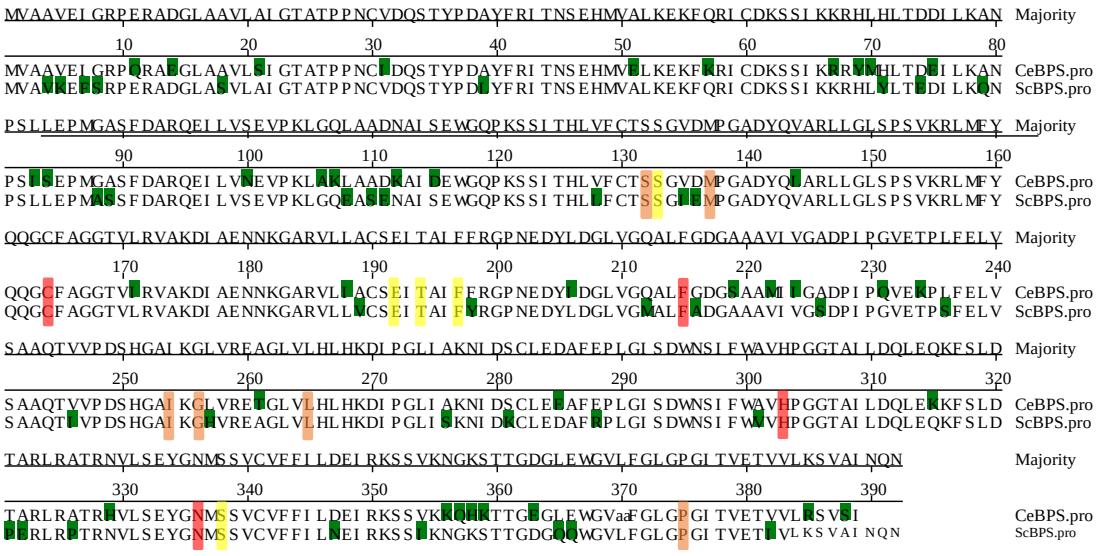

Figure 67. Amino acids alignment of *Centaurium erythraea* BPS and *Swertia chirata* BPS.

As mentioned above, the similarity between the two sequences CeBPS and ScBPS was high and reached 80.8**%.** This means that around 20% of the amino acids residues have no similar partners (blue highlights). However, the two amino acid sequences had 100% similarity in amino acid residues present in the three inter-connected cavities: For catalytic residues, as shown in Fig. 67, both enzymes had four conserved amino acid residues (Cys164, Phe215, His303 and Asn336) (red highlights). For substrate binding pocket residues, both enzymes had

the same amino acids at the following sites (Ser133, Glu192, Thr194, Phe197 and Ser338) (yellow highlights). Furthermore, they showed similarity in the amino acid residues that form the cyclization pocket (Ser132, Met137, Phe215, Ile254, Gly256, Phe265 and Pro375) (brown highlights). So, comparing the two new cloned benzophenone synthases revealed identical sites, which play a critical role in the determination of the characteristics, for example, the starter substrate selectivity. This justifies that both enzymes had similar biochemical characterizations. The optimal reaction conditions for both BPSs (pH 7, 35°C, 10-15 min) were comparable with the published data for the *Hypericum* benzophenone synthases (Huang et al. 2012; Liu et al. 2003; Nualkaew et al. 2012; Zodi 2011). However, some other properties were not observed in the other BPSs cloned from *Hypericaceae* , exemplified by the finding that both enzymes (CeBPS and ScBPS) lost more than 50% of activity after storage at different temperature conditions (0°C, 4°C, -20°, -80°C) (Fig. 28 and 29). For this reason, the proteins were used immediately (freshly) after purification on Ni-NTA agarose and were not suitable for usage after some days of storage. In addition, both enzymes were not dependent on the dithiothreitol (DTT) concentration, as shown by incubating both BPSs at various concentrations of DTT (10, 25, 50, 100, 200, 250, 500, and 1000 µM). We observed that the maximum activity of BPSs started to decrease in the presence of DTT compared with the standard incubation with 0 µM DTT. DTT is was used to decrease the oxidation risk in purifying enzymes that have catalytic cysteine. They are prevented from formation of non-specific intramolecular disulfide linkages, which alter its configuration. In some proteins, adding DTT plays a critical role. For example, the activity of BPS from crude protein extracts of *C. erythraea* was strictly dependent on DTT (25 µM), leading to maximum activity of the enzyme (Beerhues 1996). In this connection, HaBPS showed maximum activity when the incubation contained 50 µM DTT. When omitting DTT, the activity of the enzyme was reduced by approximately 40% (Liu et al. 2003). This means that some specific characters were detected in both enzymes (CeBPS and ScBPS) but not in the previously cloned BPSs. For both CeBPS and ScBPS, it was an incentive for us to test the substrate specificity with different CoA esters. The enzymes were incubated after purification under the optimal assay conditions with a serious of CoA esters (Fig. 35). Three different predominant enzymatic products were detected: 2,3` ,4,6-THB, 2,4,6-THB, and styrylpyrone in five different incubations. 2,3` ,4,6-THB was the main enzymatic product upon incubation of the enzymes with three related 3-hydroxybenzoyl-CoA substrates: 3-hydroxybenzoyl-CoA, 3-(3-hydroxybenzoyloxy)benzoyl-CoA, and 3-(3-hydroxybenzoyloxy)3-hydroxylbenzoyloxy)-benzoyl-CoA. The maximum activity was detected for 3-(3-hydroxy**benzoyloxy)benzoyl-CoA**. All substrates could form the same linear tetraketide intermediate after three malonyl-CoA condensations. Catalyzed by C6 to C1 Claisen condensation, 2,3` ,4,6-THB was formed as a final product. These results were supported by the activity of previous cloned BPSs, as mentioned above. The absolute amounts of the individual enzymatic products obtained were estimated based on their absolute peak areas in the HPLC chromatograms obtained at the same experimental conditions. CeBPS and ScBPS failed to form a product when incubated with 2-hydroxybenzoyl-CoA and 4-hydroxybenzoyl-CoA. Also, the wild-type of HaBPS and the T135L mutant were inactive with the last two substrates (Klundt et al. 2009). The second best substrate was cinnamoyl-CoA with

CeBPS (72%) and ScBPS (94%). CeBPS and ScBPS catalyzed the addition of only two acetyl units to the starter molecule. The triketide is the final linear intermediate formed and then cyclizes into styrylpyrone via C-5 keto-enol oxygen to C1 lactonization. On the other hand, we failed to detect an enzymatic product when using *p*-coumaroyl-CoA as substrate. This result is comparable with the activity of the T135L mutant of wild-type HaBPS (Klundt et al. 2009). The T135L mutant catalyzes the iterative condensation of benzoyl-CoA with two malonyl-CoAs to give a linear intermediate triketide that undergoes intramolecular cyclization via C-5 keto-enol oxygen to C-1 lactonization. The T135L mutant was not active with 3-hydroxybenzoyl-CoA. The homology models of the active site cavity of the T135L mutant showed that both starter substrates, benzoyl-CoA and 3-hydroxybenzoyl-CoA, are covalently attached to the catalytic cysteine 167 and that the triketide is redirected into a new pocket where no further chain elongation takes place. Moreover, in case of 3-hydroxybenzoyl-CoA, the study showed the formation of a hydrogen bond with the backbone carbonyl and amide group of Gly-166, which explained that the triketide intermediate of 3-hydroxybenzoyl-CoA may be trapped in the new pocket and may play a role as inhibitor (Fig. 68). The same explanations may be true for our results in this study, when CeBPS and ScBPS are active with cinnamoy-CoA but are not active with *p*-coumaroyl-CoA as starter substrate.

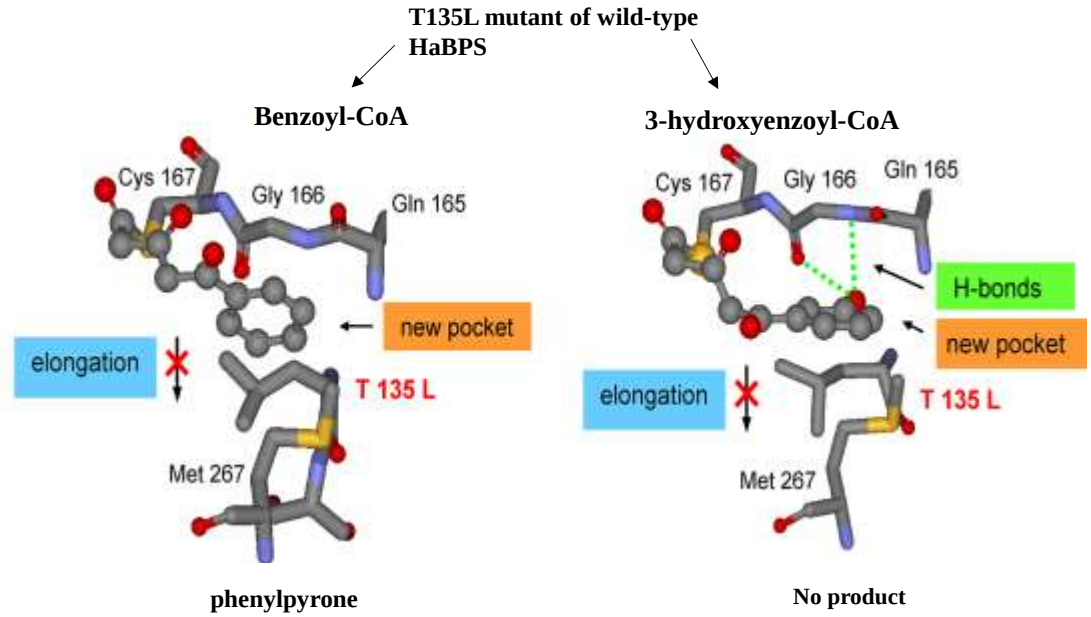

Figure 68. CHS based homology models of the active site cavities of the T135L mutant. Adapted from Klundt et al. (2009).

Generally, type III PKSs utilize various substrates to form different enzymatic products. To exemplify, BPSs were cloned from several *Hypericaceae*: *H. androsaemum* HaBPS (Liu et al. 2003), *H. calycinum* HcBPS (Zodi 2011) , *H. sampsonii* HsBPS (Huang et al. 2012), and *Garcinia mangostana* GmBPS (Nualkaew et al. 2012)). Although they showed variant substrate specificities, they all had 100 % maximum activity with benzoyl-CoA as starter substrate and 2,4,6-THB was the main product. HaBPS exhibited 18.8 % and 10.9 % maximum

activity with 3-hydroxybenzoyl-CoA and *N*-methylanthraniloyl-CoA, respectively, to form 2,3` ,4,6-THB and 1,3-dihydroxy-*N*-methylacridone as the products. HsBPS had, besides the activity with benzoyl-CoA, 66% relative activity with 3-hydroxybenzoyl-CoA and derailment activity with 2-hydroxybenzoyl-CoA (salicoyl-CoA), leading to 2,3` ,4,6-THB and 4-hydroxycoumarin as products, respectively. HcBPS showed 37% relative activity with 3-hydroxybenzoyl-CoA and 2,3` ,4,6-THB was the producd. Biphenyl synthase from *Sorbus aucuparia* (SaBIS), another type III PKS, also used benzoyl-CoA as preferred starter substrate and 3,5-dihydroxybiphenyl was the final product. Furthermore, SaBIS showed 68% and 52% of the maximum activity with 3-hydroxybenzoyl-CoA and 2-hydroxybenzoyl-CoA, respectively, leading to the formation of 6-(3-hydroxy-phenyl)-4-hydroxy-2-pyrone and 4-hydroxycoumarin (Liu et al. 2007). All above BPSs of *Hypericum* species and BIS from *S. aucuparia* did not accept CoA esters of cinnamic acid as starter molecules. An exception was GmBPS which showed more variation in the usage of starter substrates, consequently different types of products were formed (phloroglucinol, triketide lactone, and tetraketide lactone), resulting from activity with benzoyl-CoA 100%, acetyl-CoA 19% , phenylacetyl-CoA 12%, hexanoyl-CoA 11%, cinnamoyl-CoA 15%, *p*-coumaroyl-CoA 9% and 2-hydroxybenzoyl-CoA 10% of the maximum activity (Nualkaew et al. 2012). The shape and size of the active site of type III PKSs affect the selectivity of starter substrate and the number of malonyl-CoAs needed for condensation. Our results showed high selectively between the related aromatic substrates, for example, cinnamoyl-CoA and *p*-coumaroyl-CoA. CeBPS and ScBPS could use cinnamoyl-CoA with 2x malonyl-CoA condensation and styrylpyrone was the product formed in the active site, with a high percentage of relative activity being reached (72% and 94% of maximum activity, respectively). Upon one addition of a hydroxyl group as in *p*-coumaroyl-CoA, the enzymes failed to use it, no enzymatic product was detected. Intriguingly, the promiscuous substrate selectivity was shown with three related 3-hydroxybenzoyl-CoA substrates possessing one, two and three benzoyl residues. CeBPS and ScBPS had a similar order of selectivity with the three related substrates. CeBPS showed 100% activity with 3-(3-hydroxybenzoyloxy)benzoyl-CoA, 56% with 3-((3-hydroxybenzoyloxy)3-hydroxylbenzoyloxy)-benzoyl-CoA, and 46% with 3-hydroxybenzoyl-CoA. ScBPS showed 100% with 3- (3-hydroxybenzoyloxy)benzoyl-CoA, 74% with 3-((3-hydroxybenzoyloxy)3-hydroxylbenzoyloxy)-benzoyl-CoA, and 42% with 3-hydroxybenzoyl-CoA.

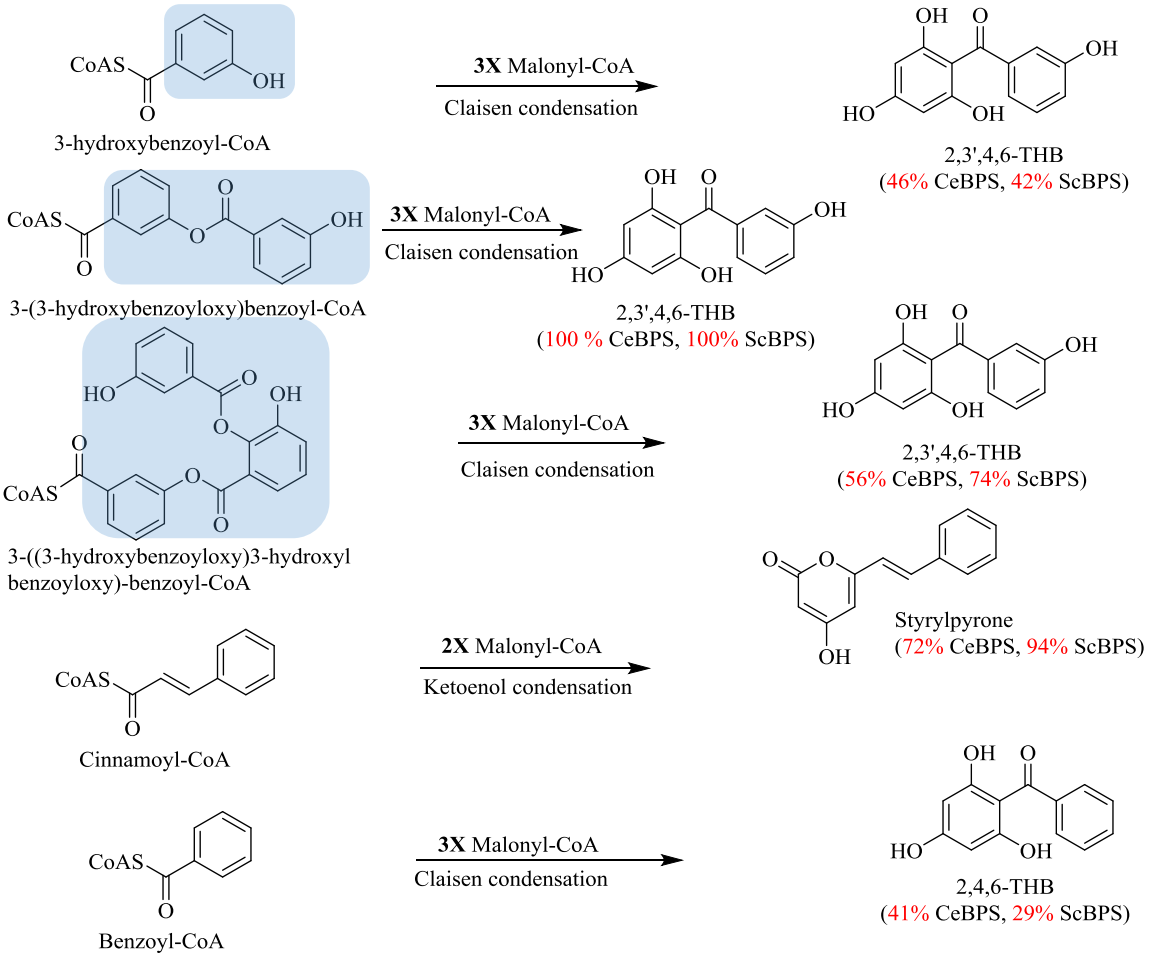

Figure 69. Enzymatic products formed by condensation of malonyl-CoAs with five preferred starter substrates for CeBPS and ScBPS.

The recently cloned GmBPS generated with large aromatic substrates, e.g. cinnamoyl-CoA and *p*-coumaroyl-CoA, only triketide lactones as products (Nualkaew et al. 2012). By contrast, CeBPS and ScBPS used the large aromatic substrates like cinnamoyl-CoA, 3-(3-hydroxybenzoyloxy)benzoyl-CoA and 3-((3-hydroxybenzoyloxy)3-hydroxylbenzoyloxy)-benzoyl-CoA) to generate both types of products: benzophenone and triketide lactone. This suggested that the active site size of both CeBPS and ScBPS may be larger than that of GmBPS. One of the most essential properties in engineering an enzyme for selective catalysis is changing the substrate selectivity by redirecting the specificity towards novel substrates or expanding and narrowing the substrate selectivity. To make this explicit, the mutation part (site-directed mutagenesis) plays a dramatic and sense effect on the explanation of the results. Based on the crystal structure of MsCHS2, the three amino acids T197, G256, S338 were supposed to play a critical role in controlling the starter substrate selectivity and the number of malonyl-CoA condensations by steric modulation of the active site cavity, thereby providing clarification for the starter molecule preference (Jez et al. 2001). More specifically, the triple

mutation of MsCHS2 (T197L, G256L, and S338I) transformed the enzyme into a functional 2-pyrone synthase (2-PS), which used a different substrate (acetyl-CoA vs. *p*-coumaroyl-CoA) and formed a new product (triacetic acid lactone vs. naringenin) (Jez et al. 2000). This result provided us a first insight into the structural basis of the volume and shape of the active site to affect the functional diversity of type III PKSs (Abe and Morita 2010; Dana et al. 2006). Many studies were done for different type III PKSs on the inert active site residues (T197, G256, S338), which control the starter substrate specificity and polyketide chain elongation by steric modulation of the initiation/elongation cavity (Abe et al. 2005; Abe et al. 2004). After we cloned the new benzophenone synthases, a general comparison was achieved with the most interesting PKSs of type III, most of which were cloned in our laboratory. Phenylpyrone synthases were cloned from cell cultures of *C. erythraea* CePPS (Agarwal 2013) (unpublished results) and from root cultures of *S. chirata* ScPPS (Agarwal 2013). The first BPS was cloned from *H. androsaemum* HaBPS (Liu et al., 2003) and compared with chalcone synthase from *Medicago sativa* MsCHS2. In ScBPS and CeBPS, some positions (Fig. 70) were promising sites, which were supposed to play a vital role in controlling the starter substrate selectivity and the number of malonyl-CoA condensations by steric modulation of the active-site cavity and providing an illustration for the starter molecule preference of both new BPSs. CeBPS and ScBPS had similar amino acids residues in all critical positions (initiation pocket and elongation pocket), as mentioned above (Fig. 67). So, the first promising sites for mutation in the future are S135, T197, F200, G260 to be transformed into I135, I197, T200, A260. These changes are expected to show an effect at the level of starter substrate selectivity and product formation. HaBPS was transformed into a functional phenylpyrone synthase by a single mutation in the active site cavity T135L, so the enzyme was dramatically changed in both substrate and product specificities (Klundt et al. 2009). Furthermore, the effect of all possible amino acids in position 135 of *H. sampsonii* BPS wild-type enzyme was studied and the results showed that only a single amino acid substitution (T135K) switched the substrate specificity of HsBPS wild-type from benzoyl-CoA and 3-hydroxybenzoyl-CoA to salicoyl-CoA (Abdelaziz 2014). This change was not in the substrate specificity but at the level of product specificity from benzophenone after three malonyl-CoA additions (Claisen condensation) to 4-hydroxycoumarin after only one malonyl-CoA addition (spontaneous lactonization).

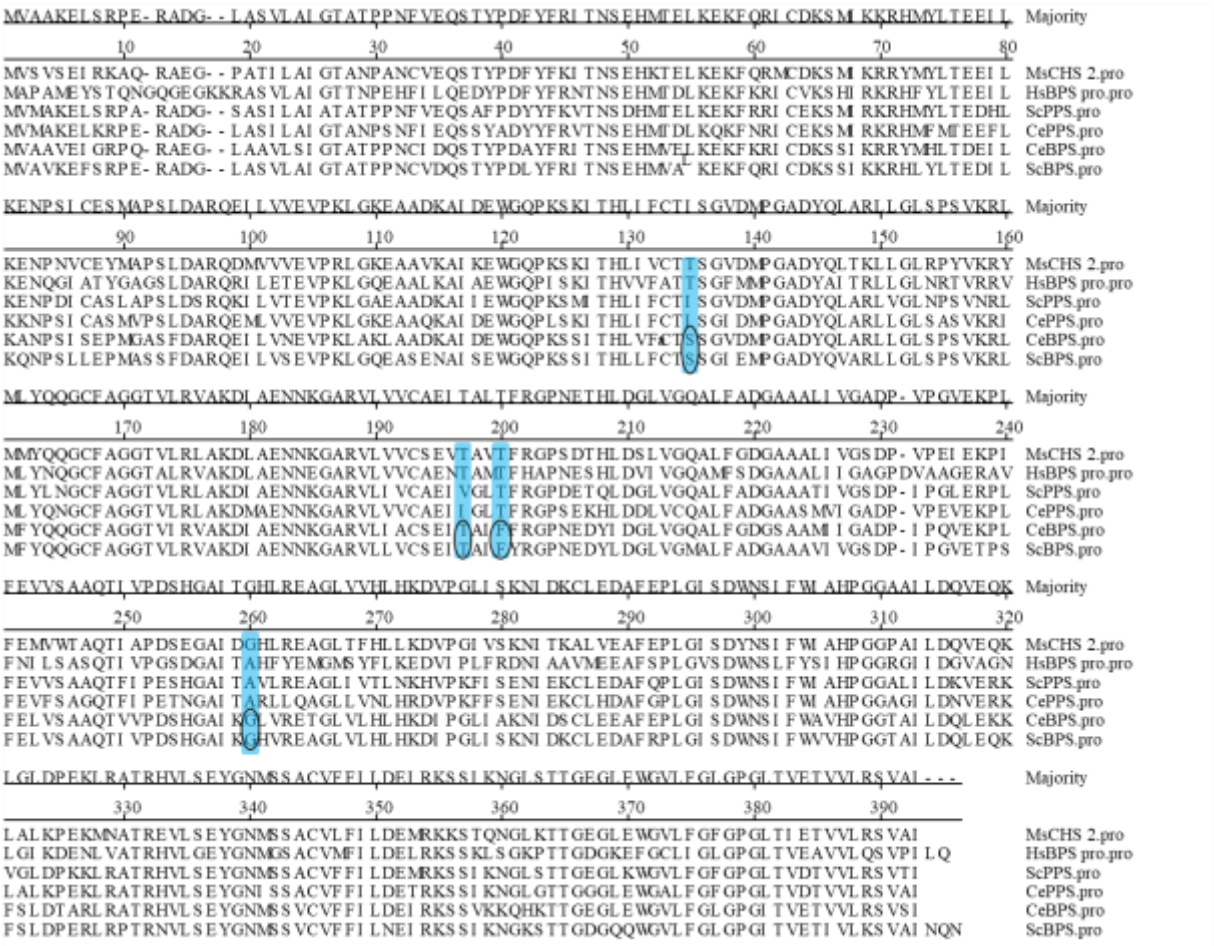

Figure 70. Amino acid sequence alignment of CeBPS, ScBPS, HaBPS (accession number AAL79808), CePPS, ScPPS and MsCHS2 (accession number P30074).

The article of Jez et al. (2001) showed that there is a direct relationship between the structural variation in the active site cavity and the functional alteration in the cyclization reaction. The 3D structure of the active site of the enzyme and the shape and size of the starter molecules are main factors to optimal stabilization of the intermediate formation. Site direct mutations at inert active site residues of CeBPS and ScBPS, as marketed in Fig. 70, as well as X-ray crystallographic studies will give us more explanation and illustration about the substrate specificity and polyketide chain formation.

The kinetic analysis of both enzymes, CeBPS and ScBPS, indicated that both enzymes accepted 3-(3-hydroxybenzoyloxy)benzoyl-CoA with more efficiency than cinnamoyl-CoA. The catalytic efficiency (K_{cat}/K_m) values for 3-(3-hydroxybenzoyloxy)benzoyl-CoA were about 1.5-2.4 fold higher than for cinnamoyl-CoA with CeBPS and ScBPS (Table 4). In case of CeBPS, the K_{cat}/K_m value for 3-((3-hydroxybenzoyl)-oxy)benzoyl-CoA was 1.5, 2.6, 19, 20.5 fold higher than for cinnamoyl-CoA, 3-(3-hydroxybenzoyloxy)3-hydroxylbenzoyloxy)-benzoyl-CoA, 3-hydroxybenzoyl-CoA and benzoyl-CoA, respectively. Also, ScBPS showed the highest catalytic efficiency with 3-(3-hydroxybenzoyloxy) benzoyl-CoA, which was 2.4,

2.5, 5, and 14 fold higher than those for cinnamoyl-CoA, 3-((3-hydroxybenzoyloxy)3-hydroxylbenzoyloxy)-benzoyl-CoA, 3-hydroxybenzoyl-CoA and benzoyl-CoA, respectively.

Table 4. Catalytic efficiency of *Centaurium erythraea* and *Swertia chirata* benzophenone synthases.

Substrates	K_{cat}/K_m (min^{-1} M^{-1}) CeBPS	K_{cat}/K_m (min^{-1} M^{-1}) ScBPS
3-(3-hydroxybenzoyloxy) benzoyl-CoA	162500	122300
Cinnamoyl-CoA	145925	56444
3-((3-hydroxybenzoyloxy)3-hydroxylbenzoyloxy)-benzoyl-CoA	62500	49394
3-hydroxybenzoyl-CoA	8421	25008
Benzoyl-CoA	8075	9598

4.3.2 *CeBPS* gene expression

Kinetic analysis of the recombinant protein and expression studies give more explanation about the role of benzophenone synthases in xanthone biosynthesis. In Hypericaceae, such as *Hypericum calycinum*, the transcript level of *HcCYP81AA1* was increased after yeast extract treatment, which was associated with xanthone formation. The transcript levels increased rapidly post-elicitation, reached the maximum level at 8h and then decreased. Also, the transcript level for *HcCPR2*, which indirectly contributes to the biosynthesis of xanthones, undergoes similar changes (El-Awaad et al. 2016). The upregulation was not only for *HcCYP81AA1* and *HcCPR2* but also for cinnamate:CoA ligase (CNL), which catalyzes the formation of cinnamic acid, one building block of the xanthone scaffold in this family (Gaid et al. 2012). The preliminary study for expression analysis of *CeBPS* did not yield the expected result, as mentioned above for *Hypericaceae*. The variation observed in the transcript level for CeBPS post-elicitation with Ye agreed with the constant xanthone level in cell cultures of *C. erythraea* post elicitation. In cell cultures of *Swetia chirata*, the pattern of *ScBPS* expression was studied in the leaves and two types of root cultures (root 1 = root from plantlet; root 2 = root from callus) without treatment by elicitation as shown in Fig. 71 (Agarwal 2013). The results showed that the expression of *ScBPS* was higher in roots 1 than in leaves and roots 2.

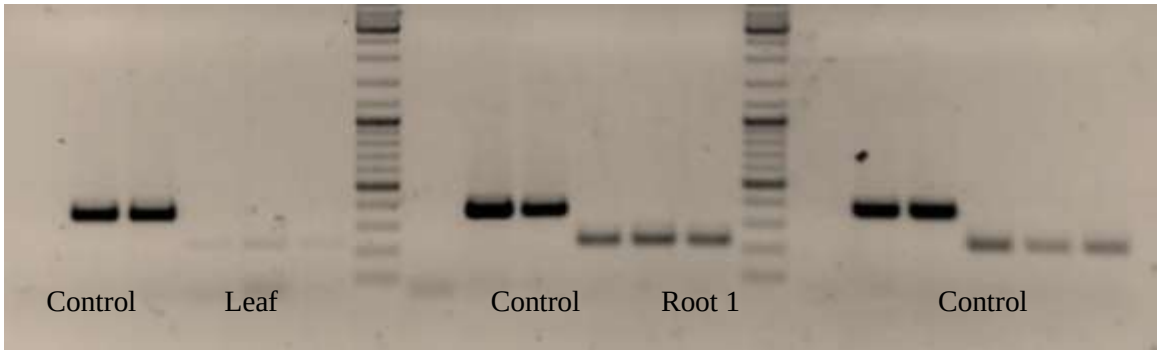

Figure 71. *ScBPS* expression pattern in *S. chirata* leaf, root 1 (from plantlet) and root 2 (from callus) (Agarwal 2013).

4.4 Accumulation of xanthones in cell cultures of *C. erythraea*

In vivo plants of Gentianaceae were observed to contain metabolite profiles including iridoids and xanthones. In contrast, *in vitro* cultures were almost devoid of any iridoid (Beerhues and Berger 1994). An extensive study was performed with two species of *Centaurium*, i.e. *C. erythraea* Rafn and *C. littorale* (Turner) Gilmour. Xanthones were the main components, but the iridoids were below the detection limit. Cell suspension cultures of two species were established from the stems and shown to contain 3,5,6,7,8-pentamethoxy-1-*O*-primeverosylxanthone as a major component. This compound was accumulated in the cultures parallel with the growth. In this study, the tissue cultures were established from leaves of *in vitro* plants, seeds for which were from variant geographical sources (Stuttgart, Ulm, and Karlsruhe). The previously established callus in our laboratory (Fig. 12.1) was transferred in LS liquid medium supplemented with 1 mg/l NAA and 1 mg/l 2,4 D (Fig. 12.2). Afterwards, we started with the best growing cell suspension cultures. The cultured cells were elicited with two elicitors: MeJ and YE at final concentrations of 100 µM and 3 g/l, respectively, in order to change the pattern of metabolite constituents and stimulate xanthone biosynthesis pathway. Significant changes were observed in cell cultures of *C. erythraea* and *C. littoralle* after addition of MeJ and YE (Beerhues and Berger 1995). Cell suspension cultures of *C. erythraea* responded to MeJ and YE and exhibited the accumulation of 1-hydroxy-3,5,6,7-tetramethoxyxanthone and 1,5-dihydroxy-3-methoxyxanthone, respectively. Likewise, *C. littorale* formed both new compounds, but their amounts increased only after a lag phase of 25 h. In contrast, many cell cultures producing compounds post-induction excrete the major proportion of these constituents into the culture medium (Beerhues and Berger 1995; Hauffe et al. 1986; Keßmann and Barz 1987; Liswidowati et al. 1991). The newly established cell suspension cultures of *C. erythraea* (Ce_St and Ce_Kr) showed different responses compared with the previous study after addition of MeJ and YE. The extraction was carried out for the metabolites from the cells and the media. The cells were separated from the media around 48h after the onset of treatment by elicitors. The HPLC analysis of extracts from these cells failed to detect any change in the xanthone pattern in the chromatogram at wavelengths 319 nm and 289 nm (Fig. 54).

Cell cultures of *Hypericum androsaemum*, when grown in modified B5 medium, were shown to accumulate prenylated xanthone aglycones and their glucosides (Schmidt et al. 2000a). The cultures showed no appreciable changes in the pattern of constituents post elicitation with methyl jasmonate.

Xanthones were the main accumulated constituents observed in the metabolite profile of cell cultures of *C. erythraea* (Ce_Kr). The major reproducible peak was peak 2 (Fig. 54), which was detected in untreated cells and post-induction. It was identified as 1,5-dihydroxy-3-methoxyxanthone by comparison of its UV-Spectrum with authentic xanthones available in our laboratory. The 5-hydroxy group of 1,5-dihydroxy-3-methoxyxanthone corresponds to the 3-hydroxy group of 3-hydroxybenzoic acid, which is the physiological substrate in xanthone biosynthesis in this plant family (Beerhues 1996). It was accumulated post-treatment with yeast extract in two cell cultures of *Centaurium* species (Beerhues and Berger 1995). The roots of *Canscora decussata* (Gentianaceae) showed the presence of this compound between variant types of xanthone derivatives (Chaudhuri and Ghosal 1971). Cell suspension cultures of *C. erythraea* contained 1-hydroxy-3,5,6,7,8-pentamethoxyxanthone accumulating in untreated cells (peak 3, Fig. 54). In addition, the roots of *Eustoma grandiflorum* (Gentianaceae) also accumulated this derivative of xanthones (Sullivan et al. 1977).

The two major peaks observed in the HPLC chromatograms were in the media extracts after MeJ and YE treatment at 319 nm and 289 nm (Fig. 50). The two peaks were reproducibly present after a time interval from induction with MeJ and YE at one to five days. On the 2nd day, the highest level of peaks was observed. Therefore, it was intriguing for us to collect and analyse these peaks. As a result, the UV spectra and mass spectra indicated that both peaks were not related to the characteristic xanthone pattern (Fig. 51). In both UV spectra, the characteristic maxima of xanthones are absent compared with all available data referring to UV spectra (Agarwal 2013; Du et al. 2012; Jia et al. 2012; Scharnhop 2008; Shekarchi et al. 2010; Singh 2014; Wang 2008) This is also true for xanthone references available in our group. Cell cultures of *C. erythraea* contained xanthones in the untreated cells and the total xanthone content did not specifically respond to induction by yeast extract during a long time interval up to 96 h (Fig. 56).

Studies were also carried out with root cultures of *S. chirata* by Agarwal (2013); Singh (2014). The acetone extract of metabolites was found to contain variant oxygenated xanthones and derivative of xanthones, in addition to amarogentin. By contrast, the acetone extract of callus and cell suspension cultures of *Exacum affine* (Gentianaceae) did not contain any related peaks for xanthones, except after treating the cultures with 100 µM MeJ. A putative xanthone aglycone was detected in medium extract, while no xanthones were detected intracellularly (Singh 2014).

4.5 Biphenylcarboxylate synthase (BICS) from *Gentiana lutea*

Chemical synthesis of the biphenyl carboxylate moiety was reported by Wang et al. (2000). While the biosynthesis pathway was not studied at the enzyme or gene level. The study of this intermediate was started in our group by Swiddan (2010) and is up to date still an interesting point. The biosynthesis of amarogentin was postulated to be catalyzed by BICS, which catalyzes the formation of an unusual 3,3` ,5-trihydroxybiphenyl-2-carboxylate moiety using 3-hydroxybenzoyl-CoA and malonyl-CoA as starter and extender substrates, respectively (Fig. 11). In recent years, there is an increase in the number of studies that observe interesting novel pharmacological activities of amarogentin. So, the aim was the molecular cloning of a BICS cDNA from Gentianaceae (*G. lutea* and/or *S. chirata*), which are rich sources of amarogentin. Previously, a fragment was cloned from *G. lutea* with 741 bp length and 83% identity with CHS but no identity with BPS or BIS. Based on this fragment, we could obtain the full length sequence of putative BICS. The ORF length was 1170 bp and showed 74% identity with CHS after blasting the sequence in NCBI data bank. The amino acid sequence of the cloned gene (GL.put BICS) was aligned with putative BICS sequences available in the data bank, *Gentiana acaulis* Ga.BICS and *Gentiana lutea* CHS (GL.CHS). The results showed 96% identity of the new sequence with Ga.BICS and 69% identity with chalcone synthase. When tested for functionality, the purified enzyme failed to show any activity with 3-hydroxybenzoyl-CoA. Similarly, the test of the purified enzyme with 3-(3-hydroxybenzoyloxy)benzoyl-CoA as starter substrate in a standard incubation showed a negative result.

5 Summary

- The Gentianaceae family includes interesting herbaceous medicinal plants such as *Centaurium erythraea*, *Swertia chirata*, and *Gentiana lutea*. These plants are rich sources for bioactive compounds such as xanthones and amarogentin, which were reported to have a wide range of important pharmaceutical usages.

- Benzophenone synthase (BPS) is responsible for the formation of the C_{13} skeleton of benzophenones, which are main intermediates in xanthone biosynthesis. BPS is a relatively new member of type III PKSs. To date, all BPSs were cloned from *Hypericaceae* such as *H. androsaemum*, *H. sampsonii*, *H. calycinum* and *H. perforatum* ssp *angustifolium* and *Garcinia mangostana*. For all, the preferred starter substrate is benzoyl-CoA, leading to the formation of 2,4,6- trihydroxybenzophenone after three iterative condensations with malonyl-CoA via C_6 to C_1 Claisen condensation.

- A first goal of this work was successfully achieved by cloning a full-length cDNA for **BPS** with a 1170 bp ORF from cell suspension cultures of *C. erythraea* after elicitation with MeJ and YE, starting with degenerate primers derived from conserved regions of type III PKSs. Another full-length cDNA with a 1179 bp ORF has recently been cloned in our group from root cultures of *S. chirata*. Both new **BPSs** shared 80.8% identity at the amino acid level. They were successful expressed in *E. coli* and functionally characterized.

- Both **BPSs** had a pH optimum between 7 and 7.5 and a temperature optimum at 35°C. The enzymes dramatically lost activity upon storage at different temperatures (0, 4, -20, -80 °C). Their activity was not stimulated by addition of DTT.

- In Gentianaceae, 3-hydroxybenzoyl-CoA appears to be the physiological starter substrate for **BPS** to form the tetraketide intermediate 2,3` ,4,6-tetrahydroxybenzophenone after iterative condensation with three molecules of malonyl-CoA. For the first time, three related CoA esters with a varying number of 3-hydroxybenzoyl residues were tested as substrates (3-hydroxybenzoyl-CoA, 3-(3-hydroxybenzoyloxy)benzoyl-CoA and 3-(3-hydroxybenzoyloxy)3-hydroxylbenzoyloxy)-benzoyl-CoA). All of them resulted in the formation of an identical product, i.e. 2,3` ,4,6-tetrahydroxybenzophenone, however, the catalytic efficiencies differed. Both CeBPS and ScBP**S** exhibited the highest catalytic efficiency with 3-(3-hydroxybenzoyloxy)benzoyl-CoA (K_{cat}/K_m = 162500 and 122300, respectively). In addition, both BPSs had relatively high activity with cinnamoyl-CoA and formed the triketide intermediate styrylpyrone after iterative condensation with

only two molecules of malonyl-CoA. This activity has so far only been observed with BPS from *Garcinia mangostana*.

- The transcripts level of **CeBPS** was not clearly enhanced after elicitation with yeast extract in cell cultures of *C. erythraea*, as shown by semiquantitative RT-PCR.

- The biosynthesis of amarogentin, especially the formation of the 3,3` ,5-trihydroxybiphenyl-2-carboxylate moiety, was postulated to be catalyzed by biphenylcarboxylate synthase (**BICS**) as a type III PKS. In this study, root cultures of *S. chirata* and *G. lutea* were used as mRNA sources. A full-length sequence putatively encoding BICS was ampliefied from *G. lutea* genomic DNA. The ORF comprised 1170 bp. The protein shared ~ 96% identity with a putative *Gentiana acaulis* BICS in the databank. The ORF was successfully expressed in *E. coli* but neither 3-hydroxybenzoyl-CoA nor benzoyl-CoA were accepted as starter substrates.

Prospective work

- In the past years, the explanation and analysis of structures and functions of type III polyketide synthases were dramatically increased due to cloning and characterization of novel enzymes. Thus, crystallization and structural analysis of both new enzymes (CeBPS and ScBPS) will provide essential information on the nature of the active site cavities. These studies should be supported by site-directed mutagenesis targeting essential residues. Finally, one may achieve amazing changes in the substrate and/or product specificities of the new BPSs.

- It is still challenging to do further attempts toward cloning a full-length sequence for BICS from *G. lutea* and/or *S. chirata*, which are the major sources of amarogentin. This compound was found to have interesting pharmacological activities, such as inhibition of DNA topoisomerase I from *Leishmania donovani*. It also inhibits the proliferation of cancer cells and induces apoptosis in a mouse skin carcinogenesis model.

6 References

Abd El-Mawla AM, Beerhues L (2002) Benzoic acid biosynthesis in cell cultures of *Hypericum androsaemum*. Planta 214: 727-733

Abd El-Mawla AM, Schmidt W, Beerhues L (2001) Cinnamic acid is a precursor of benzoic acids in cell cultures of *Hypericum androsaemum* L. but not in cell cultures of *Centaurium erythraea* RAFN. Planta 212: 288-293

Abdelaziz S (2014) Site-directed mutagenesis of Hypericum benzophenone synthases. dissertation TU Braunschweig

Abe I (2008) Engineering of Plant Polyketide Biosynthesis. Chemical and Pharmaceutical Bulletin 56: 1505-1514

Abe I (2010) Engineered biosynthesis of plant polyketides: structure-based and precursor-directed approach. Top Curr Chem 297: 45-66

Abe I, Morita H (2010) Structure and function of the chalcone synthase superfamily of plant type III polyketide synthases. Natural product reports 27: 809-838

Abe I, Takahashi Y, Morita H, Noguchi H (2001) Benzalacetone synthase. European Journal of Biochemistry 268: 3354-3359

Abe I, Utsumi Y, Oguro S, Morita H, Sano Y, Noguchi H (2005) A Plant Type III Polyketide Synthase that Produces Pentaketide Chromone. Journal of the American Chemical Society 127: 1362-1363

Abe I, Utsumi Y, Oguro S, Noguchi H (2004) The first plant type III polyketide synthase that catalyzes formation of aromatic heptaketide. FEBS letters 562: 171-176

Abe T, Morita H, Noma H, Kohno T, Noguchi H, Abe I (2007) Structure function analysis of benzalacetone synthase from Rheum palmatum. Bioorganic & medicinal chemistry letters 17: 3161-3166

Aberham A, Pieri V, Croom Jr EM, Ellmerer E, Stuppner H (2011) Analysis of iridoids, secoiridoids and xanthones in *Centaurium erythraea*, Frasera caroliniensis and *Gentiana lutea* using LC–MS and RP-HPLC. Journal of pharmaceutical and biomedical analysis 54: 517-525

Aberham A, Schwaiger S, Stuppner H, Ganzera M (2007) Quantitative analysis of iridoids, secoiridoids, xanthones and xanthone glycosides in *Gentiana lutea* L. roots by RP-HPLC and LC-MS. Journal of pharmaceutical and biomedical analysis 45: 437-442

Agarwal P (2013) Molecular cloning of a type III polyketide synthase from root cultures of *Swertia chirata*. Master thesis at TU-Braunschweig

Alliegro MC (2000) Effects of Dithiothreitol on Protein Activity Unrelated to Thiol–Disulfide Exchange: For Consideration in the Analysis of Protein Function with Cleland's Reagent. Analytical Biochemistry 282: 102-106

Arino A, Arberas I, Leiton MJ, Renobales Md, Dominguez JB (1997) The extraction of yellow gentian root (*Gentiana lutea* L). Zeitschrift fuer Lebensmittel-Untersuchung und -Forschung (Germany) 205: 295-299

Austin MB, Noel JP (2003) The chalcone synthase superfamily of type III polyketide synthases. Natural product reports 20: 79-110

References

Bajpai MB, Asthana RK, Sharma NK, Chatterjee SK, Mukherjee SK (1991) Hypoglycemic Effect of Swerchirin from the Hexane Fraction of *Swertia chirayita*. Planta medica 57: 102-104

Banerjee S, Sur TP, Das PC, Sikdar S (2000) Assessment of the antiinflammatory effects of *Swertia chirata* in acute and chronic experimental models in male albino rats. Indian J. Pharmacol 32: 21–24

Barillas W, Beerhues L (1997) 3-Hydroxybenzoate:coenzyme A ligase and 4-coumarate:coenzyme A ligase from cultured cells of *Centaurium erythraea*. Planta 202: 112-116

Beerhues L (1996) Benzophenone synthase from cultured cells of *Centaurium erythraea*. FEBS letters 383: 264-266

Beerhues L, Berger U (1994) Xanthones in cell suspension cultures of two *Centaurium* species. Phytochemistry 35: 1227-1231

Beerhues L, Berger U (1995) Differential accumulation of xanthones in methyl-jasmonate- and yeast-extract-treated cell cultures of *Centaurium erythraea* and *Centaurium littorale*. Planta 197: 608-612

Beerhues L, Liu B (2009) Biosynthesis of biphenyls and benzophenones--evolution of benzoic acid-specific type III polyketide synthases in plants. Phytochemistry 70: 1719-1727

Bennett G, Lee H-H (1989) Xanthones from Guttiferae. Phytochemistry 28: 967-998

Bentley R, Trimen H (1880) Medicinal Plants. London: J and A Churchill

Bhatt A, Rawal RS, Dhar U (2006) Ecological features of a critically rare medicinal plant, *Swertia chirayita*, in Himalaya. Plant Species Biology 21: 49-52

Birnboim HC, Doly J (1979) A rapid alkaline extraction procedure for screening recombinant plasmid DNA. Nucleic Acids Research 7: 1513-1523

Bode HB, Müller R (2003) Possibility of Bacterial Recruitment of Plant Genes Associated with the Biosynthesis of Secondary Metabolites. Plant Physiology 132: 1153

Boumendjel A, Boccard J, Carrupt P-A, Nicolle E, Blanc M, Geze A, Choisnard L, Wouessidjewe D, Matera E-L, Dumontet C (2008) Antimitotic and Antiproliferative Activities of Chalcones: Forward Structure–Activity Relationship. Journal of Medicinal Chemistry 51: 2307-2310

Bradford MM (1976) A rapid and sensitive method for the quantitation of microgram quantities of protein utilizing the principle of protein-dye binding. Analytical Biochemistry 72: 248-254

Bruneton J (1995) Pharmacognosy, phytochemistry, medicinal plants. Lavoisier Publishing, Paris

Cao E, Chen Y, Cui Z, Foster PR (2003) Effect of freezing and thawing rates on denaturation of proteins in aqueous solutions. Biotechnology and Bioengineering 82: 684-690

Cao T-W, Geng C-A, Ma Y-B, He K, Wang H-L, Zhou N-J, Zhang X-M, Tao Y-D, Chen J-J (2013) Xanthones with Anti-Hepatitis B Virus Activity from *Swertia mussotii*. Planta medica 79: 697-700

Capasso F, Gaginella T, Grandolini G, Izzo A (2003) Phytotherapy: a quick reference to herbal medicine. Springer Science & Business Media

References

Chaudhuri RK, Ghosal S (1971) Xanthones of *Canscora decussata* schult. Phytochemistry 10: 2425-2432

Chen Y, Huang B, He J, Han L, Zhan Y, Wang Y (2011) *In vitro* and *in vivo* antioxidant effects of the ethanolic extract of *Swertia chirayita*. J Ethnopharm 136

Chin Y-W, Kinghorn AD (2008) Structural Characterization, Biological Effects, and Synthetic Studies on Xanthones from Mangosteen (*Garcinia mangostana*), a Popular Botanical Dietary Supplement. Mini-reviews in organic chemistry 5: 355-364

Clarke CB (1885) Verbenaceae, in The Flora of British India, Vol. IV, ed Hooker J. D., editor. (London: L. Reeve and Co;). 560–604

Cohen SN, Chang ACY, Hsu L (1972) Nonchromosomal Antibiotic Resistance in Bacteria: Genetic Transformation of *Escherichia coli* by R-Factor DNA. Proceedings of the National Academy of Sciences of the United States of America 69: 2110-2114

Crockett SL, Poller B, Tabanca N, Pferschy-Wenzig E-M, Kunert O, Wedge DE, Bucar F (2011) Bioactive xanthones from the roots of *Hypericum perforatum* (common St John's wort). Journal of the Science of Food and Agriculture 91: 428-434

Cushnie TPT, Lamb AJ (2005) Antimicrobial activity of flavonoids. International Journal of Antimicrobial Agents 26: 343-356

Dagert M, Ehrlich SD (1979) Prolonged incubation in calcium chloride improves the competence of *Escherichia coli* cells. Gene 6: 23-28

Dana CD, Bevan DR, Winkel BSJ (2006) Molecular modeling of the effects of mutant alleles on chalcone synthase protein structure. Journal of Molecular Modeling 12: 905-914

David SS (1998) Plant secondary metabolism The Netherlands: Kluwer Acadimic Publishers 147: 483-485

de Carvalho PB, Ferreira EI (2001) Leishmaniasis phytotherapy. Nature's leadership against an ancient disease. Fitoterapia 72: 599-618

Dibyenda DM (2015) A brief Review on Plant Type III Polyketide Synthases, an Important Group of Enzyme of Secondary Metabolism. Research Journal of Recent 4.(10): 138-147

Du X-G, Wang W, Zhang Q-Y, Cheng J, Avula B, Khan IA, Guo D-A (2012) Identification of xanthones from *Swertia punicea* using high-performance liquid chromatography coupled with electrospray ionization tandem mass spectrometry. Rapid Communications in Mass Spectrometry 26: 2913-2923

Duckworth P (2012) The synthesis of intermediates to probe the biosynthesis of bacillaene. Master Thesis. University of Bristol,Cantock's Close, Bristol, BS8 1TS, U.K

Eckermann S, Schroder G, Schmidt J, Strack D, Edrada RA, Helariutta Y, Elomaa P, Kotilainen M, Kilpelainen I, Proksch P, Teeri TH, Schroder J (1998) New pathway to polyketides in plants. Nature 396: 387-390

El-Awaad I (2016) Cytochrome P450 enzymes involved in xanthone biosynthesis in Hypericum species. Dissertation TU Braunschweig

El-Awaad I, Bocola M, Beuerle T, Liu B, Beerhues L (2016) Bifunctional CYP81AA proteins catalyse identical hydroxylations but alternative regioselective phenol couplings in plant xanthone biosynthesis. Nature Communications 7: 11472

References

El-Seedi H, El-Barbary M, El-Ghorab D, Bohlin L, Borg-Karlson A, Goransson U, Verpoorte R (2010) Recent insights into the biosynthesis and biological activities of natural xanthones. Curr Med Chem 17: 854-901

Ferrer J-L, Jez JM, Bowman ME, Dixon RA, Noel JP (1999) Structure of chalcone synthase and the molecular basis of plant polyketide biosynthesis. Nat Struct Mol Biol 6: 775-784

Flores-Sanchez IJ, Verpoorte R (2009) Plant Polyketide Synthases: A fascinating group of enzymes. Plant Physiology and Biochemistry 47: 167-174

Frandsen R (2010) Polyketide biosynthesis.

Fukai T, Oku Y, Hou AJ, Yonekawa M, Terada S (2005) Antimicrobial activity of isoprenoid-substituted xanthones from *Cudrania cochinchinensis* against vancomycin-resistant enterococci. Phytomedicine 12: 510-513

Gaid MM, Sircar D, Müller A, Beuerle T, Liu B, Ernst L, Hänsch R, Beerhues L (2012) Cinnamate:CoA Ligase Initiates Biosynthesis of a Benzoate-Derived Xanthone Phytoalexin in *Hypericum calycinum* Cell Cultures. Plant Physiology

Gargi N, Sukriti D, Susmita D, Bratati D (2015) Antioxidant, anti-acetylcholinesterase and anti-glycosidase properties of three species of Swertia, their xanthones and amarogentin: A comparative study. Pharmacognosy Journal 7

Ghosal S, Sharma PV, Chaudhuri RK, Bhattacharya SK (1973a) Chemical Constituents of the Gentianaceae V: Tetraoxygenated Xanthones of *Swertia chirata* Buch.-Ham. Journal of pharmaceutical sciences 62: 926-930

Ghosal S, Sharma PV, Chaudhuri RK, Bhattacharya SK (1973b) Chemical constituents of the gentianaceae V: Tetraoxygenated xanthones of *swertia chirata* buch.-ham. Journal of pharmaceutical sciences 62: 926-930

Haraguchi H, Tanaka Y, Kabbash A, Fujioka T, Ishizu T, Yagi A (2004) Monoamine oxidase inhibitors from *Gentiana lutea*. Phytochemistry 65: 2255-2260

Hartmann T (2007) From waste products to ecochemicals: Fifty years research of plant secondary metabolism. Phytochemistry 68: 2831-2846

Hauffe K, Hahlbrock K, Scheel D (1986) Elicitor-stimulated furanocoumarin biosynthesis in cultured parsley cells: S-Adenosyl-Lmethionine:bergaptol and S-adenosyl-L-methionine:xanthotoxol

O-methyltransferases. . Z Naturforsch 41c: 228-239

Hertweck C (2009) The Biosynthetic Logic of Polyketide Diversity. Angewandte Chemie International Edition 48: 4688-4716

Huang L, Wang H, Ye H, Du Z, Zhang Y, Beerhues L, Liu B (2012) Differential expression of benzophenone synthase and chalcone synthase in *Hypericum sampsonii*. Nat Prod Commun 7: 1615-1618

I**inuma M, Tosa H, Tanaka T, Asai F, Kobayashl Y, Shimano R, Miyauchi K-I** (1996) Antibacterial Activity of Xanthones from Guttiferaeous Plants against Methicillin-resistant Staphylococcus aureus. Journal of Pharmacy and Pharmacology 48: 861-865

Jang M, Cai L, Udeani GO, Slowing KV, Thomas CF, Beecher CWW, Fong HHS, Farnsworth NR, Kinghorn AD, Mehta RG, Moon RC, Pezzuto JM (1997) Cancer

Chemopreventive Activity of Resveratrol, a Natural Product Derived from Grapes. Science 275: 218-220

Jantan I, Mohd Yasin YH, Jalil J, Murad S, Idris MS (2009) Antiplatelet aggregation activity of compounds isolated from Guttiferae species in human whole blood. Pharmaceutical Biology 47: 1090-1095

Jez JM, Austin MB, Ferrer J-L, Bowman ME, Schröder J, Noel JP (2000) Structural control of polyketide formation in plant-specific polyketide synthases. Chemistry & Biology 7: 919-930

Jez JM, Bowman ME, Noel JP (2001) Structure-Guided Programming of Polyketide Chain-Length Determination in Chalcone Synthase. Biochemistry 40: 14829-14838

Jia B, Li S, Hu X, Zhu G, Chen W (2015) Recent Research on Bioactive Xanthones from Natural Medicine: *Garcinia hanburyi*. AAPS PharmSciTech 16: 742-758

Jia J, Chen T, Wang P, Chen G, You J, Liu Y, Li Y (2012) Preparative Separation of Methylswertianin, Swerchirin and Decussatin from the Tibetan Medicinal Plant Swertia Mussotii Using High-speed Counter-current Chromatography. Phytochemical Analysis 23: 332-336

Joshi P, Dhawan V (2005) *Swertia chirayita* – An overview. Current Science 89(4): 635-640

Kaouadji M, Vaillant I, Mariotte A-M (1986) Polyoxygenated Xanthones from *Centaurium erythraea* Roots. Journal of Natural Products 49: 359-359

Karan M, Vasisht K, Handa SS (1999) Morphological and chromatographic comparison of certain Indian species of Swertia. J. Med. Aromat. P19lant Sci 19: 995–963

Keil M, Härtle B, Guillaume A, Psiorz M (2000) Production of Amarogentin in Root Cultures of *Swertia chirata*. Planta medica 66: 452-457

Keßmann H, Barz W (1987) Accumulation of isoflavones and pterocarpan phytoalexins in cell suspension cultures of different cultivars of chickpea (Cicer arietinum). Plant Cell Reports 6: 55-59

Klundt T, Bocola M, Lutge M, Beuerle T, Liu B, Beerhues L (2009) A single amino acid substitution converts benzophenone synthase into phenylpyrone synthase. The Journal of biological chemistry 284: 30957-30964

Kumar V, Sood H, Chauhan RS (2015) Detection of intermediates through high-resolution mass spectrometry for constructing biosynthetic pathways for major chemical constituents in a medicinally important herb, *Swertia chirayita*. Natural Product Research 29: 1449-1455

Kumar V, Van Staden J (2015) A Review of *Swertia chirayita* (Gentianaceae) as a Traditional Medicinal Plant. Frontiers in Pharmacology 6: 308

Kumarasamy Y, Nahar L, Cox PJ, Jaspars M, Sarker SD (2003) Bioactivity of secoiridoid glycosides from *Centaurium erythraea*. Phytomedicine 10: 344-347

Kusšar A, Zupančič A, Šentjurc M, Baričevicč D (2006) Free radical scavenging activities of yellow gentian (*Gentiana lutea* L.) measured by electron spin resonance. Human & Experimental Toxicology 25: 599-604

Laemmli UK (1970) Cleavage of Structural Proteins during the Assembly of the Head of Bacteriophage T4. Nature 227: 680-685

Lange D (1998) Europe's medicinal and aromatic plants: their use, trade and conservation. TRAFFIC International, Cambridge

Li D-H, Li C-X, Jia C-C, Sun Y-T, Xue C-M, Bai J, Hua H-M, Liu X-Q, Li Z-L (2016) Xanthones from *Garcinia paucinervis* with *in vitro* anti-proliferative activity against HL-60 cells. Archives of Pharmacal Research 39: 172-177

Li R, Kenyon GL, Cohen FE, Chen X, Gong B, Dominguez JN, Davidson E, Kurzban G, Miller RE, Nuzum EO, Rosenthal PJ, McKerrow JH (1995) *In Vitro* Antimalarial Activity of Chalcones and Their Derivatives. Journal of Medicinal Chemistry 38: 5031-5037

Li X, Liu S, Huang H, Liu N, Zhao C, Liao S, Yang C, Liu Y, Zhao C, Li S, Lu X, Liu C, Guan L, Zhao K, Shi X, Song W, Zhou P, Dong X, Guo H, Wen G, Zhang C, Jiang L, Ma N, Li B, Wang S, Tan H, Wang X, Dou QP, Liu J (2013) Gambogic Acid Is a Tissue-Specific Proteasome Inhibitor *In Vitro* and *In Vivo*. Cell Reports 3: 211-222

Liebisch H, Bernasch H, Schütte H (1973) Zur Biosynthese der Tropanalkaloide. Die Biosynthese des Cochlearins. Z Chem 372-373

Liswidowati, Melchior F, Hohmann F, Schwer B, Kindl H (1991) Induction of stilbene synthase by *Botrytis cinerea* in cultured grapevine cells. Planta 183: 307-314

Liu B, Beuerle T, Klundt T, Beerhues L (2004) Biphenyl synthase from yeast-extract-treated cell cultures of *Sorbus aucuparia*. Planta 218: 492-496

Liu B, Falkenstein-Paul H, Schmidt W, Beerhues L (2003) Benzophenone synthase and chalcone synthase from *Hypericum androsaemum* cell cultures: cDNA cloning, functional expression, and site-directed mutagenesis of two polyketide synthases. The Plant journal : for cell and molecular biology 34: 847-855

Liu B, Raeth T, Beuerle T, Beerhues L (2007) Biphenyl synthase, a novel type III polyketide synthase. Planta 225: 1495-1503

Liu B, Raeth T, Beuerle T, Beerhues L (2009) A novel 4-hydroxycoumarin biosynthetic pathway. Plant Molecular Biology 72: 17

Lukačin R, Schreiner S, Matern U (2001) Transformation of acridone synthase to chalcone synthase. FEBS letters 508: 413-417

Lukačin R, Schreiner S, Silber K, Matern U (2005) Starter substrate specificities of wild-type and mutant polyketide synthases from Rutaceae. Phytochemistry 66: 277-284

Lukačin R, Springob K, Urbanke C, Ernwein C, Schröder G, Schröder J, Matern U (1999) Native acridone synthases I and II from *Ruta graveolens* L. form homodimers. FEBS letters 448: 135-140

Mandel M, Higa A (1970) Calcium-dependent bacteriophage DNA infection. Journal of Molecular Biology 53: 159-162

Marshall BJ, Ratledge C (1972) Salicylic acid biosynthesis and its control in *Mycobacterium smegmatis*. Biochimica et Biophysica Acta (BBA) - General Subjects 264: 106-116

Masters K-S, Bräse S (2012) Xanthones from Fungi, Lichens, and Bacteria: The Natural Products and Their Synthesis. Chemical reviews 112: 3717-3776

Matsumoto K, Akao Y, Kobayashi E, Ohguchi K, Ito T, Tanaka T, Iinuma M, Nozawa Y (2003) Induction of Apoptosis by Xanthones from Mangosteen in Human Leukemia Cell Lines. Journal of Natural Products 66: 1124-1127

References

Medda S, Mukhopadhyay S, Basu MK (1999) Evaluation of the *in vivo* activity and toxicity of amarogentin, an antileishmanial agent, in both liposomal and niosomal forms. The Journal of antimicrobial chemotherapy 44

Menković N, Šavikin-Fodulović K, Savin K (2000) Chemical Composition and Seasonal Variations in the Amount of Secondary Compounds in *Gentiana lutea* Leaves and Flowers. Planta medica 66: 178-180

Meszaros S, de Laet J, Smets E (1996) Phylogeny of Temperate Gentianaceae: A Morphological Approach. Systematic Botany 21: 153-168

Moon UR, Sircar D, Barthwal R, Sen SK, Beuerle T, Beerhues L, Mitra A (2015) Shoot cultures of *Hoppea fastigiata* (Griseb.) C.B. Clarke as potential source of neuroprotective xanthones. Journal of Natural Medicines 69: 375-386

Moreno PRH, van der Heijden R, Verpoorte R (1994) Elicitor-mediated induction of isochorismate synthase and accumulation of 2,3-dihydroxy benzoic acid in *Catharanthus roseus* cell suspension and shoot cultures. Plant Cell Reports 14: 188-191

Morita H, Kondo S, Kato R, Wanibuchi K, Noguchi H, Sugio S, Abe I, Kohno T (2007) Crystallization and preliminary crystallographic analysis of an acridone-producing novel multifunctional type III polyketide synthase from *Huperzia serrata*. Acta crystallographica. Section F, Structural biology and crystallization communications 63: 576-578

Morita H, Noguchi H, Schröder J, Abe I (2001) Novel polyketides synthesized with a higher plant stilbene synthase. European Journal of Biochemistry 268: 3759-3766

Mroueh M, Saab Y, Rizkallah R (2004a) Hepatoprotective activity of *Centaurium erythraea* on acetaminophen-induced hepatotoxicity in rats. Phytotherapy Research 18: 431-433

Mroueh M, Saab Y, Rizkallah R (2004b) Hepatoprotective activity of *Centaurium erythraea* on acetaminophen- induced hepatotoxicity in rats. Phytotherapy Research 18: 431-433

Mustafa AM, Caprioli G, Ricciutelli M, Maggi F, Marín R, Vittori S, Sagratini G (2015) Comparative HPLC/ESI-MS and HPLC/DAD study of different populations of cultivated, wild and commercial *Gentiana lutea* L. Food Chemistry 174: 426-433

Negi JS, Bisht VK, Singh P, Rawat MSM, Joshi GP (2013) Naturally Occurring Xanthones: Chemistry and Biology. Journal of Applied Chemistry 2013: 9

Nielsen SF, Christensen SB, Cruciani G, Kharazmi A, Liljefors T (1998) Antileishmanial Chalcones: Statistical Design, Synthesis, and Three-Dimensional Quantitative Structure−Activity Relationship Analysis. Journal of Medicinal Chemistry 41: 4819-4832

Niiho Y, Yamazaki T, Nakajima Y, Yamamoto T, Ando H, Hirai Y, Toriizuka K, Ida Y (2006) Gastroprotective effects of bitter principles isolated from Gentian root and Swertia herb on experimentally-induced gastric lesions in rats. Journal of Natural Medicines 60: 82-88

Nualkaew N, Morita H, Shimokawa Y, Kinjo K, Kushiro T, De-Eknamkul W, Ebizuka Y, Abe I (2012) Benzophenone synthase from *Garcinia mangostana* L. pericarps. Phytochemistry 77: 60-69

Obolskiy D, Pischel I, Siriwatanametanon N, Heinrich M (2009) *Garcinia mangostana* L.: a phytochemical and pharmacological review. Phytotherapy Research 23: 1047-1065

Osbourn A, Lanzotti V (2009) Plant-derived Natural Products "Synthesis, Function, and Application". Springer Science+Business Media, LLC

References

Öztürk N, Herekman-Demir T, Öztürk Y, Bozan B, Başer KHC (1998) Choleretic activity of *Gentiana lutea* ssp. symphyandra in rats. Phytomedicine 5: 283-288

Pant N, Jain DC, Bhakuni RS (2000) Phytochemicals from genus Swertia and their biological activities. Indian Journal of Chemistry 39B: 565-586.

Peres V, Nagem T (1997) Trioxygenated naturally occurring xanthones. Phytochemistry 44: 191-214

Peters S, Schmidt W, Beerhues L (1997) Regioselective oxidative phenol couplings of 2,3′,4,6-tetrahydroxybenzophenone in cell cultures of *Centaurium erythraea* RAFN and *Hypericum androsaemum* L. Planta 204: 64-69

Phoboo S, Bhowmik PC, Jha PK, Shetty K (2014) Phenolic-Linked Antioxidant, anti-Diabetic, and anti-Hypertensive Potential of Wild and Cultivated *Swertia chirayita* (Roxb. ex Flem.) Karst. Using in vitro Assays. Journal of Herbs, Spices & Medicinal Plants 20: 55-69

Phoboo S, Pinto MDS, Barbosa ACL, Sarkar D, Bhowmik PC, Jha PK, Shetty K (2013) Phenolic-Linked Biochemical Rationale for the Anti-Diabetic Properties of *Swertia chirayita* (Roxb. ex Flem.) Karst. Phytotherapy Research 27: 227-235

Piatczak E, Wielanek M, Wysokinska H (2005) Liquid culture system for shoot multiplication and secoiridoid production in micropropagated plants of *Centaurium erythraea* Rafn. Plant Science 168: 431-437

Piątczak E, Wysokińska H (2013) Encapsulation of *Centaurium eryhthraea* RAFN – An effecient method for regeneration of transgenic plants. Acta biologica Cracoviensia Series Botanica, p 37

Rai LK, P. P, Sharma E (2000) Conservation threats to some medicinal plants of the Sikkim Himalaya. Biol. Cons 93: 27–33

Ray S, Majumder HK, Chakravarty AK, Mukhopadhyay S (1996) Amaraogentin, a naturally occurring secoiridoid glycoside and a newly recognized inhibitor of topoisomerase I from *Leishmania donovani*. J Nat Prod 59

Reimold U, Kröger M, Kreuzaler F, Hahlbrock K (1983) Coding and 3' non-coding nucleotide sequence of chalcone synthase mRNA and assignment of amino acid sequence of the enzyme. The EMBO Journal 2: 1801-1805

Resmi MS, Verma P, Gokhale RS, Soniya EV (2013) Identification and characterization of a type III polyketide synthase involved in quinolone alkaloid biosynthesis from Aegle *marmelos Correa*. The Journal of biological chemistry 288: 7271-7281

Sakaitani M, Rusnak F, Quinn NR, Tu C, Frigo TB, Berchtold GA, Walsh CT (1990) Mechanistic studies on trans-2,3-dihydro-2,3-dihydroxybenzoate dehydrogenase (Ent A) in the biosynthesis of the iron chelator enterobactin. Biochemistry 29: 6789-6798

Sambrook J, Russell DW (2001) Molecular cloning: a laboratory manual, 3rd edn. (NewYork:Cold Spring Harbor Laboratory Press)

Saxena RS, Gupta B, Saxena KK, Singh RC, Prasad DM (1984) Study of anti-inflammatory activity in the leaves of Nyctanthes arbor tristis Linn. — an Indian medicinal plant. Journal of Ethnopharmacology 11: 319-330

Scharnhop H (2008) Untersuchengen zur Biosynthese aromatischer Sekundärmetabolite in Zellkulturen von *Sorbus aucuparia* L. und *Centaurium erythraea* RAFN. Dissertation TU Braunschweig, Braunschweig

Schimmer O, Mauthner H (1996) Polymethoxylated xanthones from the herb of *Centaurium erythraea* with strong antimutagenic properties in *Salmonella typhimurium*. Planta medica 62: 561-564

Schmidt W, Abd El-Mawla AMA, Wolfender J-L, Hostettmann K, Beerhues L (2000a) Xanthones in Cell Cultures of *Hypericum androsaemum*. Planta medica 66: 380-381

Schmidt W, Beerhues L (1997) Alternative pathways of xanthone biosynthesis in cell cultures of *Hypericum androsaemum* L. FEBS letters 420: 143-146

Schmidt W, Peters S, Beerhues L (2000b) Xanthone 6-hydroxylase from cell cultures of *Centaurium erythraea* RAFN and *Hypericum androsaemum* L. Phytochemistry 53: 427-431

Schröder J (1999) The chalcone/stilbene synthase-type family of condensing enzymes. Comprehensive Natural Products Chemistry vol. 1, Elsevier, Amsterdam: 749-771

Shekarchi M, Hajimehdipoor H, Khanavi M, Adib N, Bozorgi M, Akbari-Adergani B (2010) A validated method for analysis of Swerchirin in *Swertia longifolia* Boiss. by high performance liquid chromatography. Pharmacognosy Magazine 6: 13-18

Shimizu Y, Ogata H, Goto S (2017) Type III Polyketide Synthases: Functional Classification and Phylogenomics. Chembiochem : a European journal of chemical biology 18: 50-65

Siebert M, Severin K, Heide L (1994) Formation of 4-hydroxybenzoate in *Escherichia coli*: characterization of the ubiC gene and its encoded enzyme chorismate pyruvate-lyase. Microbiology 140: 897-904

Singh P (2014) Molecular cloning of 3-hydroxybenzoate: Co ligase from Gentianaceae. Master thesis at TU-Braunschweig

Skrzypczak L, Wesolowska M, Skrzypczak E (1993) Gentiana Species: *In Vitro* Culture, Regeneration, and Production of Secoiridoid Glucosides. In: Bajaj YPS (ed) Medicinal and Aromatic Plants IV. Springer Berlin Heidelberg, Berlin, Heidelberg, pp 172-186

Staunton J, Weissman KJ (2001) Polyketide biosynthesis: a millennium review. Natural product reports 18: 380-416

Sullivan G, Stiles FD, Rosler K-HA (1977) Phytochemical Investigation of Xanthones of *Eustoma grandiflorum* (Raf.) Shinners. Journal of pharmaceutical sciences 66: 828-831

Suzuki O, Katsumat aY, Oya M (1978) Biochemical Pharmacology. 27: 2075-2078

Swiddan A (2010) Biphenyl synthase from Gentian and Pear. dissertation TU Braunschweig

Ueno C, Kakuda R, Kikuchi M, Yaoita Y, Machida K, Kikuchi M (2003) On the chemical constituents of *Gentiana radix* III. J Tohoku Pharm Univ 50: 81-84

Valentão P, Fernandes E, Carvalho F, Andrade PB, Seabra RM, Bastos ML (2001) Antioxidant Activity of *Centaurium erythraea* Infusion Evidenced by Its Superoxide Radical Scavenging and Xanthine Oxidase Inhibitory Activity. Journal of Agricultural and Food Chemistry 49: 3476-3479

Valentão P, Fernandes E, Carvalho F, Andrade PB, Seabra RM, Bastos ML (2003) Hydroxyl radical and hypochlorous acid scavenging activity of small Centaury (*Centaurium*

erythraea) infusion. A comparative study with green tea (*Camellia sinensis*). Phytomedicine 10: 517-522

van der Sluis WG, Labadie RP (1981) Secoiridoids and Xanthones in the Genus Centaurium. Planta medica 41: 150-160

VanHaelen M, Vanhaelen-Fastre R (1983) Quantitative determination of biologically active constituents in medicinal plant crude extract by thin-layer chromatography densitiometry. J chromatogr 281: 263-271

Vieira L, Kijjoa A (2005) Naturally-occurring xanthones: Recent developments. Curr Med Chem 12: 2413-2446

Waltenberger B, Liu R, Atanasov GA, Schwaiger S, Heiss HE, Dirsch MV, Stuppner H (2015) Nonprenylated Xanthones from *Gentiana lutea, Frasera caroliniensis*, and *Centaurium erythraea* as Novel Inhibitors of Vascular Smooth Muscle Cell Proliferation. Molecules 20

Wang C-Z, Maier UH, Zenk MH (2000) Synthesis of 3,3‘,5-Trihydroxybiphenyl-2-carboxylic Acid, a Component of the Bitterest Natural Product Amarogentin and Its Coenzyme A and N-Acetyl Cysteamine Thiol Esters. Journal of Natural Products 63: 371-374

Wang CZ, Maier UH, Keil M, Zenk MH, Bacher A, Rohdich A, Eisenreich W (2003) Phenylalanine-independent biosynthesis of 1, 3, 5, 8-tetrahydroxyxanthone: aretrobiosynthetic NMR study with root cultures of *Swertia chirata*. European Journal of Biochemistry 270: 2950-2958

Wang D (2008) Qualitative and quantitative analysis of Swertia herbs by high performance liquid chromatography diode array detector-mass spectrometry (HPLC-DAD-MS). Chem Pharm Bull 56

Wang S-n, Li Q, Jing M-h, Alba E, Yang X-h, Sabaté R, Han Y-f, Pi R-b, Lan W-j, Yang X-b, Chen J-k (2016) Natural Xanthones from *Garcinia mangostana* with Multifunctional Activities for the Therapy of Alzheimer’s Disease. Neurochemical Research 41: 1806-1817

Wanibuchi K, Zhang P, Abe T, Morita H, Kohno T, Chen G, Noguchi H, Abe I (2007) An acridone-producing novel multifunctional type III polyketide synthase from Huperzia serrata. The FEBS Journal 274: 1073-1082

Weiss RF (1988) Aerztezeitschr Naturheilverf 29: 429-436

Wu Y-P, Zhao W, Xia Z-Y, Kong G-H, Lu X-P, Hu Q-F, Gao X-M (2013) Three Novel Xanthones from *Garcinia paucinervis* and Their Anti-TMV Activity. Molecules 18: 9663

Ya BQ, Nian LC, Li C, Gen XP (1999) Protective effect of swerchirin on hematopoiesis in 60Co-irradiated mice. Phytomedicine 6: 85-88

Yue Y-D, Zhang Y-T, Liu Z-X, Min Q-X, Wan L-S, Wang Y-L, Xiao Z-Q, Chen J-C (2014) Xanthone Glycosides from *Swertia bimaculata* with α-Glucosidase Inhibitory Activity. Planta medica 80: 502-508

Zhou M, Zhou K, Zhao Y-L, Xiang N-J, Zhang T-D, Wang Y-D, Dong W, Ji B-K, Li L-M, Lou J, Li G-P, Hu Q-F (2015a) Three new prenylated xanthones from *Comastoma pedunculatum* and their anti-tobacco mosaic virus activity. Phytochemistry Letters 11: 245-248

Zhou N-J, Geng C-A, Huang X-Y, Ma Y-B, Zhang X-M, Wang J-L, Chen J-J (2015b) Anti-hepatitis B virus active constituents from *Swertia chirayita*. Fitoterapia 100: 27-34

References

Zodi R (2011) Molecular cloning of benzophenone synthase from *Hypericum calycinum* cell cultures and attempts toward transformation of *Hypericum perforatum*. Dissertation TU Braunschweig, Braunschweig

7 Appendix

7.1 Graphical representation of enzyme kinetics for CeBPS and ScBPH through Michaelis- Menten and Lineweaver-Burk plots

7.1.1 Graphical representation of additional enzyme kinetics for CeBPS (3.1.4.8.1)

7.1.1.1 Cinnamoyl-CoA

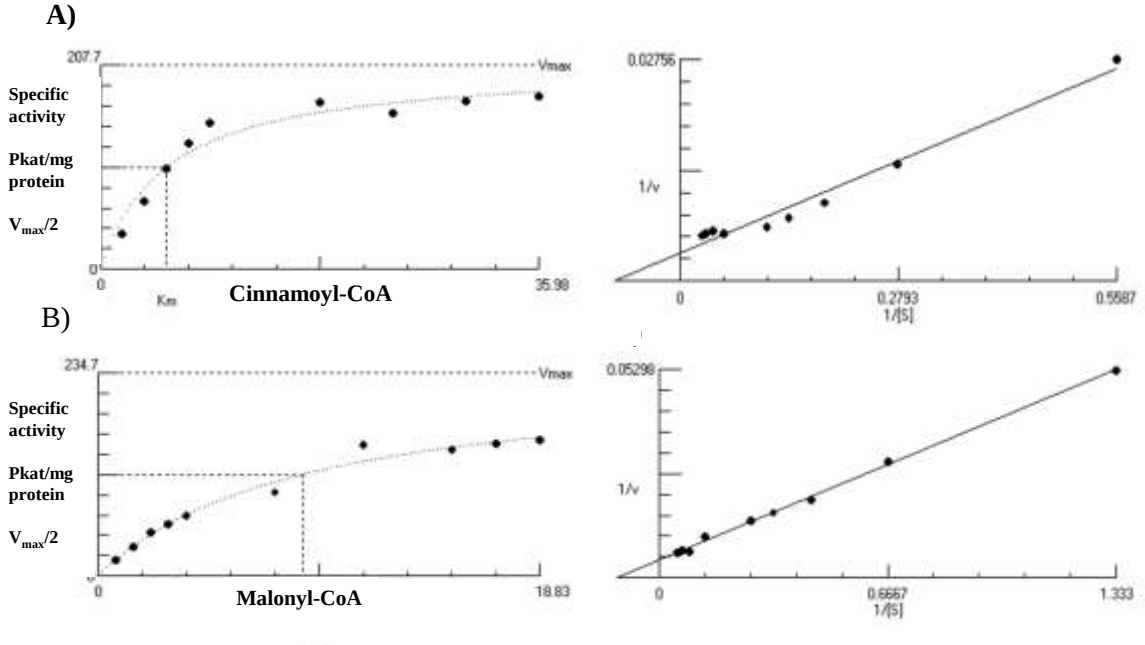

Figure 72. Graphical representation of enzyme kinetics for CeBPS through Michaelis-Menten and Lineweaver-Burk plots. A) Cinnamoyl-CoA, B) Malonyl-CoA.

7.1.1.2 3-((3-hydroxybenzoyloxy)3-hydroxylbenzoyloxy)-benzoyl-CoA

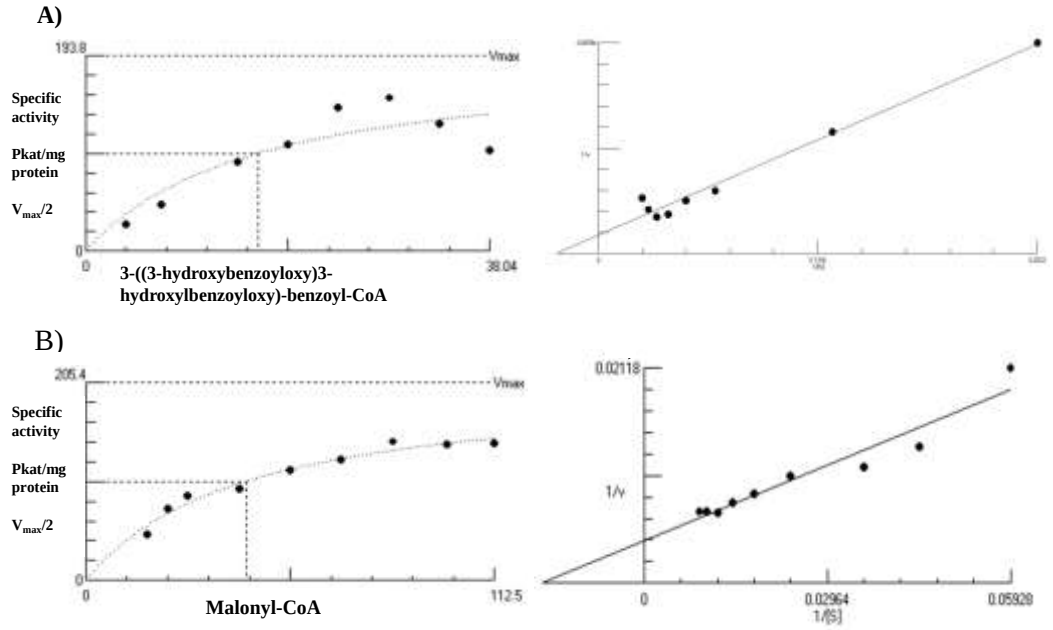

Figure 73. Graphical representation of enzyme kinetics for CeBPS through Michaelis-Menten and Lineweaver-Burk plots. A) 3-((3-hydroxybenzoyloxy)3-hydroxylbenzoyloxy)-benzoyl-CoA, B) Malonyl-CoA.

7.1.1.3 3-hydroxybenzoyl-CoA

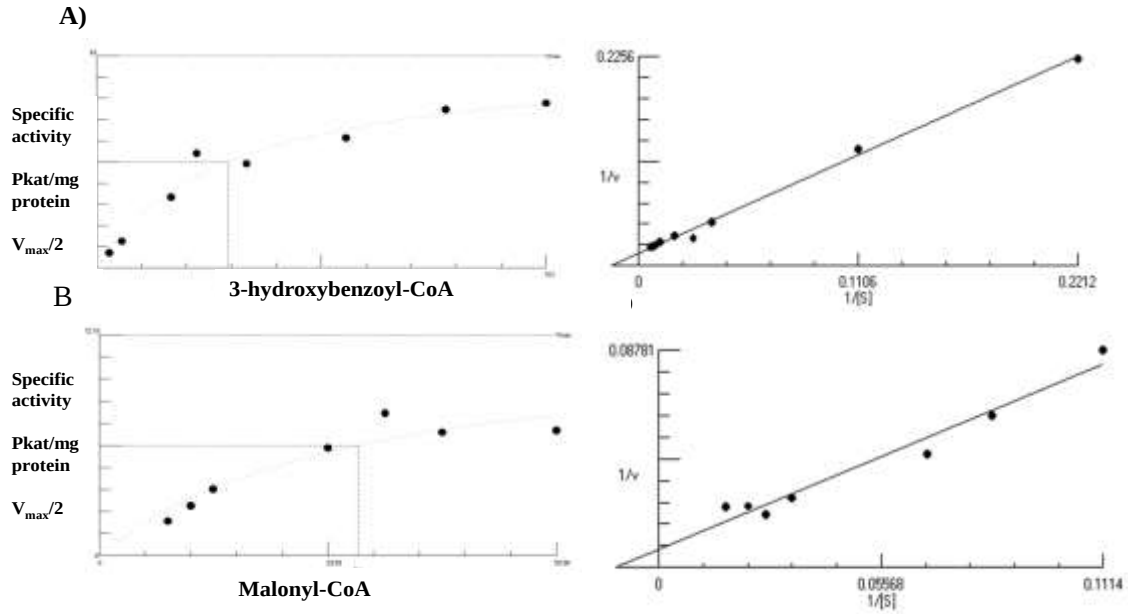

Figure 74. Graphical representation of enzyme kinetics for CeBPS through Michaelis-Menten and Lineweaver-Burk plots. A. 3-hydroxybenzoyl-CoA, B. Malonyl-CoA.

7.1.1.4 Benzoyl-CoA

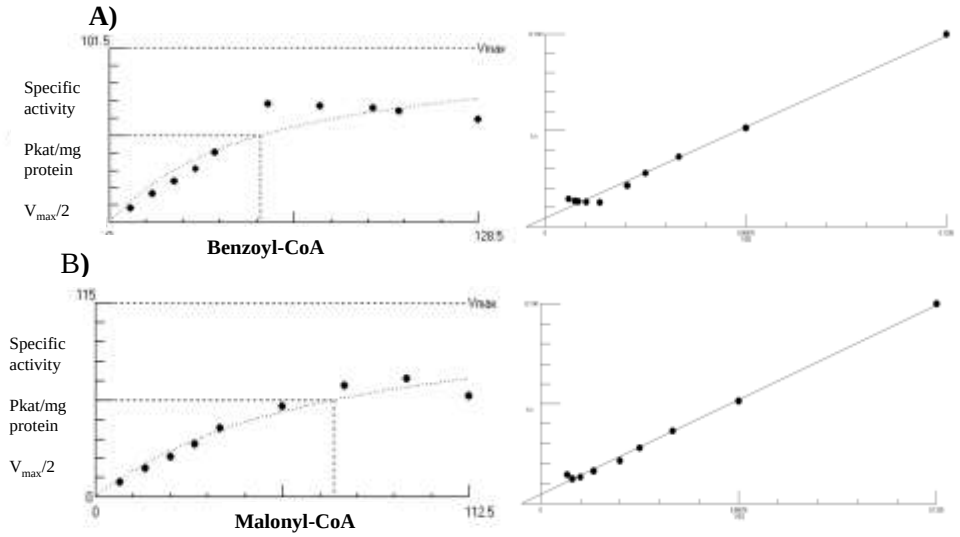

Figure 75. Graphical representation of enzyme kinetics for CeBPS through Michaelis-Menten and Lineweaver-Burk plots. A) benzoyl-CoA, B) Malonyl-CoA.

7.1.2 Graphical representation of additional enzyme kinetics for ScBPS (3.1.4.8.2)

7.1.2.1 Cinnamoyl-CoA

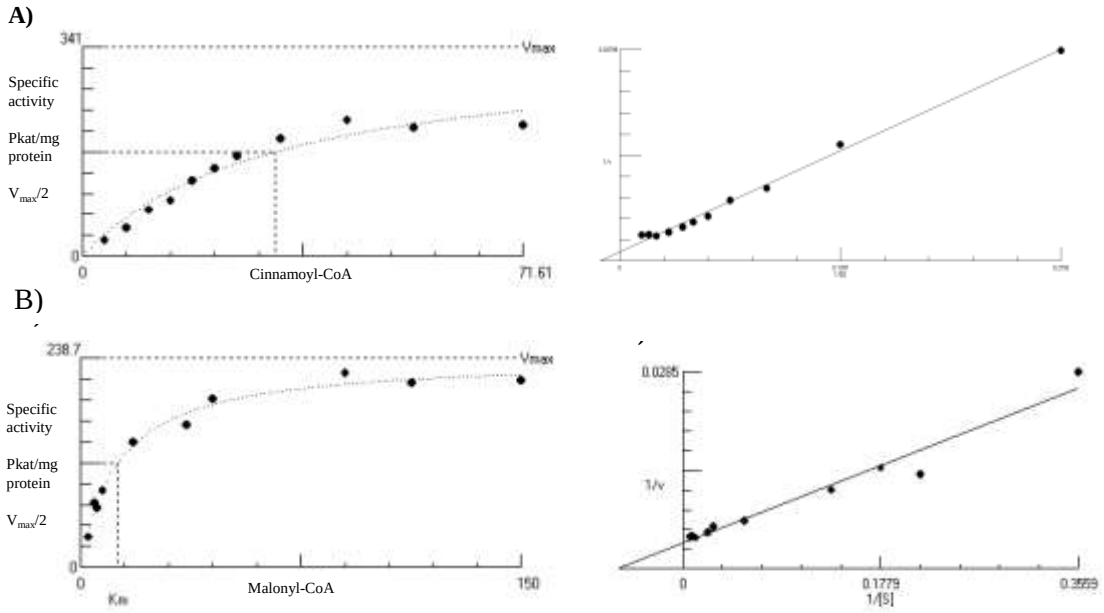

Figure 76. Graphical representation of enzyme kinetics for ScBPS through Michaelis-Menten and Lineweaver-Burk plots. A) Cinnamoyl-CoA, B) Malonyl-CoA.

7.1.2.2 3-((3-hydroxybenzoyloxy)3-hydroxylbenzoyloxy)-benzoyl-CoA

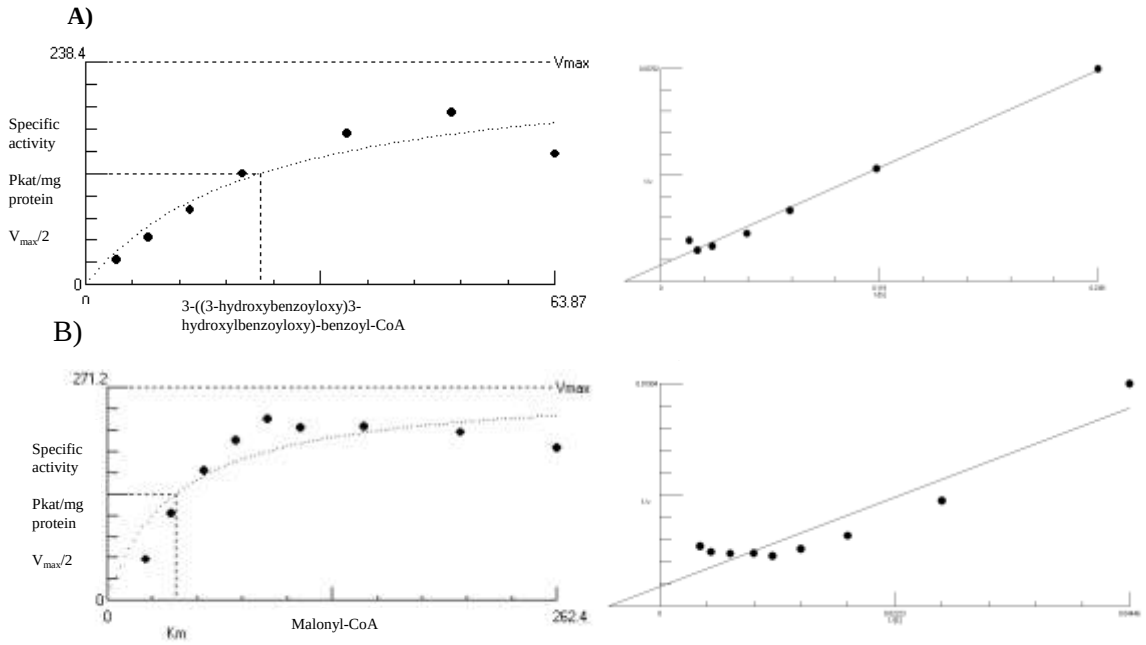

Figure 77. Graphical representation of enzyme kinetics for ScBPS through Michaelis-Menten and Lineweaver-Burk plots. A) 3-((3-hydroxybenzoyloxy)3-hydroxylbenzoyloxy)-benzoyl-CoA, B) Malonyl-CoA.

7.1.2.3 3-hydroxybenzoyl-CoA

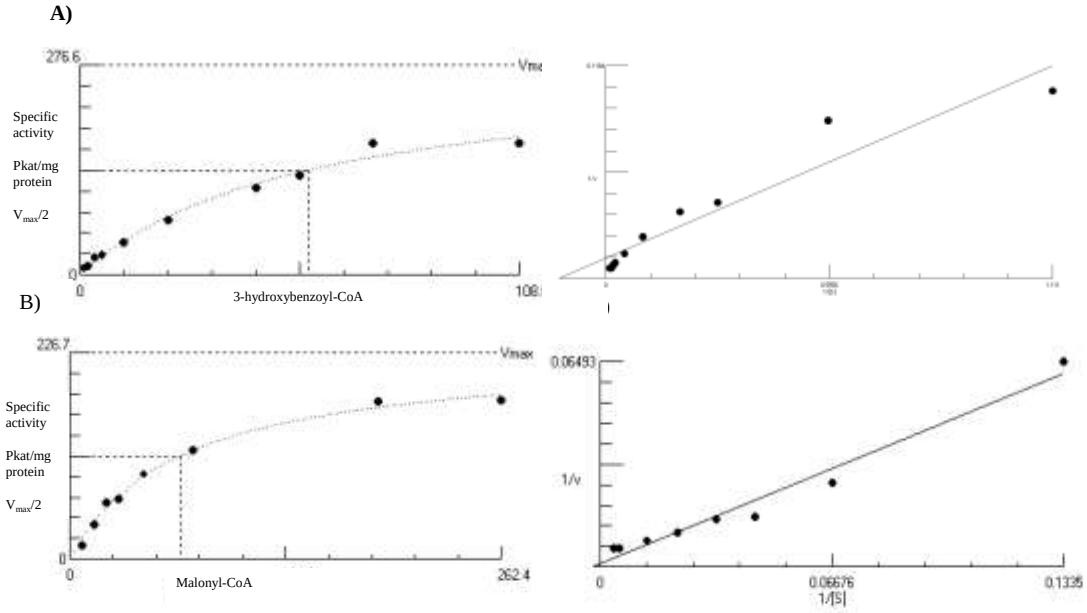

Figure 78. Graphical representation of enzyme kinetics for ScBPS through Michaelis-Menten and Lineweaver-Burk plots. A) 3-hydroxybenzoyl-CoA, B) Malonyl-CoA.

7.1.2.4 Benzoyl-CoA

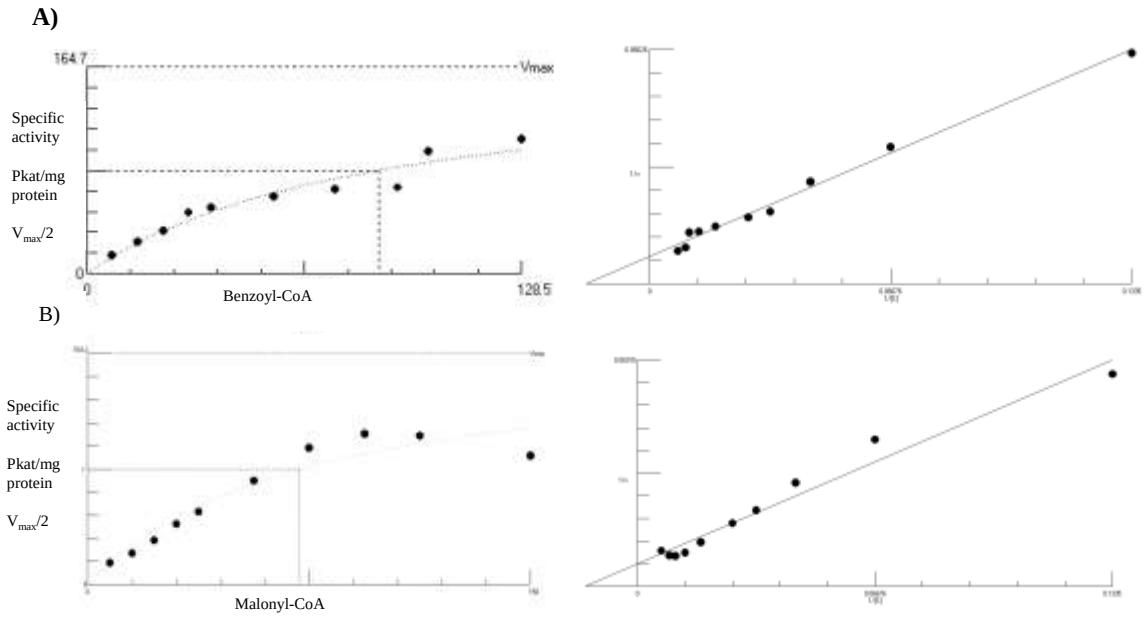

Figure 79. Graphical representation of enzyme kinetics for ScBPS through Michaelis-Menten and Lineweaver-Burk plots. A) Benzoyl-CoA, B) Malonyl-CoA.